OKLAHOMA
GEOLOGICAL
SURVEY

BULLETIN 151

Isoteline Trilobites of the Viola Group (Ordovician: Oklahoma): Systematics and Stratigraphic Occurrence

Lisa Amati
State University of New York at Potsdam

2014

Oklahoma Geological Survey
G. Randy Keller, *Director*

BULLETIN 151 ISSN 0078-4389

Isoteline Trilobites of the Viola Group (Ordovician: Oklahoma): Systematics and Stratigraphic Occurrence

Lisa Amati
Department of Geology,
State University of New York at Potsdam
Potsdam, New York 13676

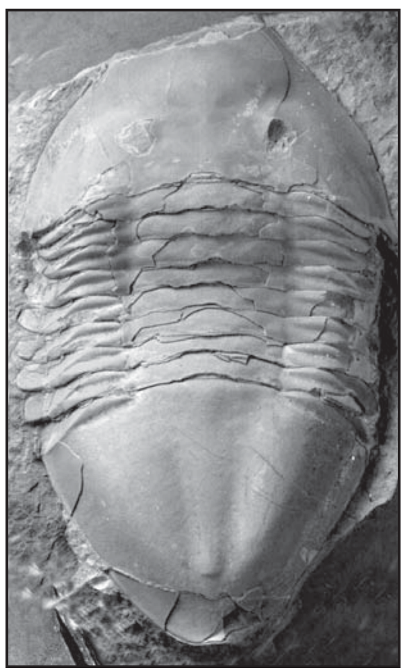

The University of Oklahoma
Norman
2014

TITLE PAGE ILLUSTRATION

From Plate12, Figure 2, page 85: *Isotelus* cf. *I. iowensis*; OU 3119 (BQ-Float) nearly complete individual, front of cephalon and rear of pygidium broken x0.75 in dorsal view.

This publication is issued by the Oklahoma Geological Survey as authorized by Title 70, Oklahoma Statutes, 1981, Sections 231–238. Copies have not been printed, but are available on-line through the OGS website. An electronic copy has been deposited with the Publications Clearinghouse of the Oklahoma Department of Libraries.

CONTENTS

TABLE

FIGURES

PLATES

Isoteline Trilobites of the Viola Group (Ordovician: Oklahoma): Systematics and Stratigraphic Occurrence

Lisa Amati
Department of Geology,
State University of New York at Potsdam
Potsdam, New York 13676

ABSTRACT. — In this paper, I describe eleven species of isoteline trilobites from the Upper Ordovician (Katian) Viola Group, including six species of *Isotelus* (*I. kimmswickensis* Bradley, 1930, *I. violaensis* new species, *I. bradleyi* new species, *I. skapaneidos* new species, *Isotelus* cf. *I. walcotti* Walcott, 1918, *Isotelus* cf. *I. iowensis* Owen, 1852), one species of *Ectenaspis* (*E. burkhalteri* new species), two species of *Stegnopsis* (*S. wellingensis* new species, *S. erythragora* new species) and two species of *Anataphrus* (*A. megalophrys* new species, *A. kermiti* new species). A formal analysis of phylogenetic relationships within the Isotelinae is beyond the scope of this study, so my rediagnoses and evaluation of the phylogenetic context of the four genera occurring in the Viola Group are provisional. *Isotelus* and *Ectenaspis* likely form a monophyletic group. I define two groups within *Isotelus* based on the course of the facial sutures anterior to the palpebral lobes. I exclude a third group of trilobites traditionally classified in *Isotelus* including *I. latus* Raymond, 1913, *I ottawaensis* Wilson, 1947, *I. maximus* Locke, 1838, and *I. rex* Rudkin and others, 2003. Numerous plesiomorphic features are shared by *Stegnopsis* and *Isoteloides* including a short (exsag.) pygidium, incomplete effacement of the pygidium, genal spines in some holaspids and wide cephalic and pygidial border furrows. I consider *Anataphrus* to form a derived group with *Nahannia*, *Protopresbynileus*, *Vogdesia*, *Homotelus* and possibly *Nileoides* based on high degree of effacement of axial furrows, wide pygidial axes, and a glabella that extends to the anterior margin of the cranidium. The stratigraphic distribution of isotelines within the Viola Group is useful for correlation with other Upper Ordovician units across Laurentia in a wide range of depositional environments.

INTRODUCTION

Isotelines are large and conspicuous Ordovician trilobites that are familiar to most paleontologists. *Isotelus* Dekay, 1824, includes the largest known species of trilobite (Rudkin and others, 2003). Isotelines are also widely distributed across North America (e.g., northwestern Canada: Chatterton and Ludvigsen, 1976, and Hunda and others, 2003; Nevada: Ross and Shaw, 1972; Missouri: Bradley, 1930; Manitoba: Westrop and Ludvigsen, 1983; Ontario: Wilson, 1947; Virginia: Tripp and Evitt, 1986; Newfoundland: Whittington, 1965), and have considerable potential in regional and inter-regional correlation. However, their biostratigraphic utility is undermined by the absence of modern systematic treatment of most genera and species. For example, *I. gigas* Dekay, 1824, the type species of *Isotelus*, and *I. walcotti* Walcott, 1918, were revised recently by Rudkin and Tripp (1989), but most other members of the genus remain poorly known. Isotelines can be found in most exposures of the Viola Group in south-central Oklahoma, where they occur in a variety of lithofacies. Here, I document 11 isoteline species from the Viola Group and evaluate species described by Bradley (1930) from the coeval Kimmswick Limestone of Missouri and Illinois. Viola Group isotelines include six species of *Isotelus*, two species of *Anataphrus* Whittington, in Miller and others, 1954, two species of *Stegnopsis* Whittington, 1965, and a single species of *Ectenaspis* Raymond, 1920; eight of these species are new. A formal phylogenetic analysis of isoteline trilobites is long overdue but is beyond the scope of this monograph. Many of the taxonomic problems that need to be addressed are discussed at various points in the text.

GEOLOGIC SETTING

The Viola Group consists of Upper Ordovician (Mohawkian – Cincinnatian) carbonate that was deposited in shallow epeiric seas covering the southern mid-continent. The Southern Oklahoma aulacogen (Hoffman and others, 1974) was a narrow, fault-bounded basin within the larger Oklahoma basin. The aulacogen extended from the Texas panhandle southeast through Oklahoma to eastern Texas and formed as a result of Early Cambrian rifting (Fig. 1). Periodic reactivation of faults along the hingeline of the aulacogen provided accommodation space that allowed deposition and preservation of a thick sequence of early Paleozoic sediments (Ham and others, 1964). These units are now well-exposed in the Arbuckle Mountains of south-central Oklahoma.

Two formations make up the Viola Group: the Viola Springs Formation and the overlying Welling Formation (Fig. 2). The base of the Viola Group in south-central Oklahoma is disconformable with the underlying Bromide Formation and is marked by finely-laminated mudstone indicating onset of deep-water deposition following rapid subsidence within the aulacogen. A general shallowing-upward trend is recorded at all sections, with areas nearer the plat-

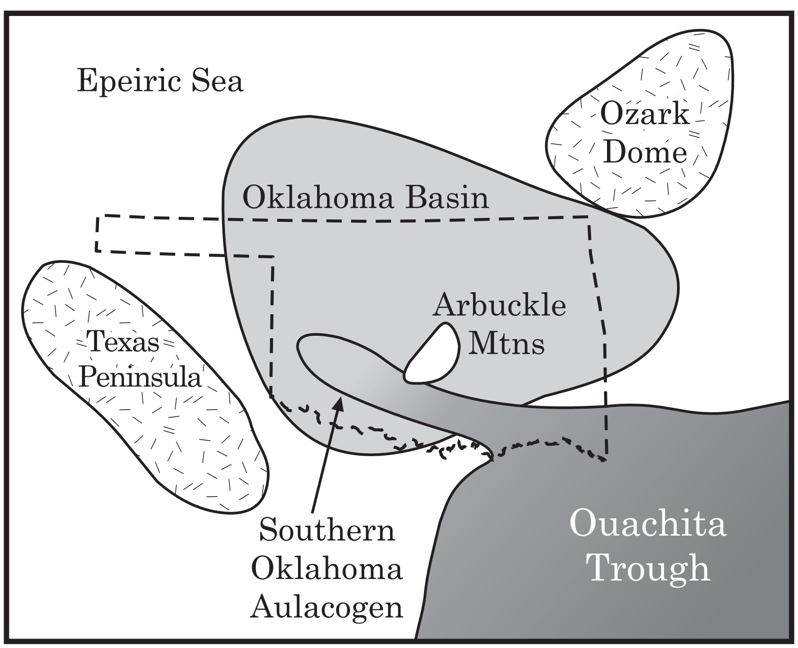

Figure 1. Generalized paleogeographic map showing the location of the modern Arbuckle Mountains in relation to the margins of the Southern Oklahoma aulacogen in the Ordovician. The Texas peninsula and Ozark dome were the only emergent features. North arrow is in modern orientation.

form shallowing more abruptly than those well within the margins of the aulacogen. Overall section thickness, as well as thickness of deep-water deposits, increases toward the center of the aulacogen.

LITHOFACIES ANALYSIS

Four lithofacies characterize the Viola Springs Formation in south-central Oklahoma and represent deposition at different depths along an environmental gradient from the shallow carbonate platform in the north to a deep ramp environment to the south within the Southern Oklahoma aulacogen. These facies are superimposed through the Viola Springs Formation indicating shallowing as the aulacogen slowly filled with sediment. A fifth lithofacies defines the Welling Formation and represents relatively shallow deposition across the environmental gradient. Following is a brief outline of Viola Group facies; a more detailed treatment can be found in Amati and Westrop (2006).

Carbonate Mudstone Lithofacies

This facies is divided into two subfacies based on sedimentary structures. The laminated carbonate mudstone subfacies consists of organic-rich, millimeter- to centimeter-scale laminae. Dark carbonate laminae are made up of slightly coarser-grained (silt grade) material and relatively lighter laminae are nearly pure carbonate mud. Carbonate layers 10-40 cm thick are separated by thin, 0.5-3 cm thick marl partings. Limestone/marl alternations reflect original heterogeneity that has been enhanced by diagenesis (Bathurst, 1987). Nodules, lenses and discontinuous beds of chert are concentrated along marl partings. The fauna is limited to rare cryptolithine trilobites and graptolites, which are abundant at some parting surfaces and oriented parallel to the hingeline of the aulacogen (Gentile and others, 1984). Absence of bioturbation, high organic content of the sediment (indicated by dark color) and limited benthic fauna suggest deposition in a low-oxygen environment (Allison and others, 1995). The high

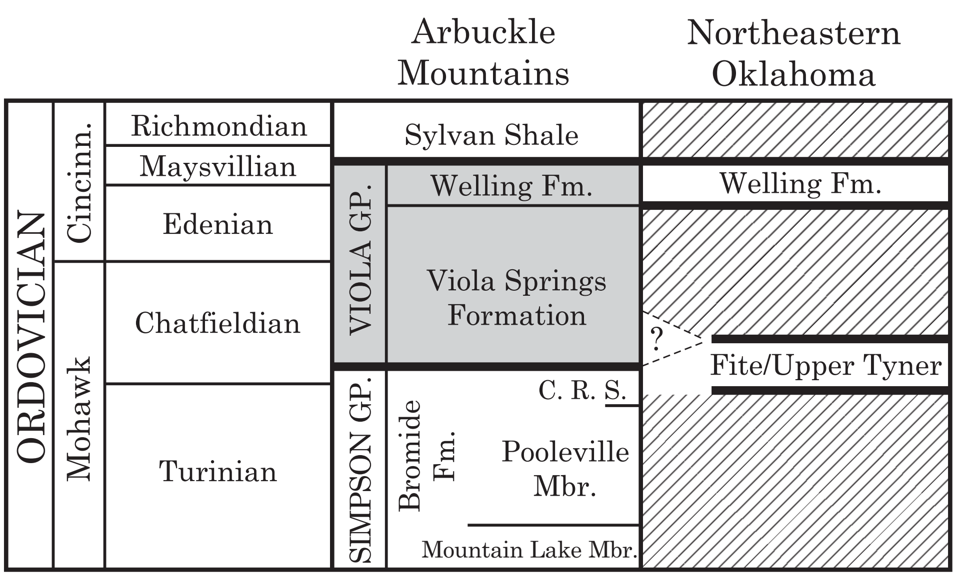

Figure 2. Late Ordovician stratigraphy for the Arbuckle Mountain region and northeastern Oklahoma. C.R.S. — Corbin Ranch Submember of the Pooleville Member of the Bromide Formation. Correlation of the Fite and Upper Tyner formations is tentative (see text for more information).

degree of sorting between laminae and the orientation of graptolites can be interpreted as evidence for deposition by, or reworking by, storm-generated geostrophic flows (Duke, 1990).

The bioturbated carbonate mudstone subfacies consist of centimeter-scale laminae similar to those of the laminated subfacies but slightly thicker on average. Degree of bioturbation becomes more intense upward in the section, indicating increasing oxygen levels. This is supported by a higher abundance of cryptolithine trilobites. Greater thickness of laminae (centimeter-scale) and increased oxygenation suggest that transportation of carbonate mud into the environment was from turbid flows (Duke, 1990; Einsele and Seilacher, 1991).

Low-diversity Wacke- to Rudstone Lithofacies

Wackestone, completely homogenized by bioturbation, occurs in 20-50 cm thick beds separated by thin (1-2 cm) marl partings. The thickness of beds and general fining-upward trend suggest deposition by distal turbid flows. *Anataphrus* trilobites are locally abundant in thick (3-10 cm) float- to rudstone layers at the tops of beds. *Anataphrus* sclerites are very abundant within these layers with rare cryptolithine cranidia. Nearly every preservable skeletal element is present (cranidia, librigenae, thoracic segments, hypostomes, pygidia) and jumbled in random orientation. Storm winnowing is unlikely to have produced these accumulations because the majority of sclerites are not found in the hydrodynamically stable, convex-up position. *Anataphrus* float- to rudstone more probably represents settling of sclerites and sediment from suspension. Karim and Westrop (2002) and Speyer and Brett (1985) provided examples of monotaxic trilobite accumulations resulting from rapid burial of biologic aggregations. The *Anataphrus* floatstone differs in that the sclerites are not preserved *in situ*, but behavioral aggregations may explain the presence of so many individuals of a single species in one place at one time. Cryptolithine fringes occur only at partings between beds and likely represent accumulation by winnowing.

High-diversity Pack- to Rudstone Lithofacies

This facies consists of centimeter-scale packages of articulate brachiopod and trilobite float- to rudstone separated by pelletal packstone layers of similar thickness. Brachiopod valves and trilobite sclerites oriented mainly in the hydrodynamically stable convex-up position indicate concentration by storm winnowing (Aigner, 1982). Marl layers between float and rudstone packages are much thinner (millimeters to few centimeters) than below and bioturbation is ubiquitous. Faunal diversity is very high with articulate brachiopods and trilobites the most abundant bioclasts. Ostracodes, gastropods, bivalves, lingulate brachiopods, receptaculitids, solitary corals, crinoids and cephalopods are also common.

Bryozoan Grain- to Rudstone Lithofacies

Well-washed, coarse skeletal debris occurs in 15-40 cm thick packages separated by scour surfaces. Fenestrate, branching and domal bryozoan colonies are the dominant bioclasts, although articulate brachiopods, crinoids and trilobites are also abundant and diverse. Iron staining at scour surfaces suggests frequent, brief subaerial exposure.

Crinoid Pack- to Rudstone Lithofacies

This facies defines the Welling Formation. Bioclasts are dominated by crinoid columnals with abundant articulate brachiopod shells and trilobite sclerites. Outside the margins of the aulacogen, bioclasts reach up to 9 cm in diameter. Ripple cross-lamination is common and little to no carbonate mud is preserved. Closer to the margins of the aulacogen, bioclasts become smaller (maximum 4 cm in diameter) and carbonate mud is more common. Within the basin of the aulacogen, bioclasts too small for identification make up a smaller proportion of sediment relative to carbonate mud.

STRATIGRAPHIC DISTRIBUTION OF LITHOFACIES

The Viola Group records an overall upward shallowing succession following subsidence within the Southern Oklahoma aulacogen. Basinal sections are thicker than those on the margin and consist almost exclusively of a succession of deep-water facies (outer ramp environments). All of the facies are represented on the platform, but deeper water lithofacies are relatively thin (Fig. 3; Appendix 2).

Basinal Sections (9-10 in Fig. 3; South Quarry, Burns Quarry in Appendix 2)

Viola Group sections deposited in basinal environments average 300 m in total thickness, with the Welling Formation accounting for about 20 m. The entire Viola Springs succession consists of relatively fine-grained limestone alternating with marl. The Pooleville Member of the Bromide Formation in the area of the Criner Hills is composed of sparsely to highly fossiliferous lime mudstone deposited in a subtidal environment. A shallowing-upward trend culminates in a floatstone rich in articulate brachiopods and receptaculitids at the top of the Pooleville. Contact with the overlying Viola Springs is abrupt and erosional but without significant relief.

The lower 17 m of the Viola Springs Formation consists of millimeter-scale laminae of the carbonate mudstone lithofacies. Degree of disturbance of laminae varies from faint interruptions, likely produced by rare small infauna or dewatering, to small-scale scours, ripples and more disruptive vertical bioturbation. This variation in abundance and type of sedimentary structures within the lower 17 m reflects changes in bottom oxygenation most likely due to minor fluctuations in relative sea level or severity of storm activity. An overall increase in biotur-

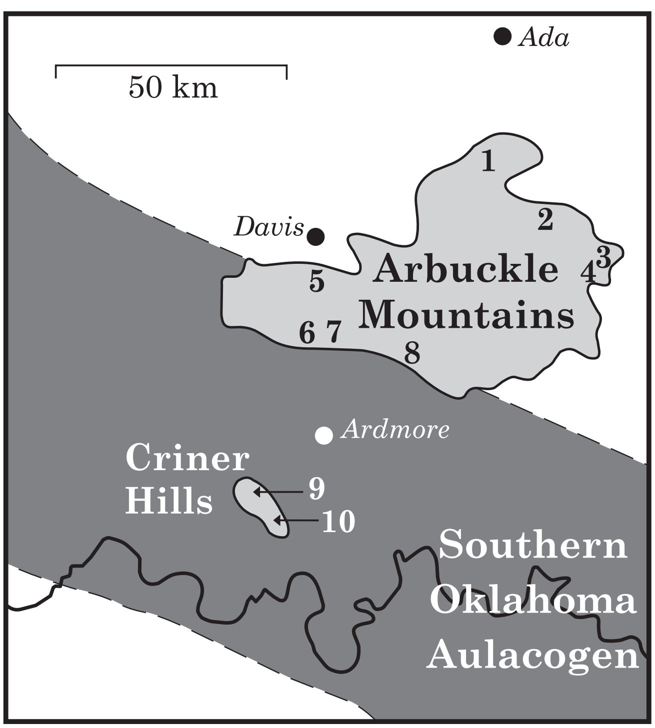

Figure 3. Viola Group collecting localities. Dark grey shading indicates inferred outline of Southern Oklahoma aulacogen in the Ordovician (see Figure 1).
1. Lawrence Quarry (LQ).
2. U.S. Highway 99 (99).
3. Mosely Creek (MC).
4. Bromide Quarry (BQ).
5. Camp Classen (CC).
6. Interstate 35 (I-35).
7. U.S. Highway 77 (77).
8. Nebo (Nebo).
9. Burns Quarry (CN).
10. South Quarry (SQ).
North arrow is in modern orientation. See Appendix 1 for locality details and Appendix 2 for stratigraphic columns.

bation upward through the section records a shallowing-upward trend. Complete burrow homogenization of carbonate mud- to wackestone by about 140 m marks the transition to the low-diversity wacke- to rudstone lithofacies. The high-diversity wacke- to rudstone and bryozoan grain- to rudstone lithofacies are absent in the basin. Exposure is limited at both sections above 192 m. The transition from the Viola Springs to the Welling Formation consists of meter-scale coarsening-upward packages of wackestone to grainstone over about a 3 m interval. This transition zone likely represents progradation of coarser debris from shallower environments during highstand.

Shelly benthic macrofossils (mainly trilobites and articulate brachiopods) are rare throughout the section. In the lower 60 m, graptolites are the only fossils preserved. Cryptolithine trilobites appear at about 60 m above the base and become more abundant up section as do sclerites of the isoteline *Anataphrus* and the remopleuridid Whittington, 1952. Articulate brachiopods and gastropods occur in low abundance in a few horizons high in the section (130-145 m).

Marginal Sections (5-8 in Fig. 3; Interstate 35, U. S. Highway 77, Nebo in Appendix 2)

The Viola Group reaches a total thickness of about 250 m at marginal sections including about 10 m of the Welling Formation. As in basinal sections, the high diversity wacke- to rudstone and bryozoan grain- to rudstone lithofacies are absent. Marginal sections shallow upward more quickly than in the basin and preserve a greater abundance of macrofossils. Limestone/marl alternations occur throughout the Viola Springs.

The Pooleville Member of the Bromide Formation also underlies the Viola Springs at sections located near the margins of the aulacogen. Moderately large (8 cm diameter) receptaculitids and solitary rugose corals are common just below the contact. A low relief erosional surface marks the contact with the Viola Springs and is topped by a thin (<1 cm) iron- and phosphate-rich layer. Overlying this is a 2 m interval consisting of rippled, ostracod-rich wacke- to packstone assigned to the Viola Springs. At about 2 m, a thin (2 cm) layer of pyrite nodules on a phosphate crust marks a transition to very dark colored, millimeter-scale laminated carbonate mudstone. Limited bioturbation at 30 m signals increased oxygenation and graptolites are more common as accumulations at partings. The low-diversity wacke- to rudstone lithofacies at marginal sections begins at 75 m where *Chondrites* becomes so abundant as to nearly obscure layers. Poorly defined, meter-scale shallowing-upward packages contain laminated beds that grade upward into increasingly bioturbated beds. Shallowing-upward packages are more distinct by 180 m, where they are also slightly coarser, shallowing from wacke- to grainstone.

Contact with the Welling Formation is gradational over about a 1 m interval. Firm grounds developed at the surface of Viola Springs wackestone are succeeded by grainstone of the Welling Formation. Welling lithology at marginal localities combines elements characteristic of both the basin and the platform. The matrix resembles the well-washed grainstone of the basin, but very large (up to 8 cm) trilobite bioclasts are more similar to those preserved on the platform.

Diversity and abundance of shelly benthic organisms is higher than in basinal sections. The carbonate mudstone lithofacies contains graptolites and rare cryptolithines as well as *Pugilator deckeri* Cooper, 1953, which is abundant at some horizons. Isotelines appear at 48 m and become more abundant upward in the section. At about 180 m, *Anataphrus* occurs in high abundance forming dense accumulations of monotaxic float- to rudstone.

Platform Sections (1-4 in Fig. 3; Lawrence Quarry and U. S. Highway 99 in Appendix 2)

A complete Viola Group section was not accessible outside the aulacogen. Total thickness as measured from wells ranges from 90-110 m with 15-25 m of Welling (Puckette and others, 2000; API Well #12300123; API Well #12370042; #1 Cummings Well, NRIS Well Database). All lithofacies are present on the platform with those representing outer ramp environments thinnest.

The contact between peritidal carbonates of the Corbin Ranch Submember (Amsden and Sweet, 1983) at the top of the Bromide, and the Viola Springs is erosional with up to 8 cm of relief. The laminated carbonate mudstone facies overlies the contact and contains abundant graptolite fragments oriented parallel to bedding. Laminae are completely obscured by bioturbation within 0.5 m of the contact, and the entire facies is only 1.5 m thick. *Isotelus* is present in the carbonate mudstone facies in addition to cryptolithines and graptolites.

Calcareous macrofossils are limited to cryptolithine and isoteline trilobites in the low-diversity wacke- to rudstone facies, which extends from 1.5-13 m above the Bromide. Planar-bedded float- to rudstone between 18 m and 23 m grades upward into the bryozoan grain- to rudstone facies. Oxidized iron at some hardground surfaces may have formed during periods of subaerial exposure.

The high-diversity wacke- to rudstone lithofacies is present only at platform localities and is at least 30 m thick. Trilobite and articulate brachiopod pavements are separated by finer pelletal wacke- to packstone layers. Trilobite biostratigraphy allows correlation to a similar lithofacies at the LQ locality (see next section for details). Higher wackestone content at the LQ locality is responsible for formation of more distinct limestone/marl alternations, although they are not as well developed as in marginal and basinal settings. Contact between the high-diversity wacke- to rudstone facies and the Welling is gradational over 0.5 m. The Welling Formation on the platform is a coarse-grained, well-washed rudstone consisting mainly of crinoidal debris with abundant large articulate brachiopod and trilobite clasts and is similar in lithology to the Welling Formation in northeastern Oklahoma (Amsden and Sweet, 1983).

Platform sections contain the greatest diversity of organisms, and trilobite diversity and abundance are highest in the high-diversity wacke- to rudstone lithofacies. The bryozoan grain- to rudstone has lower trilobite diversity but the greatest abundance. Trilobite diversity and abundance are high in the Welling but lower than in the upper Viola Springs.

STRATIGRAPHIC DISTRIBUTION OF ISOTELINES

Lithofacies of the Viola Group record changing environmental conditions along a depth gradient from the platform into the basin. Each lithofacies preserves a unique trilobite assemblage reflecting the community inhabiting that environment (Amati and Westrop, 2006). Some trilobite genera apparently were not restricted by narrow environmental tolerances and occur in multiple lithofacies. These genera can be used to correlate different but contemporaneous habitats. Trilobites provide biostratigraphic data from shallow subtidal to peritidal environments where graptolites are rare to absent. In anaerobic zones, however, graptolites must be used instead of trilobites.

Isoteline trilobites inhabited the greatest range of environments in the Viola Group. In units deposited below storm wave base, a greater abundance of cryptolithine trilobites makes them more useful for correlation, but isotelines provide higher resolution at shallower paleo-depths. *Stegnopsis wellingensis* and *Anataphrus kermiti* (new species described herein) dominate the fauna in the low-diversity wacke- to rudstone lithofacies of the Viola Springs Formation in marginal and basinal settings. Both of these species also occur in high numbers in the crinoidal grain- to rudstone lithofacies of the Welling Formation on the platform, and thus permit correlation across lithofacies boundaries.

Trilobite assemblages defined for each lithofacies can be used for correlation with assemblages from similar environments in other parts of Laurentia. Trilobite occurrences in the Viola Group are proving to be useful for correlating western Laurentia (northwest Canada, western U.S.) with central and eastern Laurentia (Trenton Group and equivalents). *Isotelus bradleyi* (new species) is very similar to *I. parvirugosus* Chatterton and Ludvigsen, 1976, from the Esbataottine Formation in the Mackenzie Mountains. *Isotelus violaensis* (new species) bears a strong resemblance to *I. copenhagenensis* Ross and Shaw, 1972, of the Copenhagen Formation in Nevada and *I. dorycephalus* Hunda and others, 2003, from the Whittaker Formation in the Mackenzie Mountains. Also from the Whittaker Formation, *A. elevatus* Hunda and others, 2003, is very similar to *A. kermiti* described herein from the Viola Group. These provide a biogeographic, and therefore biostratigraphic, connection between western and central Laurentia.

Correlations between south-central and north-central Laurentia are stronger. *Isotelus kimmswickensis* Bradley, 1930, originally described from the Kimmswick Formation in Missouri and Illinois, is also present in the Viola Group. *Ectenaspis* has been described from Iowa (the type, *E. beckeri* Slocom, 1913, from the Maquoketa Formation), southern Manitoba (*Ectenaspis* sp. Westrop and Ludvigsen, 1983) and now from Oklahoma (*E. burkhalteri*, new species).

The Trenton Group shares *I. walcotti* with a close relative in the Viola Group. An additional connection between central and eastern Laurentia is made using *Stegnopsis*, which has only been reported from Newfoundland (*S. solitarius* Whittington, 1965) and New York (*I. harrisi* Raymond, 1905—reassigned to *Stegnopsis* herein). Although data from these few species are weak, this study demonstrates the potential for greater correlation using trilobite faunas from Oklahoma.

SYSTEMATIC PALEONTOLOGY

Eleven species of isoteline trilobites from the Viola Group are assigned to four genera. Eight species are new, and all species are described and illustrated. All figured specimens of new species are stored at the Oklahoma Museum of Natural History (OU). Several specimens from the Field Museum, Chicago (P, UC) are refigured herein.

Most specimens were blackened with ink and then whitened with ammonium chloride prior to being photographed. Borrowed specimens that were not already blackened were not altered (ex. Pl. 2, Fig. 5). I cast external molds using black latex.

A locality map is provided as Figure 3. Abbreviations for locality and horizon information are detailed in Table 1.

Additional material of *I. kimmswickensis* is figured both from the Viola Group of Oklahoma and the Kimmswick Limestone of Missouri. Material from Missouri figured herein is from an active quarry operated by Holcim (US) Inc., located near the town of Clarksville, about 95 km northwest of St. Louis near the Mississippi River.

Order Asaphida Burmeister, 1843

Suborder Asaphina Salter, 1864

Family Asaphidae Burmeister, 1843

Subfamily Isotelinae Angelin, 1854

Discussion.—Current concepts of the Asaphidae go back to Jaanusson (in Moore, 1959), with a more recent emendation by Fortey (1980), who focused on features of the glabella. According to Fortey, incorporation of bacculae from the fixigenae into the glabella during the ontogeny of asaphines is an apomorphy, making the isoteline glabella plesiomorphic. But Fortey also points out that bacculae are present, and not uncommon, in asaphids outside the Asaphinae, making it a plesiomorphic feature. Some well-preserved specimens of isotelines including *Isotelus*, *Stegnopsis* and *Anataphrus*, possess bacculae on the fixigenae as meraspids (see *Isotelus gigas* Raymond, 1914, pl. 1, fig. 1; *Stegnopsis erythragora*, Pl. 18, Figs. 4a, 4c, Pl. 19, Figs. 5a-b; *Anataphrus kermiti*, Pl. 30, Fig. 1a). A major revision of the Asaphidae using through a cladistic analysis may therefore show that loss of the bacculae in late meraspid and holaspid isotelines is an apomorphy.

A major revision of the Asaphidae is long overdue, and this paper is intended as a first step towards that goal. Before relationships within the Isotelinae can be fully understood, the concepts of its constituent genera need to be better delimited. Rudkin and Tripp (1989) redescribed and reillustrated type material of *I. gigas* (the type species of the genus) and *I. walcotti*. In this paper, I describe three new species of *Isotelus* and discuss the relationships of *Isotelus*, *Ectenaspis*, *Stegnopsis* and *Anataphrus* with their presumed close relatives. For all characters discussed in the following sections, the plesiomorphic condition was determined based on comparison with asaphines such as *Asaphus* Brongniart, 1822, *Ogyginus* Raymond, 1912, and *Megistaspis* Jaanusson, 1956, and niobines like *Niobe* Angelin, 1851, and *Golasaphus* Shergold, 1971. Among closely related genera, states in *Isoteloides* Raymond, 1910a, were also used to polarize characters, as were ontogenetic data, where available.

Genus *Isotelus* Dekay, 1824

Type species.— *Isotelus gigas* Dekay, 1824

Discussion.—*Isotelus* and *Ectenaspis* share derived features that suggest they form a monophyletic group. The pygidium is triangular in outline with lateral margins that converge toward the posterior and length (sag.) that is greater relative to width (tr.) than in

Table 1
Abbreviations for Locality and Horizon Information

Lawrence Quarry (LQ)	undifferentiated Viola Springs Fm. undifferentiated Welling Fm.	LQ-VS LQ-WF
Highway 99 (99)	Viola Springs X m above Bromide Fm.	99-X
Mosely Creek (MC)	stratigraphic info. not available	MC
Bromide Quarry (BQ)	pavement at quarry floor Viola Springs X m above pavement	BQ-Pave BQ-X
Camp Classen (CC)	single horizon near top of Viola Springs	CC
Interstate Highway 35 (I-35)	Viola Springs X m above Bromide Fm. Welling Fm. X m above Bromide Fm.	I-35-X I-35-X
U.S. Highway 77 (77)	Viola Springs X m above Bromide Fm. Welling Fm. X m above Bromide Fm.	77-X 77-X
Burns Quarry (Criner North) (CN)	Viola Springs X m above Bromide Fm.	CN-X
South Quarry (Criner South) (SQ)	Viola Springs X m above Bromide Fm.	SQ-X
Nebo (Nebo)	Viola Springs X m above Bromide Fm. undifferentiated Welling Fm.	Nebo-X Nebo-Well

other closely related isotelines. The frontal region is long (sag.), and effacement of both the cranidium and pygidium is greater than in *Isoteloides*. Also unlike *Isoteloides*, the glabella expands in front of the palpebral lobes. *Ectenaspis* is a derived group defined by hyper-elongate eye-stalks and a frontal region that tapers into a dorsally curving proboscis-like extension. Elongation of the pygidium is developed to a greater degree than in *Isotelus*, and long, thin genal spines are retained in large holaspids. It is possible that recognition of a monophyletic, derived *Ectenaspis* will make *Isotelus* paraphyletic, but until a phylogenetic analysis has been performed, it is best that they are retained as separate genera. *Trigonocerca* Ross, 1951, and *Trigonocercella* Hintze, 1952, are similar to *Isotelus* and *Ectenaspis* especially in the outline of the cranidium and pygidium. Both have an apomorphic posterior extension of the pygidium, but the hypostome of *Trigonocercella* retains sharp lateral extensions of the middle body present in meraspids of other isotelines such as *Anataphrus*. This suggests that the elongate pygidium was independently derived.

Species of *Isotelus* discussed below fall into two, presently informal, groups based on the course of the facial sutures in front of the palpebral lobes. In Group I, the facial sutures are roughly parallel in front of the palpebral lobes until angling inward to intersect at the mid-line. *Isotelus gigas*, *I. copenhagenensis*, *I. kimmswickensis*, *I. homalonotoides* Walcott, 1877, and *I. violaensis* new species belong to this group. Based on a comparison with the course of the facial sutures in asaphines, this group is apomorphic. In Group II, the cranidium narrows strongly immediately in front of the palpebral lobes and widens gradually as the facial sutures curve gently forward and outward; the widest point of the cranidium in front of the palpebral lobes is at the inflection point where the facial sutures turn to become directed inward to the mid-line. This facial suture pattern, also present in *Isoteloides*, appears to be plesiomorphic and is found in *I. parvirugosus*, *I. dorycephalus*, *I. iowensis* Owen, 1852, *I. walcotti*, *I. giselae* Tripp and Evitt, 1986, *I. bradleyi* new species and *I. skapaneidos* new species.

A third group of species currently assigned to *Isotelus* shows the plesiomorphic anterior suture pattern of Group II *Isotelus* but these taxa are also very wide (tr.) relative to length (sag.) and have short (sag.), rounded pygidia with broad borders. This group consists of: *I. latus* Raymond, 1913, *I. ottawaensis* Wilson, 1947, *I. maximus* Locke, 1838, *I. rex* Rudkin and others, 2003, and possibly *I. platycephalus* Stokes, 1824. It is likely that a phylogenetic analysis will produce a clade including *Isotelus* and *Ectenaspis* that is defined by a pygidium that tapers strongly posteriorly. The latter group of species, those with broad, rounded pygidia bearing wide borders, should be excluded from the clade and I will refer to them as *"Isotelus"*.

Isotelus kimmswickensis Bradley, 1930

1930. *Isoteloides kimmswickensis*, Bradley, pl. 27, figs. 1, 2, 11.

not 1930. *Isoteloides kimmswickensis*, Bradley, pl. 27, figs. 3, 4.

not 1930. *Isoteloides* cf. *kimmswickensis*, Bradley, pl. 27, figs. 5-7.

Pls. 1-2; Pl. 3, Figs. 1-5

Type Material.—Holotype (UC28851A), incomplete internal mold of cranidium; Paratype (UC28851B), second incomplete internal mold of cranidium from same rock specimen; Paratype (UC28851C), incomplete internal mold of pygidium from same rock specimen; Paratype (UC28853), nearly complete but exfoliated pygidium; Paratype (UC28855), broken and exfoliated pygidium. Two additional specimens, UC28854, a cranidium preserving a portion of exoskeleton on the right posterior fixigena and UC28851D, an exfoliated librigena are listed by Bradley as paratypes but are more similar to *I. bradleyi*, new species and are figured on Plate 7 as *Isotelus* cf. *I. bradleyi*. Additional material from the Viola Group is also figured.

Stratigraphic Occurrence.—Type material is from the Upper Ordovician Kimmswick Limestone in Glen Park, Missouri. Additional figured material is from the Upper Ordovician Viola Springs Formation of Oklahoma (U. S. Highway 99: 99-20 to 99-36) (Appendix 2).

Diagnosis.—A species of *Isotelus* with very short (sag.) cranidium, only slightly longer than maximum width (tr.) in front of palpebral lobes. Facial sutures with only slight inflection in front of palpebral lobes then nearly parallel. Pygidium with long border, longest directly behind axis.

Description.—Cranidium only slightly longer (sag.) than wide (tr.), maximum width in front of palpebral lobes about 90% of length. Longitudinal convexity low over posterior three quarters, then slopes steeply down to frontal area. Transverse convexity low. Axial furrows shallow and broad, directed slightly inward from posterior margin to level of palpebral lobes; directed laterally for approximately one half distance in front of palpebral lobes creating "waisted" shape to glabella. Axial furrows curve inward to become preglabellar furrow. Anterior margin of glabella rounded. Occipital furrow effaced dorsally, seen faintly on internal molds (Pl. 1, Figs. 3c, 4a, 6a, 8). Occipital ring longer (sag.) medially, expressed as thin band lacking ornament. S1 distinct on some internal molds, most obvious in smaller individuals (Pl. 1, Figs. 3c, 4a). Median preoccipital tubercle located at front edge of occipital furrow, behind posterior margin of palpebral lobes, visible on internal molds, not expressed on dorsal surface of exoskeleton. Maximum width of glabella half that of posterior margin of cranidium. Palpebral regions of fixigenae taper upward into eyestalks. Palpebral lobes wider (tr.) than long (sag.), located at one third total length (sag.) in front of posterior margin, elevated slightly above maximum height of cranidium. Palpebral furrow visible on internal molds (Pl. 1, Fig. 7). Anterior branch of facial suture inflected weakly inward for very short distance then runs directly forward in front of palpebral lobe before curving gently inward toward sagittal line at angle of 50° to horizontal. Sutures form strong, anteriorly directed point at intersection (Pl. 1, Fig. 4a); facial sutures do not converge as strongly as preglabellar furrow so frontal area longest exsagittally, length (sag.) of frontal area about 15% total length. Fixigenae in front of palpebral lobes wider (tr.) than in *Isotelus* of Group II because sutures directed forward rather than inward. Posterior branch of facial suture directed toward posterior at nearly 45° to posterior margin then curving abruptly backward to join posterior margin. Posterior margin of cranidium transverse then directed backward at lateral extremity. Termination of posterior portion of fixigena rounded and deflected backward. Posterior border furrow deeply impressed, closer to posterior margin abaxially. Surface of exoskeleton where preserved without ornament (Pl. 1, Figs. 2a, 5).

Librigenae subtriangular in outline, without genal spines in moderately large holaspids; widest (tr.) point just behind eye. Posterior margin of librigena straight, directed backward. Genal angle sharp. Gena tapers anteriorly, inner margin converges on lateral margin just in front of eye. Lateral margin gently rounded; inner margin gently incised. Dorsal surface of librigena slopes gently down to lateral margin. Posterior border furrow visible on internal molds, continues from fixigena on to librigena, still deeply impressed, fades at about one half lateral distance across librigena. Lateral border absent. Eye socle furrow well-developed. No ornamentation on small portions of exoskeleton preserved. Visual surface tall, tapering upward, placed on short stalk, directed slightly outward.

Hypostome longer (sag.) than wide (tr.), width less than about 90% of length. Maculae well developed. Anterior lobe of median body weakly inflated, outlined by furrows running from midline at intersection of forks to maculae. Inflation of posterior lobe weaker than that of anterior lobe. Lateral margins of posterior lobe bowed strongly outward then angled inward to tips of forks. Posterior incision into hypostome about 1/3 total length (sag.) from posterior margin; inner margins of forks gently inclined toward midline; posterior terminations of forks sharp, intersection of forks at front of posterior lobe gently rounded. Terrace ridges weak, only preserved on small portion of one fork. Thorax unknown.

Pygidium subtriangular especially in large holaspids, width (tr.) only slightly greater than length (sag.), height approximately one half of length. Facets prominent. Axial furrows weak except on internal molds; pleural furrows visible on small holaspids and well-preserved internal molds of larger individuals (Pl. 2, Fig. 2b, 4c; Pl. 3, Fig. 5). Pleural furrow of first segment deeply impressed. Articulating half ring visible on some internal molds (Pl. 3, Fig. 5), axial rings very weak. Pleural regions slope gently, become abruptly much steeper just before lateral margin. Border furrow very shallow, arising at approximately one-third distance from anterior margin, running very close to lateral margin for most of length; longer behind posterior point of pygidium producing a short platform behind termination of axis.

Ornament of faint, wide, shallow pits (Pl. 3, Fig. 4b).

Ontogeny.—Smallest cranidium (OU11764; Pl. 1, Fig. 3) 4.5 mm long (sag.). Length (sag.) of frontal area decreases through ontogeny; length (sag.) in smallest cranidium 22% total length vs. 15% in largest cranidium (Pl. 1, Fig. 8). S1 broad, deep on internal molds, becomes effaced through development, weakly distinguishable on largest specimens (Pl. 1, Fig. 6a, 8b). Anterior facial sutures curve around maximum glabellar width in front of palpebral lobes; become less curved, more parallel in larger individuals. Smallest pygidium (OU11771; Pl. 2, Fig. 2) 3.0 mm long (sag.). Length (sag.) just under 60% width (tr.), pygidial outline only weakly triangular; length increases greatly through ontogeny to about 80% relative to width, outline becomes more triangular. Lateral border of pygidium with uniform width in smaller individuals, becoming effaced laterally and more elongate behind axis. Pleural furrows increasingly effaced with size. Axial furrows become broader.

Discussion.—Among species of Group I, *I. kimmswickensis* resembles *I. copenhagenensis* mainly in the course of the facial sutures and axial furrows (Ross and Shaw, 1972, pl. 2, figs. 4, 8, pl. 3, fig. 1). The anterior facial sutures in the former approach the mid-line at a lower angle (near 45°) than in *I. copenhagenensis* (approximately 60°). The pygidium of *I. copenhagenensis* (Ross and Shaw, 1972, pl. 2, figs. 6, 10) is shorter (sag.) and wider (tr.) than in *I. kimmswickensis* and the posterior border continues forward for a greater distance. In *I. gigas*, the facial sutures in front of the palpebral lobes are directed strongly inward for a short distance (Rudkin and Tripp, 1989, fig. 1.1). The cranidium of *I. gigas* is longer than wide while the cranidial dimensions of *I. kimmswickensis* are nearly equal. The posterior border of the pygidium in *I. gigas* is more uniform in width while that of *I. kimmswickensis* is much longer immediately behind the axis.

Isotelus violaensis, new species

?1987. *Isotelus homalonotoides* (Walcott, 1877) in DeMott, pl. 3, figs. 21-26.

Pl. 3, Figs. 6-8, Pl. 4, Pl. 5, Figs. 1-3, ?4

Etymology.—This species is very similar to *I. kimmswickensis* and is named for the correlative Viola Springs from which it comes.

Type Material.—Holotype (OU11782), exfoliated cranidium; Paratype (OU11781) small, partly exfoliated cranidium; Paratypes (OU11783, OU11788), two partial, mostly exfoliated cranidia; Paratypes (OU11784, OU11785), two external molds (photographed as latex casts); Paratypes (OU11786, OU11787, OU11789, OU11791), four pygidia of various sizes; Paratype (OU11790), internal mold of a librigena; Paratype (OU11792), hypostome.

Stratigraphic Occurrence.—The type material is from the Upper Ordovician Viola Springs Formation of Oklahoma (U. S. Highway 99: 99-39 to 99-49) (Appendix 2).

Diagnosis.—A species of *Isotelus* with facial sutures that diverge only slightly and for short distance in front of palpebral lobes then run nearly parallel until converge to mid-line. Frontal area very long (sag.), length about 20% total length of cranidium. Eye-stalks tall, extend well above maximum height of glabella. Lateral border of pygidium strongest over posterior 1/3 of pygidium, becomes much wider directly behind axis.

Description.—Very similar to *I. kimmswickensis* except for the features described below. Cranidium longer (sag.) than wide (tr.), maximum width in front of palpebral lobes just under 80% of length. Eye-stalks directed upward at steeper angle, reaching greater elevation above maximum height of cranidium, directed slightly backward (Pl. 4, Fig. 1). Frontal area longest exsagittally, relatively longer than in *I. kimmswickensis* (20% vs. 15% total length of cranidium). Palpebral furrow not preserved. Anterior branch of facial suture runs generally forward with slight adaxial deflection for short distance followed by slight abaxial deflection in front of palpebral lobe. Angle of convergence of facial sutures slightly higher than in *I. kimmswickensis*. Posterior portions of fixigenae taper more sharply than in *I. kimmswickensis*, deflected backward more sharply (Pl. 3, Figs. 6, 7a; Pl. 4, Fig. 5a). Dorsal exoskeleton virtually without ornament; faint pitting observable under magnification.

Librigenae as in *I. kimmswickensis* except slightly wider (tr.) and with taller eyestalk. Thorax unknown. Isoteline hypostome from same collection (Pl. 5, Fig. 4) assigned to this species. Anterior lobe of middle body shorter (sag.) than in *I. kimmswickensis*; forks more widely separated.

Pygidium very similar to *I. kimmswickensis* except: height lower; greater effacement of axial rings and pleural furrows on internal molds; border furrow of pygidium longer (sag.) behind axis. Exoskeleton without ornament (Pl. 5, Fig. 3b).

Ontogeny.— Smallest cranidium (OU11781; Pl. 3, Fig. 6) 6.9 mm long (sag.). Length (sag.) of frontal area becomes longer through ontogeny; maximum width of cranidium increases. Occipital and S1 furrows visible on internal molds of small individuals become effaced with growth, obsolete in most large individuals. Smallest pygidium (OU11786, Pl. 4, Fig. 3) 3.7 mm long (sag.). Ratio of length (sag.) to width (tr.) increases through ontogeny; triangular outline of pygidium becomes more pronounced. Well-developed lateral border furrow becomes effaced laterally, more elongate behind axis. Lateral margins in small specimens straight but curve inward toward posterior margin of axis in larger individuals. Effacement of axial and pleural furrows increases with size.

Discussion.—Of other Group I species, *I. violaensis* is most similar to *I. kimmswickensis*; differences are described above. *Isotelus violaensis* differs from *I. copenhagenensis* in that the pygidium of the former tapers more strongly toward the posterior and the angle of the anterior branch of the facial sutures to the sagittal line is higher (45° in *I. violaensis* versus 30° in *I. copenhagenensis*). The facial sutures of *I. violaensis* follow a similar course to those of *I. gigas* (see Rudkin and Tripp, 1989, Fig. 1) but are initially directed inward to a lesser degree in front of the palpebral lobes and the cranidium of *I. violaensis* has a lower convexity than *I. gigas*. The cranidium of *I. violaensis* is longer (width just under 80% length) than *I. kimmswickensis* (width about 90% length) but shorter than *I. gigas* (width about 65% length). The lateral portions of the posterior fixigenae taper more strongly than in either *I. kimmswickensis* or *I. gigas* and are directed backward more strongly. The posterior border of the pygidium in *I. violaensis* is wider than in *I. gigas*, especially behind the axis. The pygidium of *I. dorycephalus* is very similar to that of *I. vio-*

laensis but the cranidium of the former is of Group II type.

The pygidium of *I. homalonotoides* (Pl. 5, Fig. 6) is very similar to that of *I. violaensis*. In *I. homalonotoides*, the posterior border is slightly longer (exsag.) and maintains a uniform width to the articulating facet while the border of *I. violaensis* becomes effaced anteriorly (Pl. 5, Fig. 1a). The anterior border of the cranidium of *I. homalonotoides* is longer (exsag.) than in *I. violaensis* (Pl. 5, Fig. 5) and weak S1 glabellar furrows are retained on the internal mold of a relatively large individual.

Isotelus bradleyi, new species

?1930. *Isoteloides kimmswickensis*, Bradley, pl. 27, figs. 3, 4.

Pl. 6, Pl. 7, Figs. 1-3, Pl. 8, Figs. 1-3

Etymology.—Named in honor of J. H. Bradley, Jr.

Type Material.—Holotype (OU11796), small, mostly exfoliated cranidium missing one posterior fixigena and palpebral lobe; Paratype (OU11793), exterior mold of small cranidium (latex cast photographed); Paratypes (OU11794, OU11795, OU11797, OU11801), four small cranidia; Paratype (OU11798) exterior mold of cranidium missing the posterior fixigenae (latex cast photographed); Paratype (OU11800), external mold of cranidium showing ornament on dorsal surface, Paratype (OU11803), cranidium with distinct glabellar furrows; Paratype ()OU11799), exfoliated librigena; Paratype (OU11802), partly exfoliated librigena with visual surface preserved; Paratypes (OU11804, OU11805), two exfoliated pygidia; Paratype (OU11806), external mold of partial pygidium showing ornament of exoskeleton.

Stratigraphic Occurrence.—Type material is from the Upper Ordovician Viola Springs Formation (U. S. Highway 99: 99-08 to 99-33) of Oklahoma (Appendix 2).

Diagnosis.—A species of *Isotelus* with anterior branches of facial sutures directed inward in front of palpebral lobes then curving outward so that lateral margins of cranidium in front of palpebral lobes strongly sinuous. Anterior branches of facial sutures curve abruptly forward just before intersecting making anterior margin of cranidium sharply pointed. Ornament of coarse pits. Pygidium subtriangular but short (sag.) for genus and without border furrow.

Description.—Longitudinal convexity of glabella low; glabella nearly flat over posterior 3/4 of cranidium then slopes steeply down to anterior margin. Axial and preglabellar furrows weak, expressed mainly as change in convexity from glabella to fixigenae and frontal area. Axial furrows directed weakly adaxially from posterior margin to level of palpebral lobes, directed strongly laterally in front of palpebral lobes to widest margin of cranidium at half distance from palpebral lobes to front of cranidium. Preglabellar furrow arched, making front of glabella rounded. Occipital furrow very weak, only visible on some internal molds; very near posterior border abaxially, longer sagittally. Glabellar furrows S1, S2 and S3 visible to varying degrees on internal molds of some specimens (Pl. 6, Figs. 1, 2a, 4b, 5a; Pl. 7, Fig. 3c). Median tubercle visible on internal molds, positioned slightly in front of occipital furrow, behind posterior margin of palpebral lobes. Width (tr.) of glabella approximately half width (tr.) of posterior margin of cranidium. Fixigenae taper upward into eye-stalks. Eye-stalks positioned 1/3 total length (sag.) of cranidium in front of posterior margin, angle sharply upward above cranidium. Palbebral lobes oriented horizontally; length (sag.) moderate, nearly equal to width (tr.). Palpebral furrow weak (Pl. 6, Fig. 6); termination of palpebral lobe evenly rounded. Facial suture directed strongly inward just in front of palpebral lobe then curving anterolaterally, making lateral margin of cranidium distinctly sinuous in front of palpebral lobe. Maximum width (tr.) of cranidium in front of palpebral lobes located at about 2/3 distance from posterior margin. From widest point, facial sutures converge at 60° then curve abruptly forward just before intersecting at sagittal line. Sutures sub-parallel to preglabellar furrow until diverging forward just before intersecting, creating frontal area that is longer sagittally than exsagittally. Posterior branch of facial suture directed posterolaterally to point at about twice width (tr.) of eye-stalk then directed backward to intersect with posterior margin. Posterior margin of cranidium directed slightly backward from level of palpebral lobes so that terminations of posterior fixigenae curved slightly backward at lateral extremity. Weak posterior border furrow visible on some internal molds (Pl. 7, Fig. 1a, 3c), placed very near posterior border, positioned horizontally, becomes effaced abaxially. Ornament of densely packed, coarse pits (Pl. 6, Fig. 8; Pl. 7, Fig. 1c). Weak sagittal ridge on internal molds arises at level of S2, continues to anterior margin of glabella (Pl. 6, Fig. 5a, 6).

Librigenae without genal spines in moderately small holaspids; unknown for smaller holaspids or meraspids. Posterior margin directed only slightly backward. Genal angle sharp. Lateral margin strongly convex; widest point just behind eye. Facial suture in front of eye directed strongly laterally then curves to run anteromedially. Dorsal surface of gena gently convex. Eye socle furrow wide, shallow. Visual surface tall, directed slightly laterally from dorsal surface of gena. Posterior border furrow visible on internal molds; shallow, becomes effaced at 1/2 distance to lateral margin. Border furrow effaced. Ornament not preserved. Hypostome and thorax unknown.

Pygidium subtriangular, relatively short for genus with length (sag.) approximately 75% of width (tr.). Inflation moderate, height about 60% of length. Dorsal surface of pygidium slopes gently away from anteromedian for 3/4 distance, then slopes more steeply to lateral and posterior margins. Articulating facets prominent. Pleural furrows of first segment deeply impressed. Axial and pleural furrows weakly impressed on internal molds. Border furrow absent. Ornament of densely packed, medium-sized pits.

Ontogeny.—Smallest well-preserved cranidium (OU11794; Pl. 6, Fig. 2) 5.3 mm long (sag.). Length (sag.) of frontal area decreases through ontogeny, shape retained. S1 furrows generally more effaced with greater size with rare exceptions (Pl. 7, Fig. 3). Very fine, shallow pits increase in size and depth with growth. Small pygidia not known.

Discussion.—Among Group II species, *I. bradleyi* most closely resembles *I. parvirugosus*, especially in cranidial characters. The frontal area of *I. bradleyi* is much longer sagittally than exsagittally instead of only slightly longer. The angle of convergence of the anterior facial sutures is higher in *I. bradleyi* than in *I. parvirugosus*. In *I. bradleyi*, the longitudinal convexity is lower, especially over the posterior 3/4 of the cranidium and the eye-stalks are slightly less elevated. The pygidia of *I. bradleyi* and *I. parvirugosus* are similar in outline, but a posterior border is present in the latter. *Isotelus bradleyi* has an ornament of coarse pits and lacks genal spines in holaspids. *Isotelus dorycephalus* has a much longer border, both on the cranidium and pygidium. The cranidial outline of *I. giselae* is similar to *I. bradleyi*, but the posterior fixigenae of the former are longer (exsag.) and wider (tr.). The holaspid pygidium of *I. giselae* is unknown. The cranidium and librigenae of *Isotelus* cf. *I. harrisi* Raymond, 1905, figured by Tremblay and Westrop, 1991, (fig. 9.10-9.14) are very like *I. bradleyi*, but the facial sutures of the latter converge at a lower angle. *Isotelus instabilis* Reed, 1904, has a similar cranidial outline and lacks genal spines, but details of the anterior border aren't clear in the illustrations.

Bradley (1930) figured material of an isoteline similar to *I. bradleyi*, but attributed it to *I. gigas* (Pl. 7, Fig. 4) and *I. kimmswickensis* (Pl. 7, Fig. 5). I include it here under *Isotelus* cf. *I. bradleyi*. The assignment of Bradley's librigena is more tentative because it has a wide, shallow border furrow that is not present in the specimens from the Viola Group.

Isotelus skapaneidos, new species

Pl. 8, Figs. 4, 5; Pls. 9, 10; Pl. 11, Figs. 1, 2; Pl. 12, Fig. 1?

Etymology.—The outline of the cranidium is in the form of a spade or shovel.

Type Material.—Holotype (OU11809), partly exfoliated cranidium; Paratype (OU11811), nearly complete cranidium with left librigena; Paratypes (OU11810, OU11814, OU11816, OU11817), four cranidia; Paratype (OU11813), nearly complete, weathered individual; Paratype (OU11815), cranidial doublure with parts of both librigenae attached; Paratypes (OU11808, OU11812, OU11807), two large pygidia and one small pygidium.

Stratigraphic Occurrence.—The type material is from the Upper Ordovician Viola Springs (U. S. Highway 77: 77-202 to 77-216; Burns Quarry: CN-float) and Welling formations (Lawrence Quarry: LQ-WF) (Appendix 2).

Diagnosis.—A species of *Isotelus* with sharply pointed frontal area of cranidium; length (sag.) of frontal area about 25% total length of cranidium. Posterior portion of fixigenae long (exsag.), deflected sharply backward. Pygidium highly inflated.

Description.—Glabella very weakly convex over 3/4 of length from posterior margin then slopes sharply down to frontal area; transverse convexity stronger. Axial, preglabellar furrows shallow and wide. Behind palpebral lobes, axial furrows very faint, directed slightly adaxially; parallel lateral to palpebral lobes; directed abaxially in front of palpebral lobes then curve sharply toward center to become preglabellar furrow. Anterior margin of glabella rounded. Occipital furrow effaced, glabellar furrows faintly visible on one specimen (Pl. 11, Fig. 1a). Median pre-occipital tubercle not expressed on only exfoliated specimen. Glabellar width more than 1/2 total width of posterior margin of cranidium. Palpebral lobes at approximately 1/4 total length in front of posterior margin. Palpebral region of fixigena tapers long (exsag.) axially then tapers over short distance to become short (exsag.) at rounded terminus. Palpebral lobes oriented horizontally just below maximum height of glabella (Pl. 9, Fig. 3b; Pl. 10, Fig. 2c). Palpebral furrow not preserved. Length (exsag.) of palpebral lobes greater than width (tr.); terminations evenly rounded. Facial suture directed inward in front of palpebral lobe, then deflected gradually outward to form long (exsag.) embayment in lateral margin of cranidium. Suture curves inward at about 60% length of cranidium, continues toward sagittal line at high angle (about 40° from horizontal). Sutures parallel axial furrows from level of palpebral lobes to maximum glabellar width then diverge from preglabellar furrow to meet at mid-line forming long frontal area. Posterior branch of facial suture directed abaxially and backward for 2/3 length then directed abruptly backward to intersect posterior margin. Posterior margin of cranidium curved outward behind glabella, curved inward behind axial furrows and posterior portion of fixigenae. Fixigena behind palpebral lobe tapered laterally and directed backward. Posterior border furrow absent. Dorsal surface of exoskeleton without ornament.

Librigenae subrectangular in outline, without genal spines in moderately large holaspids. Posterior margin straight, directed backward. Genal angle sharp. Widest (tr.) point just behind eye. Gena tapers anteriorly, inner margin converges strongly on lateral margin in front of eye. Lateral margin gently rounded. Dorsal surface of librigena convex. Posterior border furrow absent. Lateral border furrow arises just in front of posterior margin, widenes (tr.) gradually forward to widest (tr.) point in front of eye. Thin (tr.) anterior portion of gena adjacent to frontal area nearly flat. Visual surface short (d-v), but more than 180° in circumference. Librigena without ornament. Ventral portion of librigena with shallow ventral flexure just in front of hypostomal embayment. Change in inflection from ventral portion to interior surface of librigena abrupt. Ankylosis of median suture nearly complete, visible for less than 15% of length (sag.) near anterior margin.

Hypostome assigned to this species only slightly longer (sag.) than wide (tr.). Lateral notch well-developed. Weak furrow separates anterior from posterior lobe of middle body; from lateral margins directed posteriorly and toward midline for short distance than transverse to connect together. Anterior lobe of median body inflated in front of maculae. Lateral margins of posterior lobe only very slightly bowed outward over most of length then directed inward to tip of forks. Interior margins of forks directed inward then nearly parallel until curve broadly forward at intersection of forks. Anterior margin nearly horizontal, deflected backward at about 45° to form front of anterior wing. Wing rounded at the extremity; in ventral view, width (tr.) of hypostome across anterior wings slightly less than width of middle body. Terrace ridges heavy developed along lateral margins of entire hypostome.

Thorax of eight segments. Axis wide (tr.), about 50% total width (tr.) of thorax, convex. Articulating furrows effaced. Adaxial 1/3 of pleural portions of thoracic segments horizontal, abaxial 2/3 deflected strongly ventrally. Articulating facets of pleurae oriented anterolaterally; extend for distal 2/3 of pleurae.

Pygidium subtriangular, length (sag.) nearly equal to width (tr.), highly inflated. Pleural furrows of first segment well defined; pleural furrows of other segments, furrows and axial rings effaced. Axial furrows very weak. Border furrow shallow, narrow, reaches nearly to anterior margin. Posterior margin of pygidium behind axis deflected upward (Pl. 8, Fig. 4b). Exoskeleton without ornament.

Ontogeny.—Smallest cranidium (OU11810; Pl. 9, Fig. 2) 26.6 mm long (sag.). Smallest pygidium (OU11807; Pl. 8, Fig. 4) 9.8 mm long (sag.). Larger individuals (Pl. 9, Figs. 1, 2; Pl. 10, Fig. 1) with short (exsag.) posterior fixigenae; axis of pygidium weakly defined (Pl. 8, Fig. 5). Smaller individuals (Pl. 9, Fig. 2; Pl. 10, Fig. 2; Pl. 11, Figs. 1, 2) with very long (exsag.) posterior fixigenae; axial furrows of pygidium much stronger (Pl. 8, Fig. 4).

Discussion.—Compared to other species in Group II, the lateral margins of cranidia in *I. skapaneidos* are very sinuous. The exceptionally well-developed anterior border of the cranidium is similar to *I. walcotti* but is much longer sagittally than exsagittally instead of being more uniform in length. *Isotelus iowensis* also has a large cranidial border but retains genal spines in the holaspids and has a strong, wide pygidial border. The frontal area of *I. gigas* is moderately long (sag.) and the pygidium tapers strongly toward the posterior but the facial sutures are those of trilobites in Group I. The cranidial outline and frontal area of *I. skapaneidos* are very similar to *I. dorycephalus* but the eyestalks of the Viola species are not elevated above the height of the glabella and the pygidium lacks a wide border.

Isotelus cf. *I. iowensis* Owen, 1852

1852. *Asaphus* (*Isotelus*) *iowensis*, Owen, table 2, fig. 3 – 5; table 2A, figs. 1 – 7.

1910. *Isotelus iowensis*, Raymond and Narraway, pl. 15, fig. 3

1913. *Isotelus iowensis*, Slocom, pl. 13, figs. 1, 2

1914. *Isotelus iowensis*, Raymond, pl. 2, Fig. 6; pl. 3, figs. 1, 2

1928. *Isotelus iowensis*, Troedsson, pl. 12, figs. 8, 9.

1947. *Isotelus iowensis*, Wilson, pl. 3, fig. 4; pl. 4

Pl. 12, Figs. 2, 3

Stratigraphic Occurrence.—Material of this species is from the Upper Ordovician Viola Springs Formation (Bromide Quarry: BQ-float; U. S. Highway 35: I-35-75) (Appendix 2).

Description.—Longitudinal convexity of cranidium very low; posterior 3/4 of cranidium flat to slightly concave; slopes steeply to anterior margin over anterior 1/4 of length. Axial and preglabellar furrows effaced, expressed only as change in convexity from glabella to fixigenae; directed abaxially in front of palpebral lobes. Glabellar furrows broad, shallow, poorly-defined depressions. Eye-stalks, palpebral lobes not preserved. Anterior branch of facial suture curves outward and forward in front of palpebral lobe, continues in broad, strongly rounded arch around lateral margin of cranidium then directed forward and adaxially. Sutures and axial furrows roughly parallel. Lateral border furrow wide on cranidium. Posterior branch of facial suture directed abaxially and slightly backward for 2/3 length, then directed abaxially and backward at about 45° to posterior margin. Posterior margin, and therefore posterior fixigenae, directed backward at lateral extremities. Posterior border furrow absent. Exoskeleton without ornament.

Librigenae wide (tr.), subtriangular in outline. Genal spines present in large holaspids; narrow (tr.), taper rapidly, broken distally. Posterior margin curved backward, nearly transverse in orientation. Posterior border furrow absent. Widest (tr.) point just behind eye-stalk, narrower (tr.) behind and toward anterior. Inner margin in front of eye converges strongly on lateral margin. Border furrow strong along entire lateral margin of gena, widest in front of eye. Anterior portion of gena very narrow (tr.). Lateral margin very gently rounded from genal spine forward to point in front of eye, then curved slightly inward lateral to maximum width of cranidium in front of palpebral lobes. Dorsal surface of librigena weakly convex. Eye-stalk and visual surface not preserved. Exoskeleton without ornament. Hypostome unknown.

Thorax of eight segments, wide (tr.), low convexity. Axis less than 45% total width of thorax. Adaxial 1/3 of pleurae nearly flat, abaxial 2/3 deflected ventrally. Pleural furrows well-defined, arise at front of segment, run laterally and backward for about 1/2 width (tr.) of pleurae then become effaced. Articulating facets long (exsag.), cover nearly entire length (exsag.) of abaxial 1/2 of pleurae.

Pygidium subtriangular, low, long (sag.), length (sag.) about 80% of width (tr.). Lateral border wide (tr.), width about equal around entire margin of pygidium. Posterior margin of pygidium upturned. Articulating facets prominent, oriented at low angle to anterior margin of pygidium. Pleural furrows of first segment well defined. Axial furrows weakest toward anterior, slightly better defined toward posterior and around posterior of axis; pleural furrows effaced. Small areas of preserved exoskeleton without ornament.

Discussion.—This species resembles *I. iowensis* in the width of the body, course of the anterior facial sutures, broad lateral border furrows on both the cephalon and pygidium and retention of genal spines in large holaspids. Further comparison is hindered by lack of preservation of the anterior of the cranidium in the Viola specimen and poor quality of the type material. Pygidia from the Viola Springs are distinctive in that the posterior terminus of the pygidium is upturned; this feature cannot be assessed for the type specimen because it is crushed.

Isotelus cf. *I. walcotti* Ulrich in Walcott, 1918

Pl. 13

1918. *Isotelus walcotti* Walcott, pl. 24, fig. 1.

1963. *Isotelus planus*, DeMott, pl. 3, figs. 12 – 20.

1987. *Isotelus* cf. *I. walcotti*, DeMott, pl. 3, figs 12 – 20.

1989. *Isotelus walcotti*, Rudkin and Tripp, figs. 1.7 – 1.9

Stratigraphic Occurrence.—Material of *Isotelus* cf. *I. walcotti* comes from the Upper Ordovician Viola Springs (U. S. Highway 99: 99-33 to 99-49.5) (Appendix 2).

Description.—Longitudinal convexity low. Posterior 2/3 of cranidium nearly flat, anterior 1/3 slopes gently to anterior margin.

Axial and preglabellar furrows expressed as change in convexity from glabella to lateral and frontal areas. Axial furrows directed inward from posterior margin to point just in front of palpebral lobes, curve outward then inward parallel with lateral margin of cranidium formed by facial sutures. Anterior margin of glabella rounded. Occipital region incompletely preserved; weak glabellar furrows (S2, S3) preserved on internal molds (Pl. 13, Fig. 1). Anterior branch of facial suture directed outward and forward in front of palpebral lobe, continues in broad, strongly rounded arch around lateral margin of cranidium then directed forward and toward mid-line at an angle of nearly 60° to sagittal line. Sutures parallel axial furrows until point of maximum width of cranidium in front of palpebral lobes then diverge from preglabellar furrow so that frontal region is longest sagittally. Lateral border of fixigena (between facial suture and axial furrow at point of maximum width in front of palpebral lobes) much wider (tr.) than in most other species. Posterior branch of facial suture directed laterally posterior to palpebral lobes; posterior portion of glabella incomplete. Ornament of very fine pits only visible under magnification.

Librigenae subrectangular in outline; narrow (tr.) and highly inflated. Genal spines present in moderately large holaspids, very thin (Pl. 13, Fig. 2). Posterior margin directed strongly backward. Posterior border furrow continues for 1/2 distance across gena. Widest (tr.) point just behind eye-stalk. Gena tapers toward anterior; inner margin converges strongly on lateral margin just in front of eye. Border furrow strong from point just behind eye forward; anterior portion of gena nearly flat. Lateral margin very gently rounded. Dorsal surface of librigena convex. Eye-stalk extends dorsally and laterally for short distance; visual surface tall and short (exsag.). Dorsal surface of exoskeleton without ornament. Hypostome and thorax unknown.

Pygidium subtriangular, length (sag.) about 75% of width (tr.). Height low, about 40% of length. Very gently concave lateral border extends around entire margin of pygidium. Articulating facets prominent, oriented at low angle to anterior margin of pygidium. Pleural furrows of first segment well defined. Axial furrows very weak, even on internal mold; pleural furrows absent. Exoskeleton not preserved.

Discussion.—The strength and width of the cranidial border furrow strongly resemble *I. walcotti* and pygidia of the species from the Viola Group and *I. walcotti* are indistinguishable. Genal spines in the holotype of *I. walcotti* are much longer and more rebust, but Viola Group specimens are on the order of 3x larger than the holotype. The visual surface in the Viola specimens is tall and short (exsag.), much taller than in *I. walcotti*. Material from the Viola Group is too sparse for confident identification.

Genus *Ectenaspis* Raymond, 1920

Type species: *Megalaspis beckeri* Slocom, 1913

Discussion.—Westrop and Ludvigsen (1983) redescribed the type of *Ectenaspis* and provided a reconstruction of the nearly complete individual. Because complete eye-stalks were unknown, those in the reconstruction are not accurate. Based on the length of the eye-stalks in the new species from the Viola Group, it is probable that those of *E. beckeri* are longer than estimated. The holotype is refigured on Plate 14 herein.

Ectenaspis burkhalteri, new species

Pls. 14, Fig. 2; 15, 16; Pl. 17, Figs. 1-4

Etymology.—The trivial name is a small way of recognizing the significant contribution Roger Burkhalter has made to the study of paleontology in Oklahoma.

Type Material.—Holotype (OU11827), cranidium with left eye-stalk and palpebral lobe preserved; Paratype (OU11828), crushed cranidium with ornament and one well-preserved palpebral lobe; Paratypes (OU11829, OU11830), two partial cranidia; Paratypes (OU11831, OU11832), portions of two librigenae; Paratype (OU11826) exfoliated hypostome; Paratypes (OU11833, OU11834, OU11835, OU11836) four pygidia of varying sizes with exoskeleton preserved.

Stratigraphic Occurrence.—The type material is from the Upper Ordovician Welling Formation, Oklahoma (Lawrence Quarry: LQ-WF; Nebo: Nebo-Well) (Appendix 2).

Diagnosis.—A species of *Ectenaspis* with border furrow of pygidium becoming obsolete through holaspid ontogeny. Weak axial rings and pleural furrows present. Cranidium wide anterior to palpebral lobes; facial sutures converge at base of proboscis.

Description.—Longitudinal convexity of cranidium low, nearly horizontal for 3/4 distance from posterior margin then slopes gently to frontal area. Frontal area tapers forward, curves dorsally; anterior margin of all specimens broken. Palpebral lobes positioned short distance behind transverse mid-line. Axial furrows effaced; lateral margins of glabella indicated by change in convexity rather than discrete furrow. Occipital furrow obsolete. Posterior branch of facial sutures sinuous; directed posteromedially then posterolaterally to posterior border furrow making front margin of posterior fixigena curved in; lateral margin of posterior fixigena rounded. Anterior branch of facial suture very gently curved inward for short distance then curved outward to anterior prolongation (Pl. 16, Fig. 1a, 2a). At frontal area, sutures curve more strongly forward; anterior termination not preserved. Glabella weakly convex (tr.) behind palpebral lobes; lateral margins of glabella obscured at level of palpebral lobes by inflated base of eye-stalks. In front of palpebral lobes, convexity of glabella slightly lower and tapering toward anterior; anterior margin of glabella narrow and rounded. Fixigenae narrow (tr.); posterior portion narrow (tr.) and concave. Posterior border furrow wide and shallow. Posterior border short (exsag.), strongly convex, deflected slightly backward distally. Palpebral areas of fixigenae with swellings angled slightly forward, taper dramatically abaxially, extend dorsolaterally to form long, thin eye-stalks (Pl. 16, Figs. 1a, 2a, 2b). Eye-stalks directed slightly forward for about half of length then curve to project laterally; directed upward at about 25° to horizontal. Palpebral lobe oriented nearly horizontally and tipped slightly forward; subcircular in outline; posterior margin more strongly rounded than anterior or lateral margins, giving the impression that the entire palpebral lobe is twisted backward. Dorsal surface of palpebral lobe strongly concave with lowest point at anteromedial edge. Palpebral furrow runs near lateral margins of lobe around entire circumference except where palpebral lobe attaches to eye-stalk. Muscle scars not expressed on dorsal or ventral surface of exoskeleton. Ornament of widely scattered, fine pustules mainly concentrated in frontal area at base of proboscis (Pl. 15, Figs. 2a, 2d). Median pre-occipital tubercle appears to be absent although internal molds not well preserved.

Librigenae long (exsag.), with long (exsag.) genal spines. Posterior margin sloping laterally and backward into curve of genal spine. Spines long, bowed outward, presumably to hug lateral margin of thorax, broken posteriorly. Posterior border furrow long (exsag.); continues across gena to spine. Width of librigena about equal from base of eye to posterior margin. Dorsal surface weakly convex. Eye-stalk very thin, long; directed outward and upward from dorsal surface. Termination and visual surface not preserved. Librigena much narrower (tr.) anteriorly. Inner margin converges gradually on lateral margin then broken. Lateral margin rounded. Exoskeleton of librigenae without ornament. Thorax unknown.

Hypostome with short (sag.) and wide (tr.) middle body; anterior lobe more strongly convex than posterior. Maculae weak on internal mold. Lateral margins flare weakly outwardat level of maculae then without curvature to posterior termination of forks.

Posterior termination of forks poorly preserved. Interior margins of forks angled inward from posterior termination of forks until ¾ of their length then directed forward before curving around to intersect. Anterior margin poorly preserved. Anterior wings directed strongly dorsally then not exposed. Faint terrace ridges preserved along lateral margins of forks.

Pygidium subtriangular in outline; tapers strongly to rounded posterior margin. Long, maximum length (sag.) approximately 75% maximum width (tr.). Axis weakly convex. Articulating facets prominent. Axial furrows weakly defined. Pleural furrows and axial wings visible on dorsal surface. Pleural furrow of the first segment deeply impressed. Articulating half ring preserved as flattened forward extension of axis. Pleural regions gently convex then abruptly steepen to lateral margin. Border furrow absent on large holaspids (Pl. 17, Fig. 4); smaller individuals with remnant of border (Pl. 16, Fig. 5). Exoskeleton of pygidium without ornament.

Ontogeny.—Smallest cranidium (OU11830; Pl. 16, Fig. 2) 13.7 mm wide (tr. across posterior fixigenae). Greater effacement of posterior border furrow, decreased convexity with development. Smallest pygidium (OU11833; Pl. 16, Fig. 5) 15.6 mm long (sag.). Short (sag.) posterior border (Pl. 16, Fig. 5b) becoming shorter through growth (Pl. 17, Fig. 2b) until obsolete (Pl. 17, Fig. 4b).

Discussion.—*Ectenaspis burkhalteri* differs from *E. beckeri* in the absence of a pygidial border furrow. In *E. beckeri*, the facial sutures converge more rapidly in front of the palpebral lobes; they are more weakly convergent in *E. burkhalteri* until directed more strongly inward at the base of the proboscis. Pustules on the cranidium are coarser and more extensively distributed in *E. burkhalteri* and pleural furrows of the pygidium show less effacement. Comparison of shape and extent of anterior prolongation precluded by consistent breakage in *E. burkhalteri*.

Genus *Stegnopsis*, Whittington, 1965

Type species.—*Stegnopsis solitarius* Whittington, 1965

Diagnosis.—A genus of isoteline with broadly divergent anterior facial sutures. Glabella without anterior expansion; frontal area broad both laterally and anteriorly. Palpebral lobes positioned far back on cranidium. Pygidium highly effaced, subcircular in outline with broad border continuing to anterior margin.

Discussion.—Whittington (1965) diagnosed *Stegnopsis* as an isoteline with wide cranidial and pygidial borders, weak axial furrows of the cranidium and strongly divergent anterior facial sutures. He speculated that *Stegnopsis* is most closely related to *Isoteloides* but differs from the latter in having palpebral lobes that are located much closer to the posterior margin and in having more divergent anterior facial sutures. *Stegnopsis* is otherwise very similar to *Isoteloides* in retention of plesiomorphic features [a short (sag.), subcircular pygidium, wide border furrows of cranidium and pygidium, wide (tr.) librigenae, genal spines in holaspids of some species, minimal anterior expansion of glabella, relict segmentation of pygidium] in comparison with asaphines and niobines. *Stegnopsis* can be distinguished from *Isoteloides* by two features in addition to those mentioned by Whittington; in *Stegnopsis*, the cranidium has uncommonly high convexity (eg. Pl. 18, Figs 1b-c, 2b; Pl. 19, Fig. 5c), and the lateral margins of the anterior lobe of the hypostome taper anteriorly (Whittington, 1965; fig. 3e). These features may be apomorphies of *Stegnopsis*, but the monophyly of the genus is currently unclear.

Stegnopsis huttoni, described by Whittington from the same formation as the type species, *S. solitarius*, has the anteriorly expanding glabella typical of *Isotelus*. It is similar to *"Isotelus" maximus* in possessing wide librigenae, holaspid genal spines and a rounded pygidium but is different in that the axial lobe of the pygidium is extremely narrow (Whittington, 1965, pl. 22, fig. 14). Although the appropriate taxonomic position of this species is currently unknown, its inclusion in *Stegnopsis* confuses the definition of that genus and it is not considered in the following discussion. It is best referred to *"Isotelus" huttoni* for now. Whittington suggests some affinity of *Stegnopsis* with *Lachnostoma* Ross, 1951, but the shape of the glabella of the latter suggests that it is an asaphine (Fortey, 1980).

Shaw (1968) remarked on the similarities between *Stegnopsis* and *I. harrisi* Raymond, 1905. He differentiated them based on characters that are present in *S. huttoni* but lacking in the type. *Isotelus harrisi* is very similar to *S. solitarius*, with the exception that the palpebral lobes are slightly farther forward in the former, and it is here reassigned to *Stegnopsis*. The two species share the following characters: anterior lobe of the hypostome without a lateral border, palpebral lobes located behind the mid-line of the glabella, strongly divergent anterior facial sutures, a wide cranidial border, a glabella that does not expand anteriorly, high convexity of the glabella, wide (tr.) librigenae, genal spines in holaspids, a short (exsag.) pygidium with a rounded posterior margin and a wide border furrow. Shaw (1968) reassigned several individuals of *I. platymarginatus* figured by Raymond (1910b, 1910c) to *S. harrisi*. Some of Raymond's figures are too poor to identify (1910b pl. 17, figs. 1-3; 1910c pl. 37, figs. 1-3) and others are examples of *Isoteloides* rather than *Stegnopsis* based on the anterior facial sutures that do not reach abaxially beyond the lateral limit of the palpebral lobes (1910b, pl. 19, fig. 3; 1910c pl. 39, fig. 3). Some of Shaw's reassignments (1910b pl. 17, figs. 4, 5; 1910c pl. 34, figs. 3-7, pl. 37, figs. 4, 5) appear to be valid. Acquisition and study of additional material, especially hypostomes, will help to improve the definition of this genus.

Hunda and others (2003) figure cranidia from the Whittaker Formation (*I. dorycephalus* pl. 4, figs. 9, 11-12) that have relatively wide cranidial borders and strongly divergent anterior facial sutures. The palpebral lobes are large and positioned far back on the cranidium, but it is difficult to determine from the figured specimens if the glabella has high convexity and expands laterally in front of the palpebral lobes. The small size of the specimens (the largest cranidium is about 4 mm long) and likely early developmental stage of the individuals makes it difficult to assess the relationships of the species.

Two isotelines from the upper Viola Springs and Welling formations are assigned to *Stegnopsis* based on a number of characters. The palpebral lobes are located well behind the mid-line of the glabella and the posterior fixigenae are therefore short (exsag.), but wide (tr.) (Pl. 17, Fig. 5; Pl. 21, Fig. 1). The palpebral lobes are large as in *S. solitarius*, the facial sutures are nearly straight and strongly divergent for a long distance in front of the palpebral lobes, and the convexity of the cranidium is very high. In both, the glabella does not expand anteriorly. The pygidia of the Viola Group species are subcircular in outline with rounded posterior margins and broad border furrows (Pl. 19, Fig. 1; Pl. 21, Fig. 3). The Viola Group species, unlike *S. solitarius*, appear to lack genal spines in holaspids (Pl. 20, Fig. 1). Hypostome unknown.

Stegnopsis wellingensis, new species

Pl. 17, Fig. 5; Pl. 18, Figs. 1-3, 7;
Pl. 19, Figs. 1-3

Etymology.—from the Welling Formation

Type Material.—Holotype (OU11837), external mold of cranidium (latex cast illustrated; Paratypes (OU11838, OU11839), two partial cranidia, one partly and the other completely exfoliated; Paratypes (OU11840, OU11844, OU11846, OU11847), four pygidia of varying sizes, mostly exfoliated; Paratype (OU11845), cast of pygidium showing details of exoskeleton.

Stratigraphic Occurrence.—The type material is from the Upper Ordovician Welling Formation (Lawrence Quarry: LQ-WF) (Appendix 2).

Diagnosis.—A species of *Stegnopsis* with facial sutures converging at front of cranidium at low angle; maximum width in front of palpebral lobes close to anterior margin. Convexity of cranidium very high.

Description.—Glabella very convex (tr. and sag.) over posterior 3/4 of length. Frontal area nearly horizontal (Pl. 18, Fig. 1b). Axial and preglabellar furrows very shallow, broad, expressed only as change in convexity from glabella to fixigenae and frontal area; not discernable at level of and behind palpebral lobes. Anterior of glabella evenly rounded, without expansion in front of palpebral lobes. Occipital furrow very weak, only visible on one internal mold (Pl. 17, Fig. 5a). Glabellar furrows not expressed. Median pre-occipital tubercle absent. Palpebral lobes far back on cranidium about 1/4 total length (sag.) of cranidium in front of posterior margin. Palpebral region of fixigena convex, tapers into laterally and slightly posteriorly directed palpebral lobe. Palpebral lobe oriented horizontally, directed slightly backward; slightly longer (exsag.) than wide (tr.), lateral margin broadly rounded. Palpebral furrow deep and wide on internal mold. Anterior branches of facial sutures directed inward for short distance in front of palpebral lobe then outward around maximum width (tr.), converge toward sagittal line at low angle to horizontal. Suture path "s"-shaped with posterior curve shorter (exsag.) than anterior curve. Maximum width (tr.) of cranidium at posterior margin. Maximum width (tr.) in front of palpebral lobes at 3/4 distance from posterior margin. Anterior facial sutures follow similar course to preglabellar furrow but separated by broad, flat frontal area. Posterior branch of facial suture runs laterally and slightly backward to distance nearly half-again width (tr.) of palpebral lobe before curving abruptly to meet posterior margin. Posterior border furrow weak. Posterior margin nearly flat, deflected only slightly backward at lateral extremities. Posterior fixigenae only slightly shorter (exsag.) distally than medially. Surface of exoskeleton without ornament. Hypostome and thorax unknown.

Pygidium subovate in outline, much wider (tr.) than long (sag.), length approximately 65% of width. Convexity very low, height approximately 35% of length. Articulating facets prominent, oriented at a low angle to horizontal. Axial furrows and pleural furrows of first segment moderately well-defined; axial rings and pleural furrows faintly preserved on internal molds (Pl. 18, Figs. 3a, 7a; Pl. 19, Fig. 2). Border furrow wide, expressed as change in slope from pleural regions to margin. Dorsal surface of exoskeleton without ornament.

Ontogeny.—Small cranidium not available. Smallest pygidium (OU11840; Pl. 18, Fig. 3) 20.5 mm long (sag.). Progressive effacement of axial furrows, posterior border furrow through ontogeny.

Discussion.—*Stegnopsis wellingensis* bears some resemblance to *I. levis* Chugaeva, 1958, in the course of the anterior facial sutures. The poor preservation of the figured specimen and lack of additional material makes further comparison impossible. *Stegnopsis wellingensis* is similar to *S. solitarius* in the course of the facial sutures and high convexity of the cranidium but the anterior border of the type is longer (sag.) and more steeply sloped. The posterior margin of the pygidium of *S. solitarius* is more broadly rounded and the border furrow is longer (sag.). The frontal area and lateral border of *S. harrisi* are much broader and the facial sutures converge at a lower angle than in *S. wellingensis*; the glabella appears to contract anteriorly in the former. The concave lateral border present in *S. harrisi* is absent in large individuals of *S. wellingensis*.

Stegnopsis erythragora, new species

Pl. 18, Figs. 4-6; Pl. 19, Figs. 4, 5; Pls. 20, 21

Etymology.—The trivial name describes the resemblance of the outline of the cranidium to the distinctive onion domes common in Red Square, Moscow.

Type Material.—Holotype (OU11853), nearly complete, small cranidium; Paratypes (OU11849, OU11852, OU11854), three partial cranidia of varying sizes; Paratype (OU11851), cast of partial cranidium; Paratype (OU11850), nearly complete weathered individual; Paratypes (OU11855, OU11856), two nearly complete pygidia; Paratype (OU11857), cast of broken pygidium showing ornament of the exoskeleton. A meraspid cranidium (OU11841), two meraspid librigenae (OU11842, OU11843), and a meraspid pygidium (OU11848) are assigned to this species.

Stratigraphic Occurrence.—The type material is from the Upper Ordovician Viola Springs (U. S. Highway 77: 77-181.5 to 77-183) and Welling formations (Nebo: Nebo-Well) of Oklahoma. Meraspid material is from the upper part of the Viola Springs Formation (Bromide Quarry: BQ-12 to BQ-18) (Appendix 2).

Diagnosis.—A species of *Stegnopsis* with very wide, evenly rounded cranidial border; anterior facial sutures directed abruptly forward just before intersecting to form sharp point. Palpebral lobes large. Librigenae without genal spines in large holaspids. Pygidium with relatively well-defined axial furrows.

Description.—Cranidium with high longitudinal convexity. Glabella slopes upward from posterior margin to level of eyes. Longitudinal convexity lower from palpebral lobes to point 3/4 distance in front of posterior margin then slopes steeply down to frontal area. Transverse convexity low. Axial and preglabellar furrows expressed as transition from convex glabella to flat border and frontal areas. Glabella without lateral expansion in front of palpebral lobes. Anterior margin of glabella evenly rounded. Axial furrows at level of palpebral lobes very shallow, become obsolete to posterior. Occipital furrow only visible on small individuals, located very close to posterior margin. Palpebral lobes positioned behind midpoint of cranidium. Palpebral region of fixigena extends upward forming short (d.-v.), long (exsag.) eye-stalk, elevated only slightly above maximum height of glabella (Pl. 21, Fig. 1b). Palpebral lobes oriented horizontally; length (exsag.) about equal to width (tr.). Palpebral furrow very weak, located at top of eye-stalk, parallels lateral margin of palpebral lobe (Pl. 20, Fig. 2a). Anterior facial sutures diverge to level of anterior margin of glabella then curve to run toward sagittal line at high angle to transverse; curve slightly inward then directed strongly forward just before intersecting to form sharp point. Maximum width of cranidium located 2/3 distance from posterior margin. Broad, flat, spade-shaped frontal area between glabella and margin of cranidium. Posterior branch of facial suture runs abaxially and slightly posteriorly well past lateral margin of palpebral lobe then deflected backward at high angle to meet posterior margin. Posterior border furrow not present. Posterior fixigena very short (exsag.), narrows only slightly abaxially. Posterior margin nearly transverse. Ornament of wide, shallow pits not visible without magnification (Pl. 21, Figs 4b). Very faint median glabellar ridge visible on internal molds (Pl. 20, Figs. 2a, 4c).

Librigenae wide (tr.), widest point at posterior margin. Genal angle rounded on holaspids. Lateral margin evenly rounded. Inner margin rounded, converges on lateral margin in front of eye. Anterior portion of librigena narrow (tr.). Dorsal surface weakly convex. Eye-stalk and visual surface not preserved.

Thorax wide (tr.), composed of eight segments. Axial furrows broad, deep. Axis wide (tr.), about 50% total width of thorax. Adaxial 1/2 of pleurae nearly horizontal, abaxial 1/2 deflected ventrally. Articulating facets wide (tr.), located on abaxial 1/2 of pleurae, become longer (exsag.) to lateral margins. Hypostome unknown.

Pygidium subovate in outline, length (sag.) about 75% of width (tr.). Inflation moderate, height about 60% of length. Border furrow wide, continues with about equal width forward to articulating facet. Articulating facets prominent, oriented at low angle to horizontal. Pleural furrows of first segment deeply impressed. Axial and pleural furrows well defined on internal molds (Pl. 21, Fig. 3a); axial rings weak. Ornament of densely packed, fine pits.

Ontogeny.—Smallest cranidium (OU11841; Pl. 18, Fig. 4) 2.3 mm long (sag.) posseses a pre-glabellar ridge and what may be bacculae; both lost by holaspid stage. Occipital furrows effaced during growth. Meraspid librigena indicates loss of genal spines through ontogeny. Smallest pygidium (OU11848; Pl. 19; Fig. 4) more triangular in outline with well-defined axial furrows but effaced plaural furrows and axial rings. Ontogenetic series of pygidia not available.

Discussion.—The glabella of *S. solitarius* is similar to that of *S. erythragora*, but the anterior facial sutures in the latter are more evenly curved around the point of maximum width. Holaspid genal spines are present in *S. solitarius* but lacking in the Viola species. Pygidia of *S. erythragora* have relict pleural furrows and well defined axis while those of *S. soliatarius* have greater effacement and are more rounded posteriorly. *Stegnopsis erythragora* is similar to *S. harrisi* in the course of the facial sutures but the widest point of the cranidium in the former is evenly rounded rather than angled. The Viola species has a parallel-sided glabella with a rounded anterior margin rather than an anterior constriction. The pygidia of *S. harrisi* and *S. erythragora* are similar in outline and border width, but the pygidium is more effaced in the former. This species differs from *S. wellingensis* in having a wider (tr.) cranidial border, and a frontal area that is formed by a lateral deflection of the facial sutures in front of the palpebral lobes and a high angle of convergence of the sutures toward the sagittal line.

Genus *Anataphrus* Whittington, 1954

Type species.—*Anataphrus borraeus* Whittington, 1954

Discussion.—Chatterton and Ludvigsen (1976) regarded *Anataphrus*, *Nahannia* Chatterton and Ludvigsen, 1976, *Protopresbynileus* Hintze, 1954, *Vogdesia* Raymond, 1910c, and *Homotelus* Raymond, 1920, as a closely related group of isotelines. They are herein regarded as a derived group united by potential apomorphies including: a glabella that reaches the anterior margin of the cranidium; extreme effacement of the axial furrows, especially on the cranidium; and wide pygidial axes. The poorly known *Nileoides* Raymond, 1920, possesses these features and may also belong to this group.

Nahannia may be monophyletic based on the short (sag.) median body of the hypostome and, possibly, the retention of genal spines in holaspids. The wide border on the pygidium, which is present in the ontogeny of *Anataphrus*, is likely to be plesiomorphic.

The status of *Anataphrus*, *Protopresbynileus* and *Nileoides* is uncertain, but all show greater effacement than *Nahannia*. Effacement of the thorax in *Anataphrus* may prove to be apomorphic. In *A. glomeratus* Dean, 1979, the position of the palpebral lobes close to the posterior margin of the cranidium and large size of the palpebral lobes make it look superficially like *Nahannia*, but absence of both a border furrow on the pygidium and of holaspid genal spines support assignment to *Anataphrus*. *Isotelus spurius* Phleger, 1933, (see Ross, 1967 pl. 4, figs. 6-9; 1970 pl. 13, figs. 3, 5, 7, 10) is highly effaced and lacks a border on the pygidium and is here reassigned to *Anataphrus*. The effacement of *Nileoides* seems to match that of *Anataphrus*, but the eyes are in a more posterior position. *Protopresbynileus* is comparable to *Anataphrus* in cranidial and pygidial effacement but the thorax is unknown. A median border spine on the hypostome could be an apomorphy but it is possible that recognition of *Protopresbynileus* will create paraphyly in *Anataphrus* and/or *Nileoides*. Until the statuses of these genera can be evaluated through a phylogenetic analysis, all should be retained.

Vogdesia is another isoteline in need of revision. It is distinct within this group mainly in having a pygidium that is elongate and posteriorly tapering rather than subcircular in outline. Weak effacement of the axial furrows of the cranidium behind the palpebral lobes and a narrow axial lobe are also distinctive. *Vogdesia* is especially problematic because the types of the type species, *V. bearsi*, have been lost, although Shaw (1968) figured topotype material and designated a neotype. *Isotelus simplex* Raymond and Narraway, 1910, (also see DeMott, 1987) lacks a frontal area but also has a short (exsag.) tapering pygidium with only moderate effacement typical of *Vogdesia* and is here tentatively reassigned to that genus. Whittington (1954) attributed some species originally assigned to *Vogdesia* to *Anataphrus* including *A. gigas*, *A. vigilans* and *A. raymondi*.

Homotelus was erected by Raymond (1920) for isotelines lacking genal spines but with wide cranidia, weak axial furrows, elevated palpebral lobes and a lateral border. Jaanusson (in Moore, 1959) added that a frontal area is lacking and the palpebral lobes are positioned slightly in front of the transverse mid-line of the cranidium. Whittington (1950) noted that the differences between *Homotelus* and *Isotelus* are small and recommended restricting the genus to the type. I agree that the genus should be restricted but feel that the lack of a frontal area on the cranidium allies *Homotelus* more closely with *Vogdesia* than *Isotelus*. Some species previously assigned to *Homotelus* (e.g., *H. bromidensis*, Esker, 1964) may belong in *Vogdesia*.

Anataphrus megalophrys, new species

Pls. 22-24; Pl. 25, Figs. 1-6

Etymology.—This species is named for the large size of the palpebral lobes.

Type material.—Holotype (OU11866), nearly complete, testate cranidium; Paratypes (OU11858 – OU11865 inclusive), eight cranidia of varying sizes, all with at least some exoskeleton preserved; Paratypes (OU11868, OU11869), two librigenae; Paratypes (OU11867, OU11870, OU11871), three hypostomes; Paratype (OU11873), articulated thorax and pygidium; Paratypes (OU11879, OU11883), two meraspid pygidia; Paratype (OU11872), small pygidium; Paratypes (OU11874, OU11875, OU11876, OU11877, OU11878, OU11880, OU11881, OU11882), eight larger pygidia.

Stratigraphic Occurrence.—The type material is from the Upper Ordovician Viola Springs Formation (U. S. Highway 99: 99-39 to 99-49.5; Lawrence Quarry: LQ-VS) (Appendix 2).

Diagnosis.—A species of *Anataphrus* with long (exsag.), wide (tr.) palpebral lobes. Pygidium long (sag.) relative to width (tr.); axial lobe weakly defined on internal molds.

Description.—Longitudinal convexity of cranidium low; anterior 1/4 of cranidium slopes at about 45° to anterior margin. Palpebral lobes at about 40% total length (sag.) from posterior margin. Axial furrows effaced except for faint impression from just behind to just in front of palpebral lobes. Occipital furrow effaced on dorsal surface; preserved on internal molds (Pl. 22, Figs. 7a, 8). Occipital ring longest sagittally reaching almost to median pre-occipital tubercle; furrow converges on posterior margin laterally; occipital ring very short (exsag.) on posterior fixigenae. Posterior branch of facial suture directed laterally and slightly posteriorly for about 1/2 distance then directed more strongly backward; turns abruptly at termination of posterior fixigena to intersect posterior margin. Anterior branch of facial suture directed slightly adaxially and forward for short distance; abruptly directed anterolaterally to maximum width then curving tightly around point of maximum width; directed anteriorly and strongly adaxially to intersect at anterior margin. Anterior margin of cranidium with short (sag.), sharp point at intersection of facial sutures (Pl. 22, Figs. 6a, 7c; Pl. 23, Fig. 1c). Glabella poorly defined; only weakly convex transversely. Posterior fixigenae become shorter (exsag.) laterally, directed weakly backward and downward. Palpebral lobes large, wide (tr.), long (exsag.); lateral termination evenly rounded, oriented horizontally, elevated only slightly above height of glabella. Median pre-occipital tubercle well defined on internal molds (Pl. 22, Fig. 8), positioned at front edge of occipital furrow. Ornament absent on dorsal surface of exoskeleton in large holaspids (Pl. 23, Fig. 1b). Small holaspids with very fine pits (Pl. 22, Fig. 3). Faint terrace ridges on anterior of cranidium present in small holaspids (Pl. 22, Fig. 2c) become fainter with increasing size (Pl. 22, Fig. 6a), absent in larger individuals (Pl. 23, Fig. 1b, 1c).

Librigenae subtriangular in outline; widest point just behind eye. Genal angle rounded in holaspids. Posterior margin rounded, lateral margin weakly convex. Inner margin converges strongly on lateral margin in front of eye then nearly parallel to lateral margin, converges only weakly until intersects with lateral margin at anterior. Dorsal surface of gena only weakly convex. Furrow at base of visual surface well defined. Visual surface continues for about 170°, tall, becomes shorter toward anterior (Pl. 23, Fig. 3a).

Hypostome wider (tr.) than long (sag.), length about 90% of width. Lateral margins bowed strongly outward; maximum width (tr.) across posterior lobe nearly equal to maximum width (tr.) across anterior margin. Maculae well-defined; positioned about 1/2 distance from anterior border to posterior border (exclusive of forks). Fork deep, making up about 50% total length (sag.) of hypostome; inner margins of forks nearly parallel; posterior terminations of forks rounded. Strong terrace ridges roughly parallel lateral margins for entire length of fork. Middle body and posterior lobe with widely scattered fine pits.

Thorax of eight segments. Axis wide (tr.), about 65% total width (tr.) of thorax, weakly convex. Articulating furrow effaced. Pleural portions of thoracic segments deflected strongly ventrally. Articulating facets of pleurae oriented anterolaterally; extend entire width (tr.); non-articulating portion becomes shorter (exsag.) distally. Short (exsag.), subtriangular process extends backward from posterior margin of thoracic segments at intersection of axial and pleural regions; process articulates with corresponding shallow facet on anterior margin of segments.

Pygidium length (sag.) about 65% of width (tr.). Axis without independent convexity except on internal molds (Pl. 24, Fig. 5b). Axial and pleural furrows effaced. Axis, as observed on internal molds, wide (tr.), about 50% total width (tr.) of pygidium, tapers toward posterior. Axial rings faintly visible on internal molds (Pl. 24, Fig. 3a, 4a-b, 5a-b). Shallow, subrectangular pits along margins of axis on large internal molds (Pl. 25, Figs. 3a, 4-5) represent apodemes on the ventral surface of the pygidium. Anterior margin transverse to very weakly rounded. Posterior margin evenly rounded. Inflation of pygidium moderate, height about 55% of length (sag.). Articulating facets well-defined. Ornament of fine terrace ridges most pronounced near articulating facets (Pl. 25, Fig. 1b). Doublure arises just behind anterior margin of articulating facet, length (exsag.) roughly uniform around entire posterior margin of pygidium. Dorsal surface of doublure parallel to dorsal surface of pygidium; anterior margin of doublure deflected backward to form relatively wide (tr.) notch at level of posterior termination of axis. Ornament of terrace ridges subparallel to anterior margin of doublure.

Ontogeny.—Smallest cranidium (OU11858; Pl. 22, Fig. 1) 1.9 mm long (sag.). Densly packed, fine pits covering dorsal surface of cranidium of (Pl. 22, Fig. 3) absent in later ontogenetic stages. Smallest pygidium (OU11872; Pl. 23, Fig. 7) 1.0 mm long (sag.). Posterior margins become more rounded through ontogeny; axial rings better defined with large size. Border furrow of pygidium lost early in ontogeny.

Discussion.—*Anataphrus megalophrys* is very similar to *A. borraeus* but has larger palpebral lobes, the cranidium in front of the palpebral lobes is narrower (tr.) and the cranidium widens (tr.) more abruptly in front of the palpebral lobes. The glabella of *A. martinensis* Ross and Shaw, 1972, is narrower and the pygidium is shorter (exsag.) than in *A. megalophrys*. *Anataphrus spurius* has a very short (exsag.) cranidium.

Anataphrus kermiti, new species

Pl. 25, Figs. 7-10; Pls. 26-31

Etymology.—Named for Kermit the Frog, who this species resembles when enrolled (Pl. 26, 2a, 2d; Pl. 31, Fig. 1b, c).

Type material.—Holotype (OU11889), nearly complete, enrolled individual; Paratype (OU11937), nearly complete enrolled individual; Paratypes (OU11938, OU11939), two nearly complete individuals; Paratypes (OU11884, OU11887, OU11908), three cranidia with strap-like palpebral lobes; Paratypes (OU11885, OU11909, OU11910), three exterior molds (latex casts illustrated) of cranidia with strap-like palpebral lobes; Paratypes (OU11888, OU11911), two cranidia with waisted palpebral lobes; Paratypes (OU11892, OU11893, OU11897), three exterior molds (latex casts illustrated) of cranidia with waisted palpebral lobes; Paratypes (OU11899, OU11906, OU11940), three cranidia lacking palpebral lobes; Paratypes (OU11914, OU11915, OU11920), three small cranidia; Paratypes (OU11898, OU11912), two librigenae; Paratypes (OU11900, OU11901), two hypostomes; Paratypes (OU11895, OU11896, OU11907, OU11913, OU11941), five pygidia; Paratypes (OU11886, OU11890, OU11894, OU11904, OU11905), five small pygidia; Paratypes (OU11918, OU11919), two meraspid cranidia; Paratypes (OU11916, OU11921, OU11922, OU11923), four meraspid librigenae; Paratypes (OU11924, OU11925), two meraspid hypostomes; Paratypes (OU11891, OU11902, OU11903, OU11917, OU11926 – OU11936 inclusive), fifteen meraspid pygidia. Figured specimens are grouped on plates by collection.

Stratigraphic Occurrence.—Type material is from the upper Viola Springs Formation (U. S. Highway 77: 77-218 to 77-219; Bromide Quarry: BQ-pave to BQ-24; Camp Classen, Mosely Creek) and Welling Formation (Lawrence Quarry: LQ-WF; Nebo: Nebo-Well) (Appendix 2).

Diagnosis.—A species of *Anataphrus* with small palpebral lobes. Exoskeleton densely pitted; anterior margin of cranidium with coarse, parallel terrace ridges. Lateral margins of hypostome only slightly curved outward. Eyes on long stalks, directed dorsally and slightly abaxially.

Description.—Longitudinal convexity of cranidium very low, nearly flat over posterior 3/4 then slopes abruptly to anterior margin. Palpebral lobes slightly behind transverse mid-line of cranidium. Axial furrows mainly effaced; weakly expressed in palpebral region. Occipital furrow effaced on dorsal surface; preserved on some internal molds (Pl. 28, Fig. 10). Occipital ring longest sagittally. Posterior border furrow absent. Posterior branch of facial sutures directed backward at about 45° for half length of posterior fixigenae then directed more sharply backward to intersect posterior margin. Posterior margin directed backward abaxially so that lateral extremities of posterior fixigenae directed backward. Anterior branch of facial suture directed adaxially so that cranidium just in front of palpebral lobe narrower (tr.) than just behind (Pl. 27, Figs. 1a, 2a). Sutures curve forward and abaxially around maximum width (tr.) in front of palpebral lobes then directed forward and adaxially to intersect at sharp point at mid-line. Glabella not defined; weakly convex transversely. Palpebral lobes wider (tr.) than long (sag.), exhibit two distinct morphologies. Most individuals (especially small holaspids) with strap-like eye-stalks: nearly equal length (sag.) over entire width (tr.), rounded termination (Pl. 25, Figs. 7, 8a, 10b; Pl. 26, Fig. 2; Pl. 29, Figs. 2, 3a). Some individuals (especially large holaspids) with waisted eye-stalk: base of eye-stalk at intersection with fixigena narrow, widens upward to termination, rounded terminal piece directed slightly backward (Pl. 26, Figs. 1a, 1c; Pl. 27, Figs. 1a, 1d, 2; Pl. 28, Fig. 1; Pl. 29, Fig. 5). Median preoccipital tubercle weak, visible only on internal molds, located just in front of occipital furrow. Ornament of fine, densely scattered pits becomes more obscure through ontogeny. Well-defined, parallel, transverse terrace ridges cover anterior 1/4 of cranidium.

Librigenae subrectangular in outline; widest point just behind eye, only slightly narrower (tr.) toward posterior margin. Genal angle and posterior margin rounded; lateral margin rounded more weakly. Inner margin converges sharply on lateral margin just in front of eye socle. Anterior portion of librigena very thin. Dorsal surface of gena weakly convex. Furrow at base of eye socle distinct. Visual surface tall, inflated, covers about 270° field of view.

Hypostome narrow (tr.) for genus, without broad lateral flare between level of maculae and posterior margin between forked projections. Lateral margins weakly rounded. Maculae well-defined; located between anterior border and posterior margin between fork. Fork deep, wide (tr.), inner margins of fork nearly parallel, posterior terminations broken. Terrace ridges parallel lateral margins of fork. Anterior wings long (exsag.). Ventral surface of hypostome nearly flat, curves slightly downward near anterior margin.

Thorax of 8 segments. Axis wide (tr.), greater than 60% total width (tr.) of thorax, weakly convex. Articulating furrow effaced. Pleural portions of thoracic segments curve evenly downward. Articulating facets of pleurae oriented anterolaterally; extend entire width (tr.), become shorter (exsag.) medially. Posterior margin of thoracic segments at intersection of axial and pleural regions with short, subtriangular posterior process; correspond to facets on anterior margin of segments.

Pygidium length (sag.) about 60% of width (tr.). Axis without independent convexity even on internal molds. Axial furrows effaced, faintly visible on internal molds. Axis width (tr.) about 60% total width (tr.) of pygidium. Anterior margin transverse; posterior margin evenly rounded. Convexity strong, height about 90% of length (sag.). Articulating facets well-defined. Ornament of deep, densely packed pits less pronounced over axis, coarse terrace ridges across pleural regions and on articulating facets.

Muscle scars visible on some well preserved cranidia and pygidia from Welling Formation at LQ locality; preserved as dark, ovate markings along axial furrows (Pl. 31, Figs. 4-5).

Ontogeny.—Smallest cranidium (OU11918; Pl. 30, Fig. 1) 1.3 mm long (sag.). Axial, preglabellar, occipital, posterior border furrows well-developed in meraspids, progressive effacement through ontogeny to obsolescence in large holaspids (except axial furrows in palpebral region). Laterally directed palpebral lobes become elevated into stalks; relative size of palpebral lobes decreases (Pl. 27, Fig 2a). Narrow glabella widens through growth. Smallest librigena (OU11921; Pl. 30, Fig. 4) 1.2 mm wide behind eye. Genal spine lost in holaspids. Smallest hypostome (OU11924; Pl. 30, Fig. 7) 1.3 mm wide (tr.) across maculae. Sharp lateral projections behind maculae lost during ontogeny. Smallest pygidium (OU11928; Pl. 30, Fig. 11) 0.8 mm long (sag.). Posteromedian notch (Pl. 30, Figs. 11a, 12a) lost at early stage. Strong axial, pleural and border furrows and axial rings gradually become effaced. Wide axis becomes wider.

Discussion.—*Anataphrus kermiti* is most similar to *A. martinensis*, especially in the outline of the cranidium. The eye-stalks of *A. martinensis* are taller than in *A. kermiti* and the axial furrows in the palpebral regions of the fixigenae are deeper. The cranidial outline and palpebral shape of *A. elevatus* Hunda and others (2003) are simlar to *A. kermiti* but the Viola species has stronger axial furrows at the level of the palpebral lobes, strap-like palpebral lobes at smaller holaspid size and bears an ornamentation of pits and terrace ridges. *Anataphrus kermiti* has much smaller palpebral lobes than *A. borraeus*. The cranidium of *A. kermiti* is longer (sag.) and the posterior fixigenae are much wider (tr.) than in *A. spurius*. This species differs from *A. megalophrys* mainly in having smaller, more strongly elevated palpebral lobes and a shorter pygidium with a more poorly-defined axis.

ACKNOWLEDGEMENTS

I am grateful to S. R. Westrop for his invaluable participation in discussions related to isoteline systematics. T. Karim contributed extensively to the collection and preparation of specimens and is one of the few people willing to work with me to try to understand the effaced. Field and lab work were undertaken in collaboration with R. Burkhalter. The Oklahoma Geological Survey provided funding for fieldwork in Oklahoma. Acknowledgement is also made to the Donors of the Petroleum Research Fund, administered by the American Chemical Society, for support of my and others' research on Ordovician trilobite faunas in Oklahoma. Additional funding was received from the Geological Society of America in the form of a Graduate Student Research Grant. I am grateful for the helpful reviews and suggestions provided by Jonathan Adrain and David Rudkin. Loans of material collected by Bradley were made available by the Field Museum.

REFERENCES

API Well #12300123 (Morris #1): T3N, R6E, Sec18, about 5 km NNE of locality LQ.

API Well #12370042 (Fittswest Unit TR40-7): T2N, R6E, Sec 36, about 3 km N of locality 99.

Aigner, T., 1982, Calcareous tempestites: Storm-dominated stratification in Upper Muschelkalk limestones (Middle Trias. SW-Germany), in Einsele, G.; and A. Seilacher. (eds.), Cyclic and Event Stratification: Springer-Verlag, Heidelberg, p. 180–198.

Allison, P. A.; Wignall, P. B.; and Brett, C. E., 1995, Palaeo-oxygenation: effects and recognition: Geological Society Special Publication, v. 83, p. 97–112.

Amati, L.; and Westrop, S. R., 2006, Sedimentary facies and trilobite biofacies along an Ordovician shelf to basin gradient, Viola Group, south-central Oklahoma: Palaios, v. 21, n. 6, p. 516–529.

Amsden, T. W.; and Sweet, W. C., 1983, Upper Bromide Formation and Viola Group (Middle and Upper Ordovician) in eastern Oklahoma: Oklahoma Geological Survey Bulletin, v. 132, 78 p.

Angelin, N. P., 1851-1878, Palaeontologica Svecica, Iconographia crustaceorum formationis transitionis: v. 1, p. 1–24, Lund.

_____, 1854, Palaeontologia Scandinavica, Lipsiae, 92 p., 41 pls.

Bathurst, R. G. C., 1987, Diagenetically enhanced bedding in argillaceous platform limestones: stratified cementation and selective compaction: Sedimentology, v. 34, p. 749–778.

Bradley, J. H., Jr., 1930, Fauna of the Kimmswick Limestone of Missouri and Illinois: Contributions from the Walker Museum, v. 2 n. 6, p. 219–290.

Brongniart, A., 1822, Des trilobites, in Brongniart, A; and Desmarest, A. G. (eds.), Histoire naturelle de crustacés fossiles, sous les rapports zoologiques et géologiques. Savoir: Les Trilobites, Levrault, Paris, p. 1–65.

Burmeister, H., 1843, Die Organisation der Trilobiten aus ihren lebenden Verwandten entwickelt; nebst einer systematischen Uebersicht aller zeither beschriebenen Arten, Berlin, 147 p.

Chatterton, B. D. E.; and Ludvigsen, R., 1976, Silicified Middle Ordovician trilobites from the south Nahanni River area, District of Mackenzie, Canada: Palaeontographica Abteilung A, v. 154, p. 1–106.

Chugaeva, M. H., 1958, Ordovician of Kazakhstan: Ordovician trilobites of the Chu-Iliyskie Mountains: Akademia Nauk USSR, Trudy Geological Institute, v. 9, p. 5–138.

Cooper, B. N., 1953, Trilobites from the lower Champlainian formations of the Appalachian Valley: Geological Society of America, Memoir 55, 69 p.

Dean, W. T., 1979, Trilobites from the Long Point Group (Ordovician), Port au Port Peninsula, southwestern Newfoundland: Geological Survey of Canada Bulletin, v. 290, 25 p., 14 pls.

Dekay, J. E., 1824, Observations on the structure of trilobites, and description of an apparently new genus: Annales of the Lyceum of Natural History, New York, v. 1, 174 p.

DeMott, L. L., 1987, Platteville and Decorah trilobites from Illinois and Wisconsin: in, Sloan, R. E., ed., Middle and Late Ordovician Lithostratigraphy and Biostratigraphy of the Upper Mississippi Valley: Minnesota Geological Survey, Report of Investigations 35, p. 63–98.

Duke, W. L., 1990, Geostrophic circulation or shallow marine turbidity currents? The dilemma of paleoflow patterns in storm-influence prograding shoreline systems: Journal of Sedimentary Petrology, v. 60, p. 870–883.

Einsele, G.; and Seilacher, A., 1991, Distinction of tempestites and turbidites: in, Einsele, G., Ricken, W., and Seilacher, A., eds., Cycles and Events in Stratigraphy: Springer-Verlag, New York, p. 377–382.

Esker, G. C., III, 1964, New species of trilobites from the Bromide Formation (Pooleville Member) of Oklahoma: Oklahoma Geological Survey Notes, v. 24, n. 9, p. 195–209.

Fortey, R. A., 1980, The Ordovician trilobites of Spitzbergen III: Norsk Polarinstitutt, v. 171, 162 p.

Gentile, L. F.; Donovan, R. N.; and Finney, S. C., 1984, Oriented graptolites as paleocurrent indicators in the lower Viola Springs Formation (Ordovician) in the Arbuckle Mountains and Criner Hills, Oklahoma: Oklahoma Geology Notes, v. 44, n. 4, p. 121–126.

Ham, W. E.; Denison, R. E.; and Merritt, C. A., 1964, Basement rocks and structural evolution of southern Oklahoma: Oklahoma Geological Survey Bulletin, v. 95, 302 p.

Hintze, L. F., 1952, Lower Ordovician trilobites from western Utah and eastern Nevada: Utah Geological and Mineralogical Survey Bulletin, v. 48, 249 p.

_____, 1954, Presbynileus and Protopresbynileus, new generic names proposed for Pseudonileus and Paranileus Hintze, preoccupied: Journal of Paleontology, v. 28, p. 119.

Hoffman, P.; Dewey, J. F.; and Burke, K., 1974, Aulacogens and their genetic relations to geosynclines, with a Proterozoic example from Great Slave Lake, Canada, in Dott, R. J., Jr.; and Shaver, R. H. (eds.), Modern and ancient geosynclinal sedimentation: Society of Economic Paleontologists and Mineralogists, Special Publication, v. 19, p. 38–55.

Hunda, B. R.; Chatterton, B. D. E.; and Ludvigsen, R., 2003, Silicified Late Ordovician trilobites from the Mackenzie Mountains, Northwest Territories, Canada: Palaeontographica Canadiana, v. 21, 87 p.

Jaanusson, V., 1956, Untersuchungen über baltoskandische Asaphiden. III. Über die Gattungen Megistaspis n. nom. und Homalopyge n. gen.: Bulletin of the Geological Institutions of the University of Upsala, v. 36, p. 59–78.

_____. 1959. Suborder Asaphina, in, Moore, R. C. (ed.), Treatise on Invertebrate Paleontology, Part O, Arthropoda, p. 334–365.

Karim, T.; and Westrop, S. R., 2002, Taphonomy and paleoecology of Ordovician trilobite clusters, Bromide Formation, south-central Oklahoma: Palaios, v.17, p. 394–403.

Locke, J. M., 1838, Second Annual Report of the Geology Survey of Ohio. Columbia.

NRIS (Natural Resources Information System) Well Database: Oklahoma Geological Survey, Norman, Oklahoma.

Owen, D. D., 1852, Report of a geological survey of Wisconsin, Iowa and Minnesota, and incidentally a portion of Nebraska Territory: Report of the Geological Survey of Wisconsin etc., Philadelphia, for 1852, 638 p. 27 pls.

Phleger, F. B., Jr., 1933, Notes on certain Ordovician faunas of the Inyo Mountains, California: Southern California Academy of Sciences Bulletin, v. 32, n. 1, p. 1–21, 2 pls.

Puckette, J.; Zuhair, A.-S.; and Sykes, M., 2000, Viola Group reservoir facies, Fitts Pool, Pontotoc County, Oklahoam: Oklahoma Geological Survey, Circular 101, p. 117–127.

Raymond, P. E., 1905, Trilobites of the Chazy Limestone: Annals of the Carnegie Museum, v. 3, p. 328-396, pls. 10–14.

_____, 1910a, Notes on Ordovician trilobites. II. Asaphidae from Beekmantown: Annals of the Carnegie Museum, v. 7, p. 35–44.

_____, 1910b, Notes on Ordovician trilobites . IV. New and old species from the Chazy: American Journal of Science, Series 4, v. 19, p. 60-80, pls. 17–19.

_____, 1910c, Trilobites of the Chazy Formation in Vermont: Report of the Vermont State Geologist, 1909-1910, p. 213–248, pls. 32–39.

_____, 1912, Notes on parallelism among the Asaphidae: Transactions of the Royal Society of Canada, v. 4, p. 111–120, 3 pls.

_____, 1913, Notes on some new and old trilobites in the Victoria Memorial Museum: Bulletin of the Victoria Memorial Museum, Geology Survey of Canada, v. 1, 45 p.

_____, 1914, Notes on the ontogeny of Isotelus gigas Dekay: Bulletin of the Museum of Comparative Zoooloy, v. 58, n. 5, 247–263, 3 pls.

_____, 1920, Some new Ordovician trilobites: Bulletin of the Museum of Comparative Zoology, v. 64, n. 2, p. 273–296.

Raymond, P. E.; and Narraway, J. E., 1910, Notes on Ordovician trilobites. III. Asaphidae from the Lowville and Black River: Annals of the Carnegie Museum, v. 7, p. 46–59.

Reed, F. R. C., 1904, The lower Palaeozoic trilobites of the Girvan District, Ayrshire. Part II: Palaeontographical Society, London.

Ross, R. J., Jr., 1951, Stratigraphy of the Garden City Formation in northeastern Utah, and its trilobite faunas: Peabody Museum of Natural History Bulletin, v. 6, 161 p., 35 pls.

_____, 1967, Some Middle Ordovician brachiopods and trilobites from the Basin Ranges, western United States: Geological Survey Professional Paper, v. 523-D, 43 p., 10 pls.

Ross, R. J., Jr.; and Shaw, F. C., 1972, Distribution of the Middle Ordovician Copenhagen Formation and its trilobites in Nevada: Geological Survey Professional Paper, v. 749, 33 p., 8 pls.

Rudkin, D. M.; and Tripp, R. P., 1989, The type species of the Ordovician trilobite genus Isotelus: I. gigas Dekay, 1824: Royal Ontario Museum, Life Sciences Contributions, v. 152, 19 p.

Rudkin, D. M.; Young, G. A.; Elias, R. J.; and Dobrzanski, E. P., 2003, The world's biggest trilobite – Isotelus rex new species from the Upper Ordovician of northern Manitoba, Canada: Journal of Paleontology, v. 77, n. 1, p. 99–112.

Salter, J. W., 1864, A monograph of the British trilobites from the Cambrian, Silurian, and Devonian formations: Palaeontographical Society, London, 224 p., 30 pls.

Shaw, F. C., 1968, Early Middle Ordovician Chazy trilobites of New York state: New York State Museum Memoir, v. 17, 162 p.

Shergold, J. H., 1971, Late Upper Cambrian trilobites from the Gola Beds, western Queensland: Commonwealth of Australia, Department of National Devleopment, Bureau of Mineral Resources, Geology and Geophysics, Bulletin 112, 127 p.

Slocom, A. W., 1913, New trilobites from the Maquoketa beds of Fayette County, Iowa: Field Museum of Natural History, Geology, v. 4, p. 43-83, pls. 13–18.

Speyer, S. E.; and Brett, C. E., 1985, Clustered trilobite assemblages in the Middle Devonian Hamilton Group: Lethaia, v. 18, p. 85–103.

Stokes, C., 1824, On a trilobite from Lake Huron, in Bigsby, J. J. (ed.), Notes on the Geography and Geology of Lake Huron: Transactions of the Geological Society, series 2, v. 1, p. 175–209.

Tremblay, J. V.; and Westrop, S. R., 1991, Middle Ordovician (Whiterockian) trilobites from the Sunblood Formation, District of Mackenzie, Canada: Journal of Paleontology, v. 65, n. 5, p. 801–824.

Tripp, R. P.; and Evitt, W. R., 1986, Silicified trilobites of the family Asaphidae from the Middle Ordovician of Virginia: Palaeontology, v. 29, n. 4, p. 705–724, pls. 54-57.

Troedsson, G. T., 1928, On the Middle and Upper Ordovician faunas of northern Greenland: Part 2: Saertryk af meddelelser om Grønland, 72, 197 p., 56 pls.

Walcott, C. D., 1877, Description of new species of fossils from the Chazy and Trenton limestones: New York State Museum of Natural History, Annual Report, 31, p. 68-71.

_____, 1918, Cambrian geology and paleontology IV. Appendages of trilobites: Smithsonian Miscellaneous Collection, v. 67, n. 4, p. 115–216.

Westrop, S. R.; and Ludvigsen, R., 1983, Systematics and paleoecology of Upper Ordovician trilobites from the Selkirk Member of the Red River Formation, southern Manitoba: Manitoba Department of Energy and Mines, Mineral Resources Division, Geological Report, GR 82-2, 51 p.

Whittington, H. B., 1950, Sixteen Ordovician genotype trilobites: Journal of Paleontology, v. 24, n. 5, p. 531–565.

_____, 1952, A unique remopleuridid trilobite: Breviora, n. 4, 9 p., 1 pl.

_____, 1954, Ordovician trilobites from Silliman's fossil mount, in Miller, A. K.; Youngquist, W.; and Collinson, C. (eds.), Ordovician cephalopod fauna of Baffin Island: Geological Society of America Memoir, v. 62, p. 119–225.

_____, 1965, Trilobites of the Ordovician Table Head Formation, western Newfoundland: Bulletin of the Museum of Comparative Zoology, v. 132, n. 4, p. 275–442, pls. 1-68.

Wilson, A. E., 1947, Trilobita of the Ottawa Formation of the Ottawa-St. Lawrence lowland: Geological Survey of Canada Bulletin, n. 9, 86 p., 10 pls.

APPENDIXES

APPENDIX 1:

Locality Details

The details of collecting localities, as numbered in Figure 3, are given below:

1 Lawrence Quarry (LQ)
Quarry owned by Holcim (US) Inc. located approximately 10 km southwest of Ada, OK.

2. U.S. Highway 99 (99)
Roadcut along west side of U.S. Highway 99, 5 km south of Fittstown, OK .

3. Mosely Creek (MC)
Creek bed 5 km north of Bromide, OK.

4. Bromide Quarry (BQ)
Abandoned quarry about 0.5 km west of Bromide, OK.

5. Camp Classen (CC)
Exposure near top of hill at Boy Scout Camp, about 7 km south west of Davis, OK near Lake Classen.

6. Interstate 35 (I-35)
Roadcut along east and west sides of northbound lanes of Interstate 35, 17 km south of Davis, OK.

7. U.S. Highway 77 (77)
Roadcut along east side of U.S. Highway 77, about 17 km south of Davis, OK.

8. Nebo (Nebo)
Hillside exposure and stream cut, about 2.5 km west of Nebo, OK and about 1.5 km south of section-line road.

9. Burns Quarry (CN)
Abandoned quarry in northern part of Criner Hills, 5 km south and 2.5 km west of I-35/I-70 interchange, southwest of Ardmore, OK.

10. South Quarry (SQ)
Abandoned quarry in southern part of Criner Hills, 1.5 km west of I-35 and 9 k south of I-70, southwest of Ardmore, OK.

APPENDIX 2:

Stratigraphic Columns

I measured and logged eight stratigraphic sections of the Viola Group in the Arbuckle Mountains and Criner Hills (Fig. 3). These are figured as stratigraphic columns on the following pages. The key below explains symbols used in the columns. Trilobite collecting horizons are indicated by arrows and described in italics.

Stratigraphic Column
Key

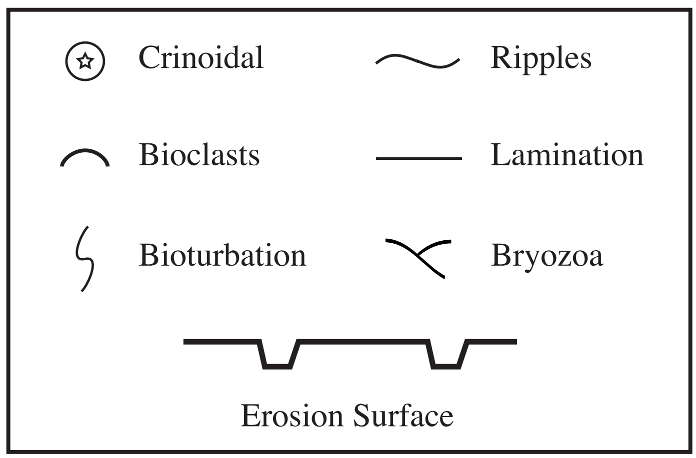

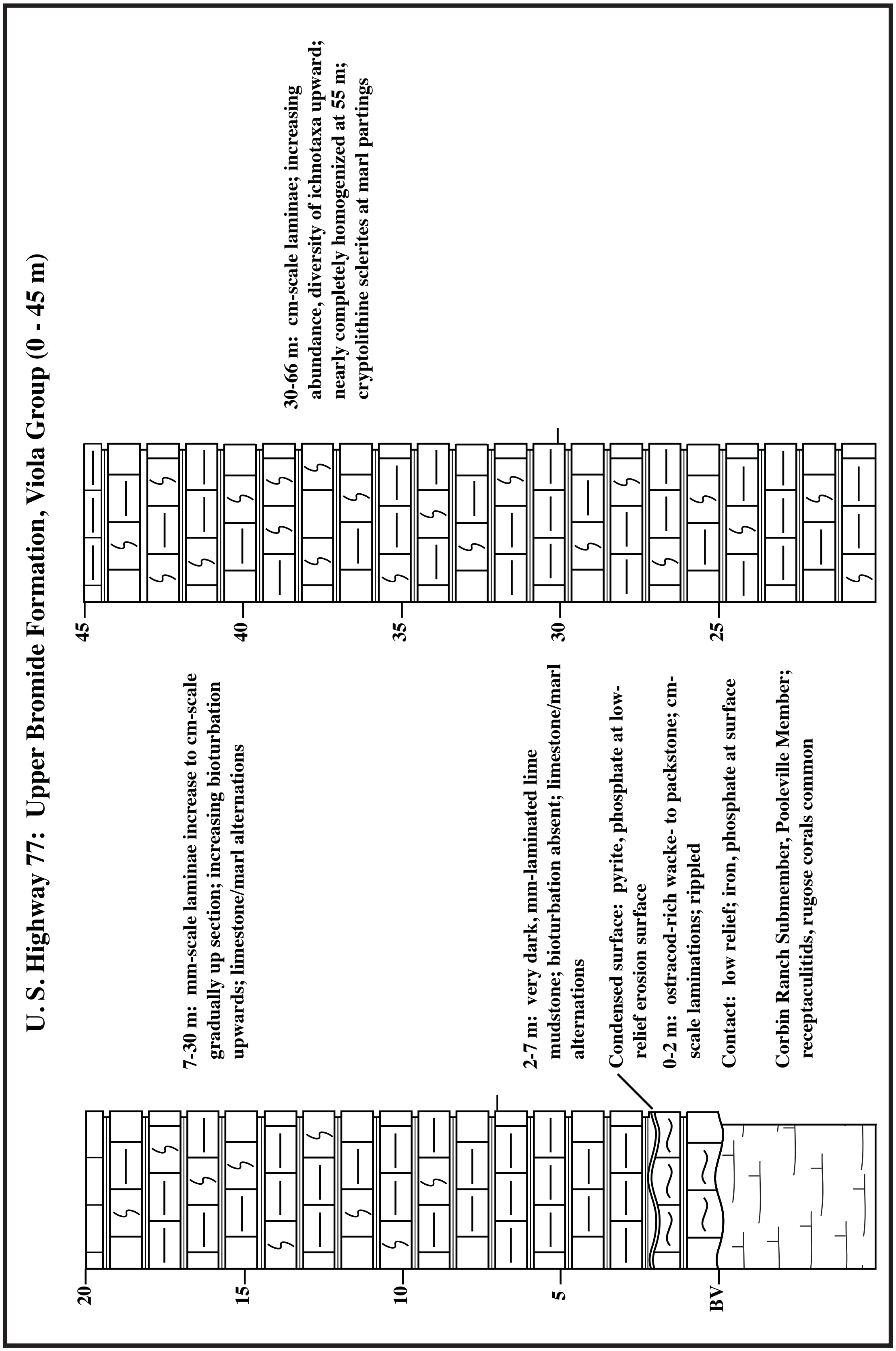
U. S. Highway 77: Upper Bromide Formation, Viola Group (0 - 45 m)
7-30 m: mm-scale laminae increase to cm-scale gradually up section; increasing bioturbation upwards; limestone/marl alternations
2-7 m: very dark, mm-laminated lime mudstone; bioturbation absent; limestone/marl alternations
Condensed surface: pyrite, phosphate at low-relief erosion surface
0-2 m: ostracod-rich wacke- to packstone; cm-scale laminations; rippled
Contact: low relief; iron, phosphate at surface
Corbin Ranch Submember, Pooleville Member; receptaculitids, rugose corals common
30-66 m: cm-scale laminae; increasing abundance, diversity of ichnotaxa upward; nearly completely homogenized at 55 m; cryptolithine sclerites at marl partings
20
15
10
5
BV
45
40
35
30
25

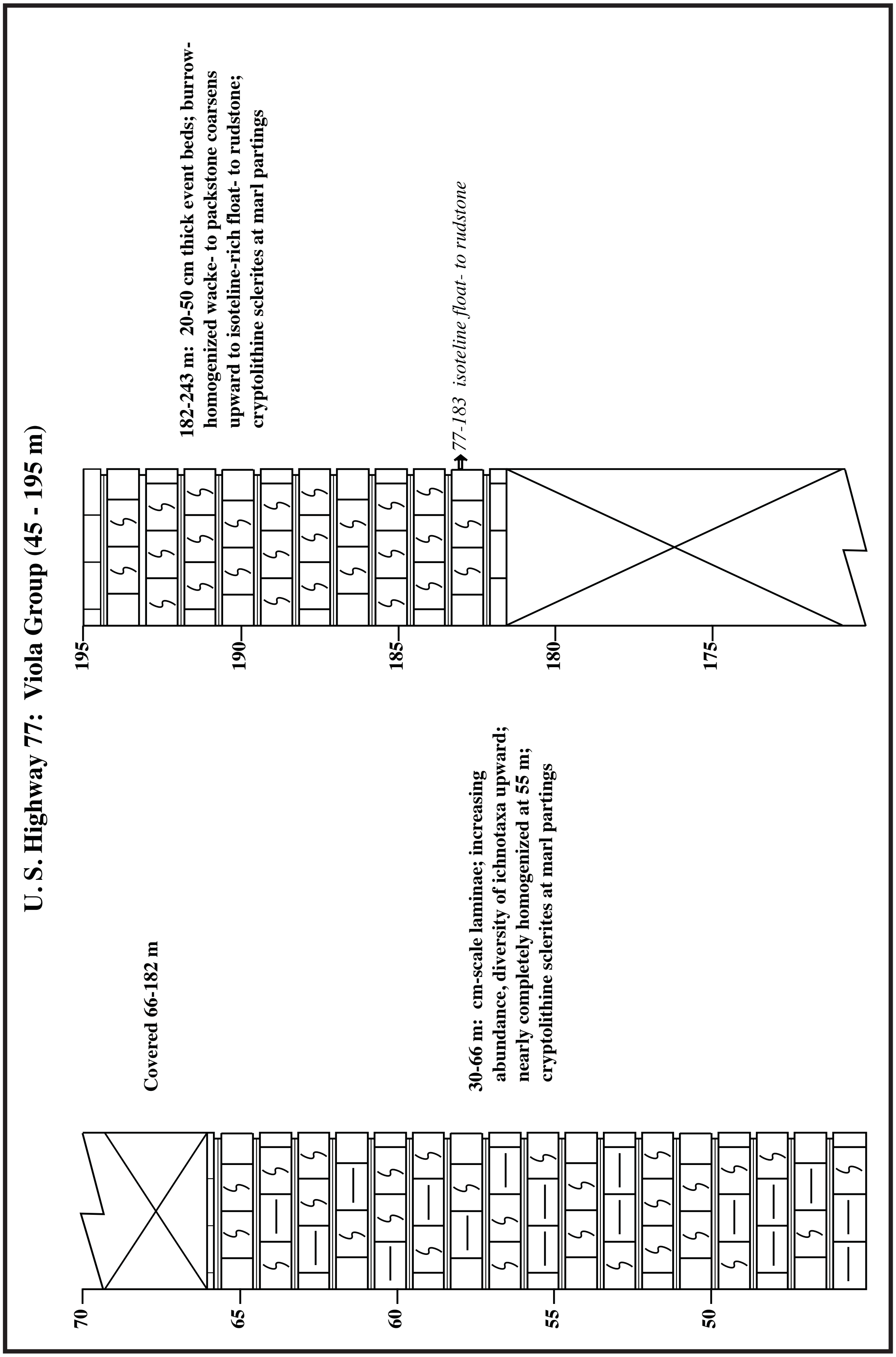
U. S. Highway 77: Viola Group (45 - 195 m)
182-243 m: 20-50 cm thick event beds; burrow-homogenized wacke- to packstone coarsens upward to isoteline-rich float- to rudstone; cryptolithine sclerites at marl partings
77-183 isoteline float- to rudstone
195
190
185
180
175
Covered 66-182 m
30-66 m: cm-scale laminae; increasing abundance, diversity of ichnotaxa upward; nearly completely homogenized at 55 m; cryptolithine sclerites at marl partings
70
65
60
55
50

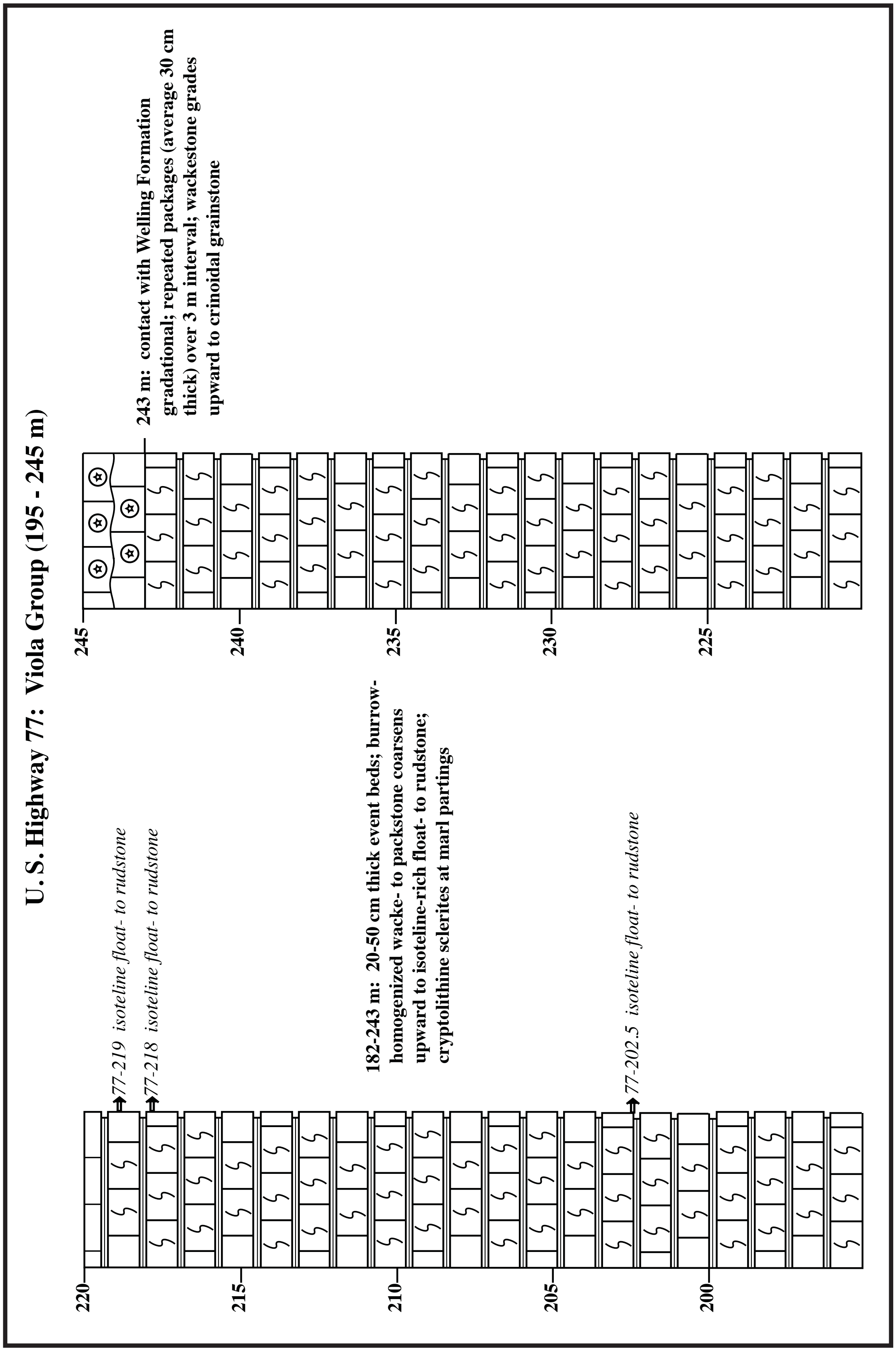
U. S. Highway 77: Viola Group (195 - 245 m)
243 m: contact with Welling Formation gradational; repeated packages (average 30 cm thick) over 3 m interval; wackestone grades upward to crinoidal grainstone
245
240
235
230
225
77-219 isoteline float- to rudstone
77-218 isoteline float- to rudstone
182-243 m: 20-50 cm thick event beds; burrow-homogenized wacke- to packstone coarsens upward to isoteline-rich float- to rudstone; cryptolithine sclerites at marl partings
77-202.5 isoteline float- to rudstone
220
215
210
205
200

U.S. Highway 77: Viola Group (245 - 252m)

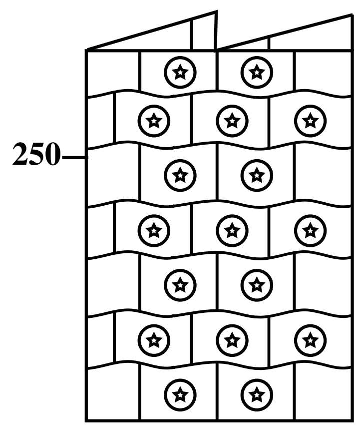

Welling Formation: crinoidal grainstone; beds separated by scours; large isoteline bioclasts (up to 8 cm diameter) occur rarely

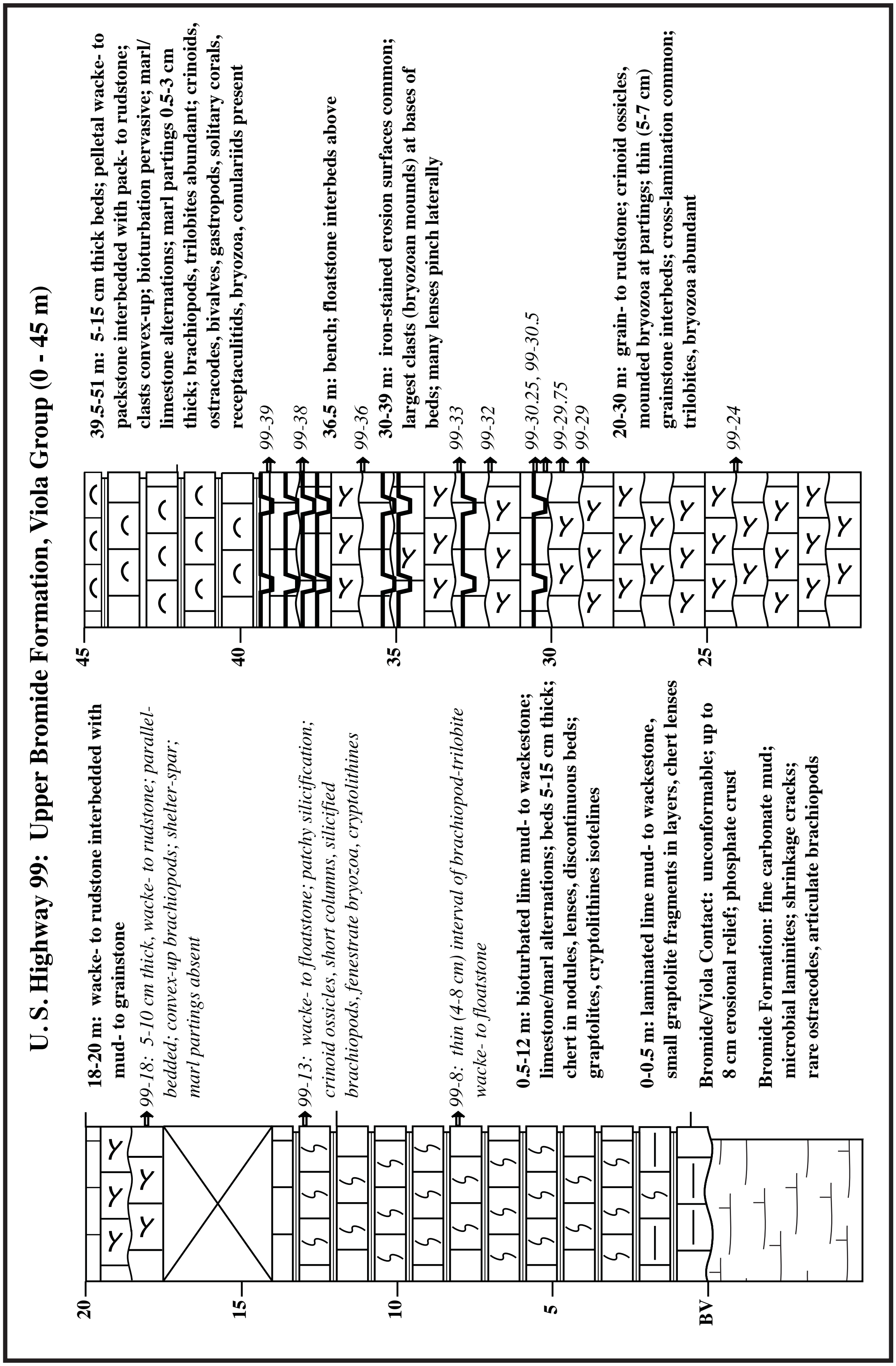
U. S. Highway 99: Upper Bromide Formation, Viola Group (0 - 45 m)
20
15
10
5
BV
18-20 m: wacke- to rudstone interbedded with mud- to grainstone
99-18: 5-10 cm thick, wacke- to rudstone; parallel-bedded; convex-up brachiopods; shelter-spar; marl partings absent
99-13: wacke- to floatstone; patchy silicification; crinoid ossicles, short columns, silicified brachiopods, fenestrate bryozoa, cryptolithines
99-8: thin (4-8 cm) interval of brachiopod-trilobite wacke- to floatstone
0.5-12 m: bioturbated lime mud- to wackestone; limestone/marl alternations; beds 5-15 cm thick; chert in nodules, lenses, discontinuous beds; graptolites, cryptolithines isotelines
0-0.5 m: laminated lime mud- to wackestone, small graptolite fragments in layers, chert lenses
Bromide/Viola Contact: unconformable; up to 8 cm erosional relief; phosphate crust
Bromide Formation: fine carbonate mud; microbial laminites; shrinkage cracks; rare ostracodes, articulate brachiopods
45
40
35
30
25
39.5-51 m: 5-15 cm thick beds; pelletal wacke- to packstone interbedded with pack- to rudstone; clasts convex-up; bioturbation pervasive; marl/limestone alternations; marl partings 0.5-3 cm thick; brachiopods, trilobites abundant; crinoids, ostracodes, bivalves, gastropods, solitary corals, receptaculitids, bryozoa, conulariids present
99-39
99-38
36.5 m: bench; floatstone interbeds above
99-36
30-39 m: iron-stained erosion surfaces common; largest clasts (bryozoan mounds) at bases of beds; many lenses pinch laterally
99-33
99-32
99-30.25, 99-30.5
99-29.75
99-29
20-30 m: grain- to rudstone; crinoid ossicles, mounded bryozoa at partings; thin (5-7 cm) grainstone interbeds; cross-lamination common; trilobites, bryozoa abundant
99-24

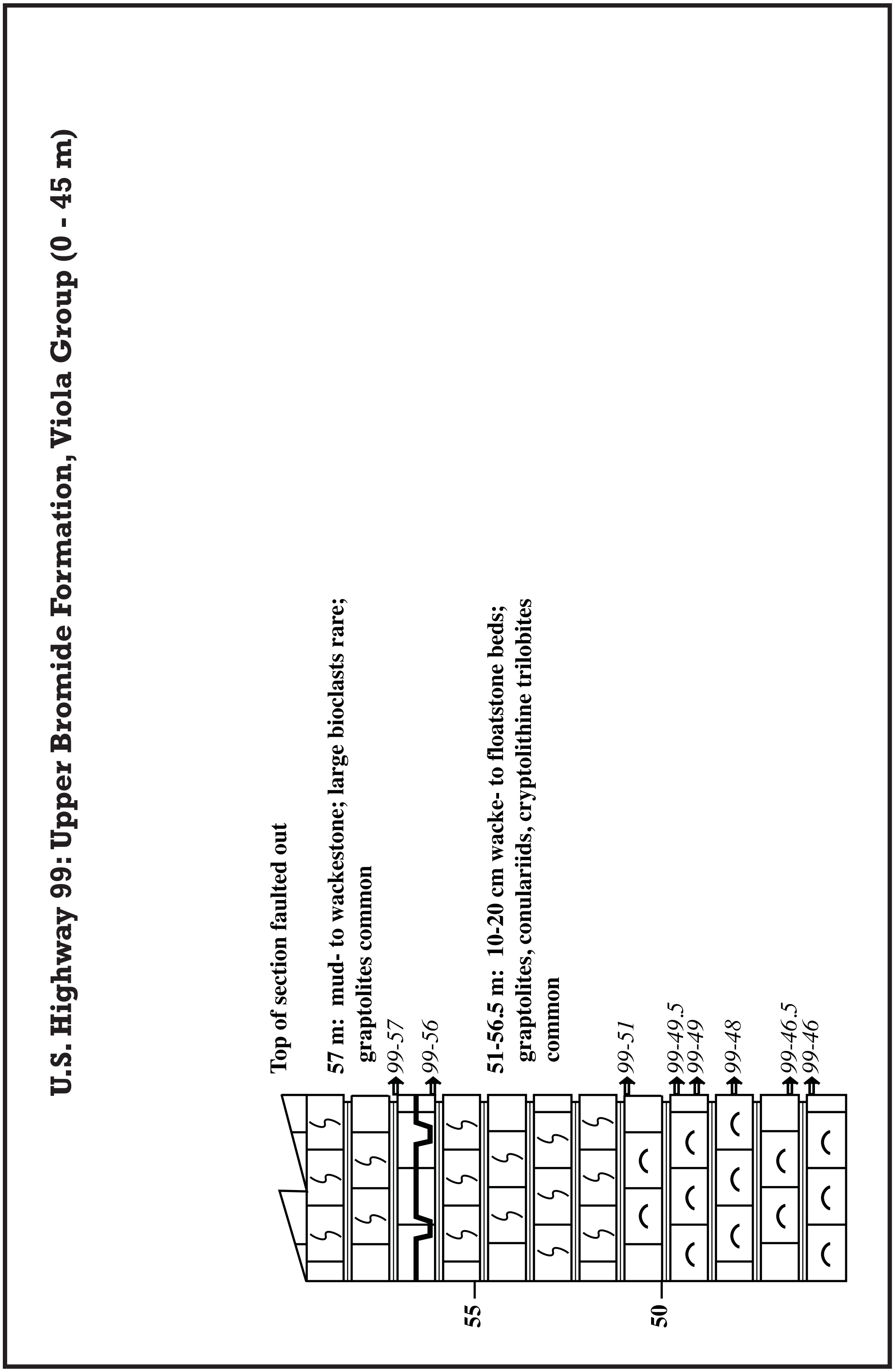
U.S. Highway 99: Upper Bromide Formation, Viola Group (0 - 45 m)
Top of section faulted out
57 m: mud- to wackestone; large bioclasts rare; graptolites common
99-57
99-56
51-56.5 m: 10-20 cm wacke- to floatstone beds; graptolites, conulariids, cryptolithine trilobites common
99-51
99-49.5
99-49
99-48
99-46.5
99-46
55
50

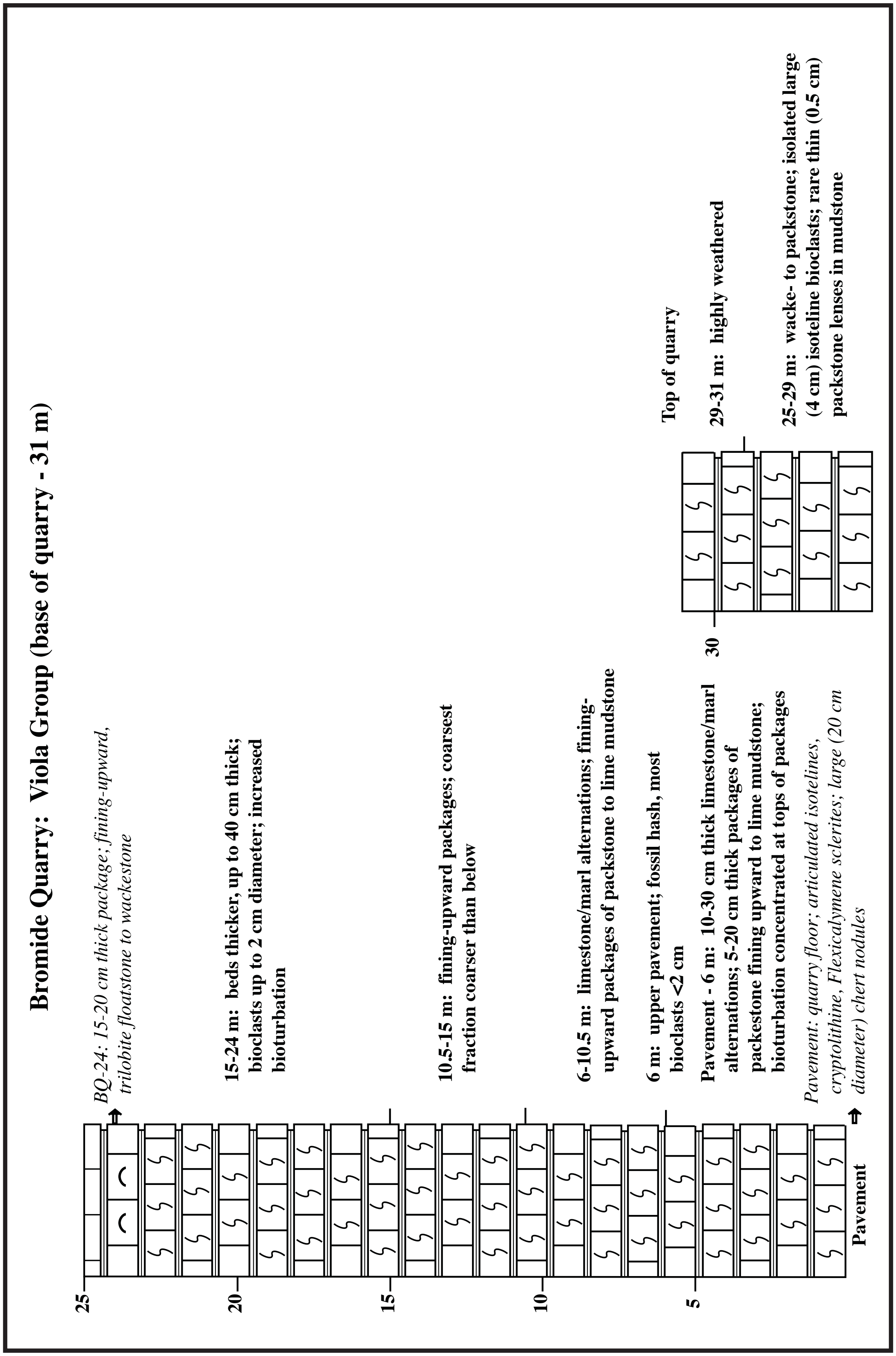
Bromide Quarry: Viola Group (base of quarry - 31 m)
BQ-24: 15-20 cm thick package; fining-upward, trilobite floatstone to wackestone
15-24 m: beds thicker, up to 40 cm thick; bioclasts up to 2 cm diameter; increased bioturbation
10.5-15 m: fining-upward packages; coarsest fraction coarser than below
6-10.5 m: limestone/marl alternations; fining-upward packages of packstone to lime mudstone
6 m: upper pavement; fossil hash, most bioclasts <2 cm
Pavement - 6 m: 10-30 cm thick limestone/marl alternations; 5-20 cm thick packages of packestone fining upward to lime mudstone; bioturbation concentrated at tops of packages
Pavement: quarry floor; articulated isotelines, cryptolithine, Flexicalymene sclerites; large (20 cm diameter) chert nodules
Pavement
25
20
15
10
5
30
Top of quarry
29-31 m: highly weathered
25-29 m: wacke- to packstone; isolated large (4 cm) isoteline bioclasts; rare thin (0.5 cm) packstone lenses in mudstone

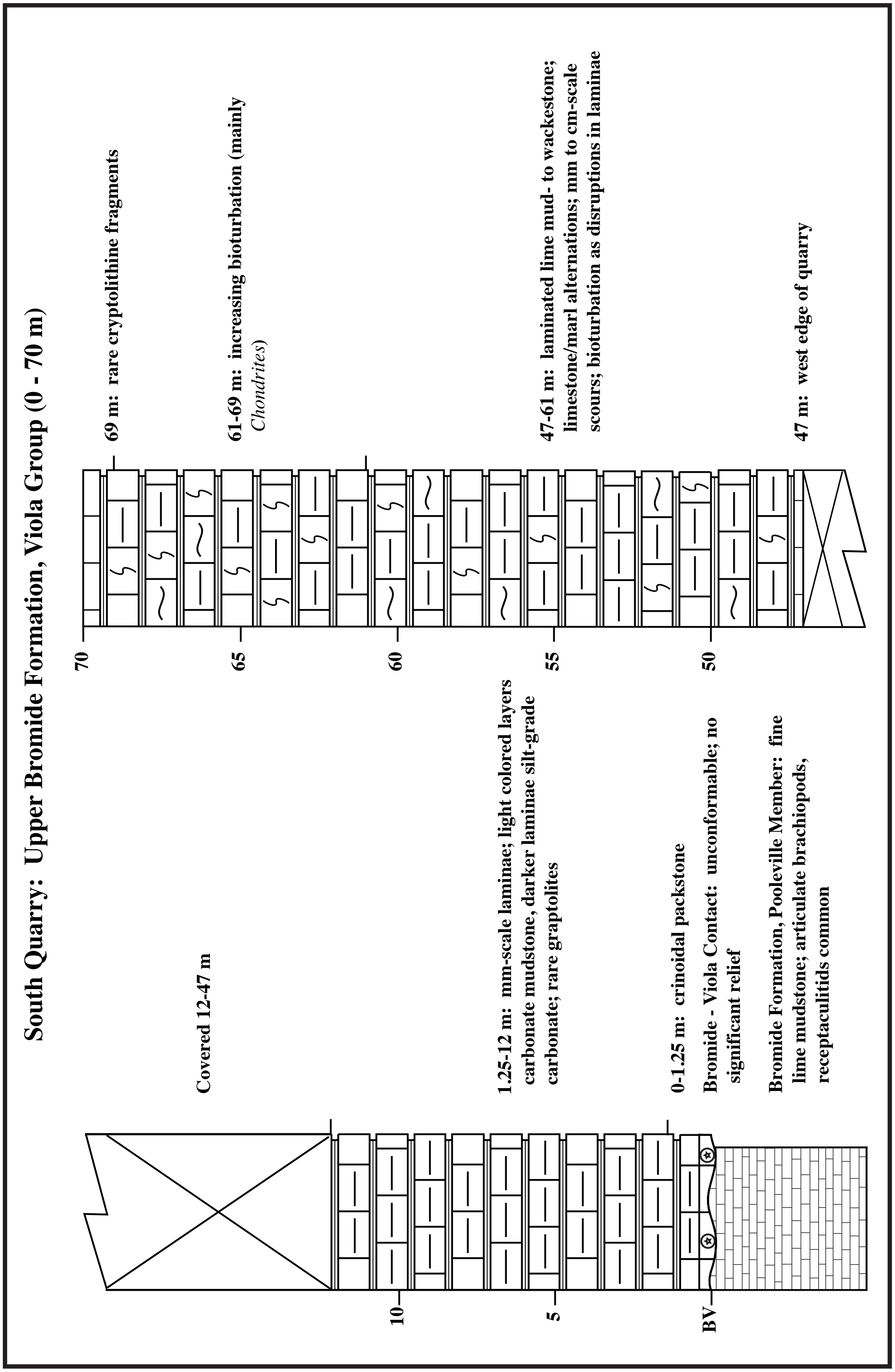
South Quarry: Upper Bromide Formation, Viola Group (0 - 70 m)
Covered 12-47 m
1.25-12 m: mm-scale laminae; light colored layers carbonate mudstone, darker laminae silt-grade carbonate; rare graptolites
0-1.25 m: crinoidal packstone
Bromide - Viola Contact: unconformable; no significant relief
Bromide Formation, Pooleville Member: fine lime mudstone; articulate brachiopods, receptaculitids common
10
5
BV
69 m: rare cryptolithine fragments
61-69 m: increasing bioturbation (mainly *Chondrites*)
47-61 m: laminated lime mud- to wackestone; limestone/marl alternations; mm to cm-scale scours; bioturbation as disruptions in laminae
47 m: west edge of quarry
70
65
60
55
50

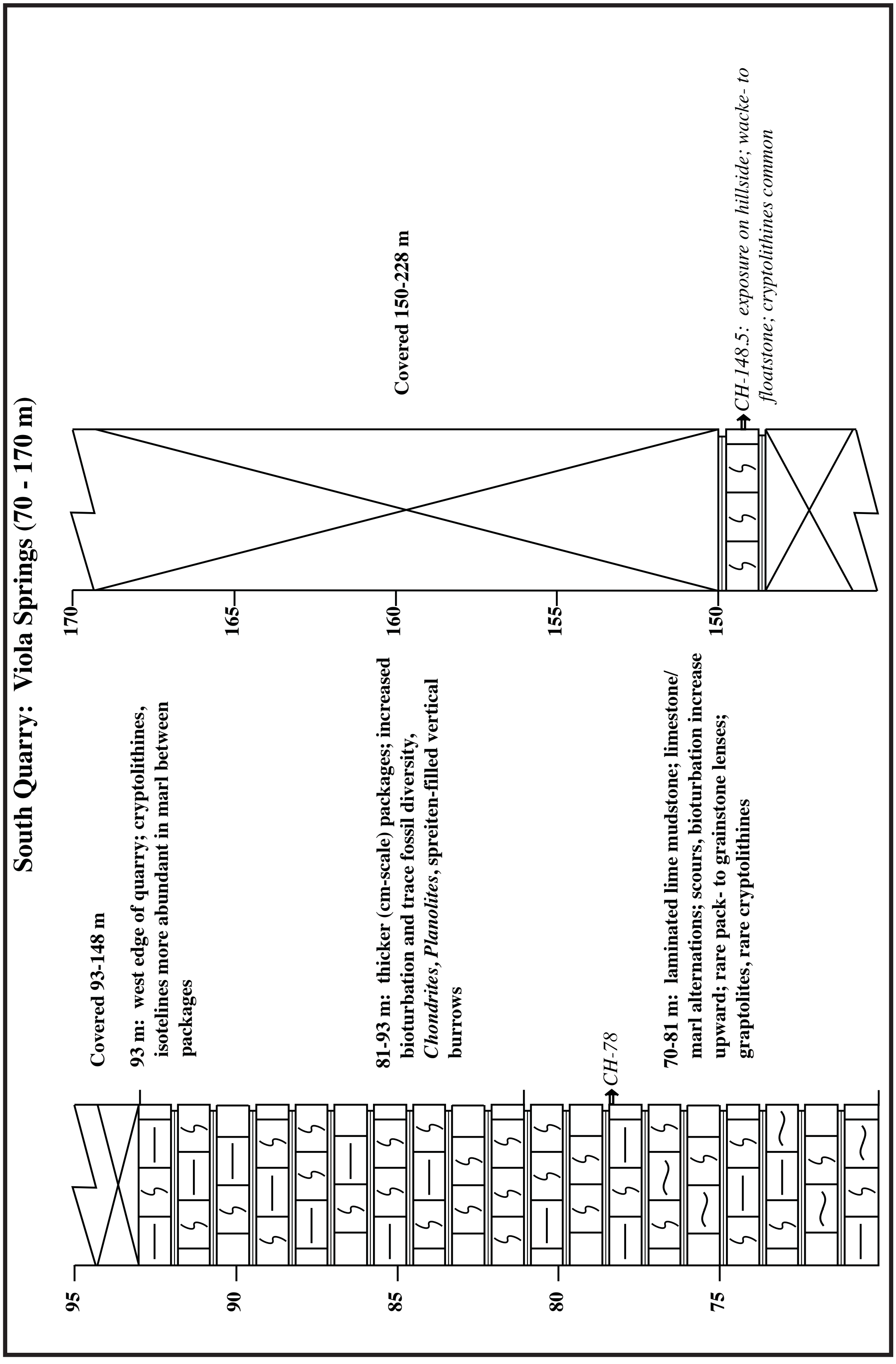
South Quarry: Viola Springs (70 - 170 m)
Covered 93-148 m
93 m: west edge of quarry; cryptolithines, isotelines more abundant in marl between packages
81-93 m: thicker (cm-scale) packages; increased bioturbation and trace fossil diversity, *Chondrites*, *Planolites*, spreiten-filled vertical burrows
CH-78
70-81 m: laminated lime mudstone; limestone/marl alternations; scours, bioturbation increase upward; rare pack- to grainstone lenses; graptolites, rare cryptolithines
95
90
85
80
75
170
165
160
155
150
Covered 150-228 m
CH-148.5: exposure on hillside; wacke- to floatstone; cryptolithines common

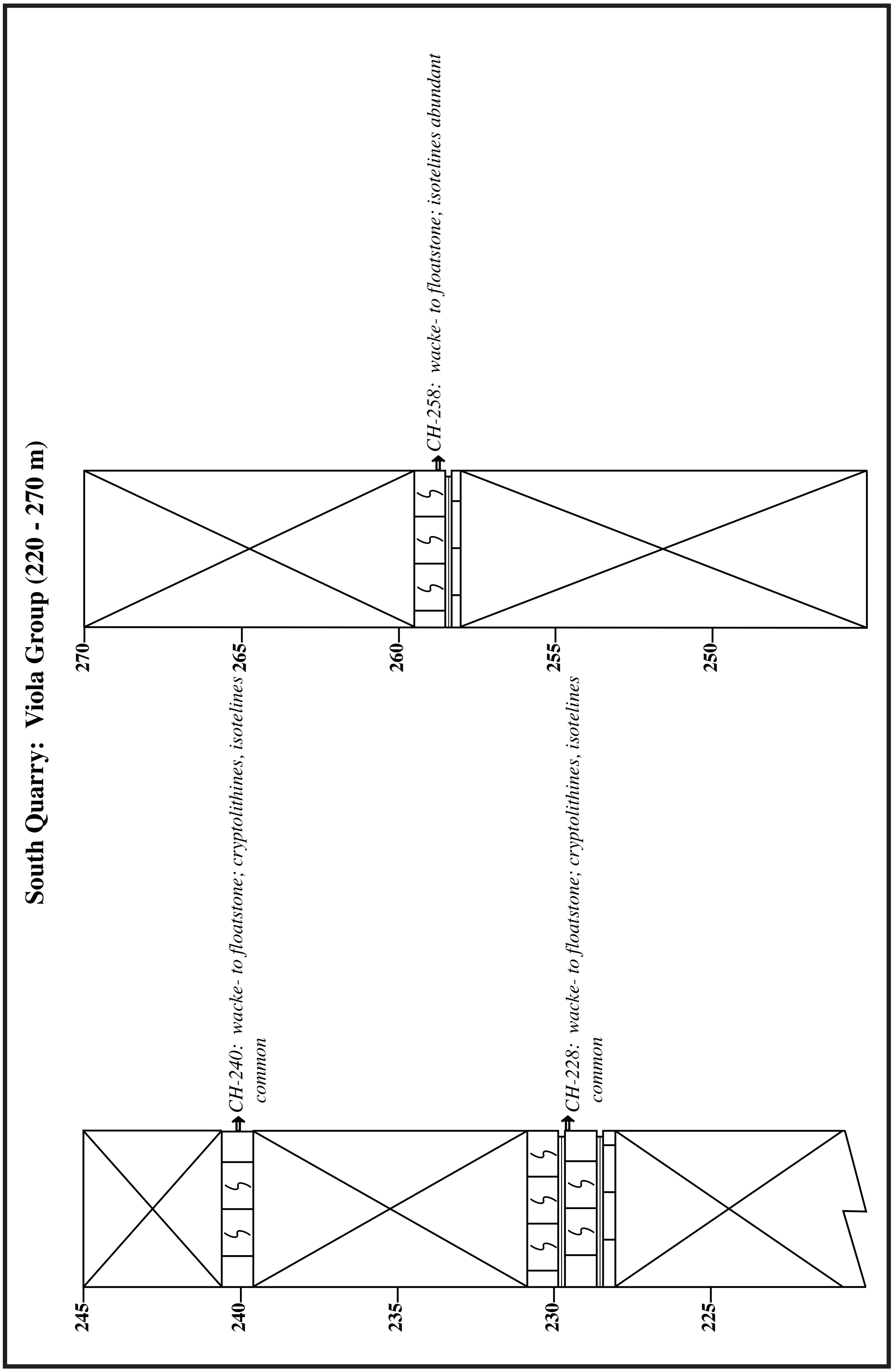
South Quarry: Viola Group (220 - 270 m)
CH-258: wacke- to floatstone; isotelines abundant
270
265
260
255
250
CH-240: wacke- to floatstone; cryptolithines, isotelines common
CH-228: wacke- to floatstone; cryptolithines, isotelines common
245
240
235
230
225

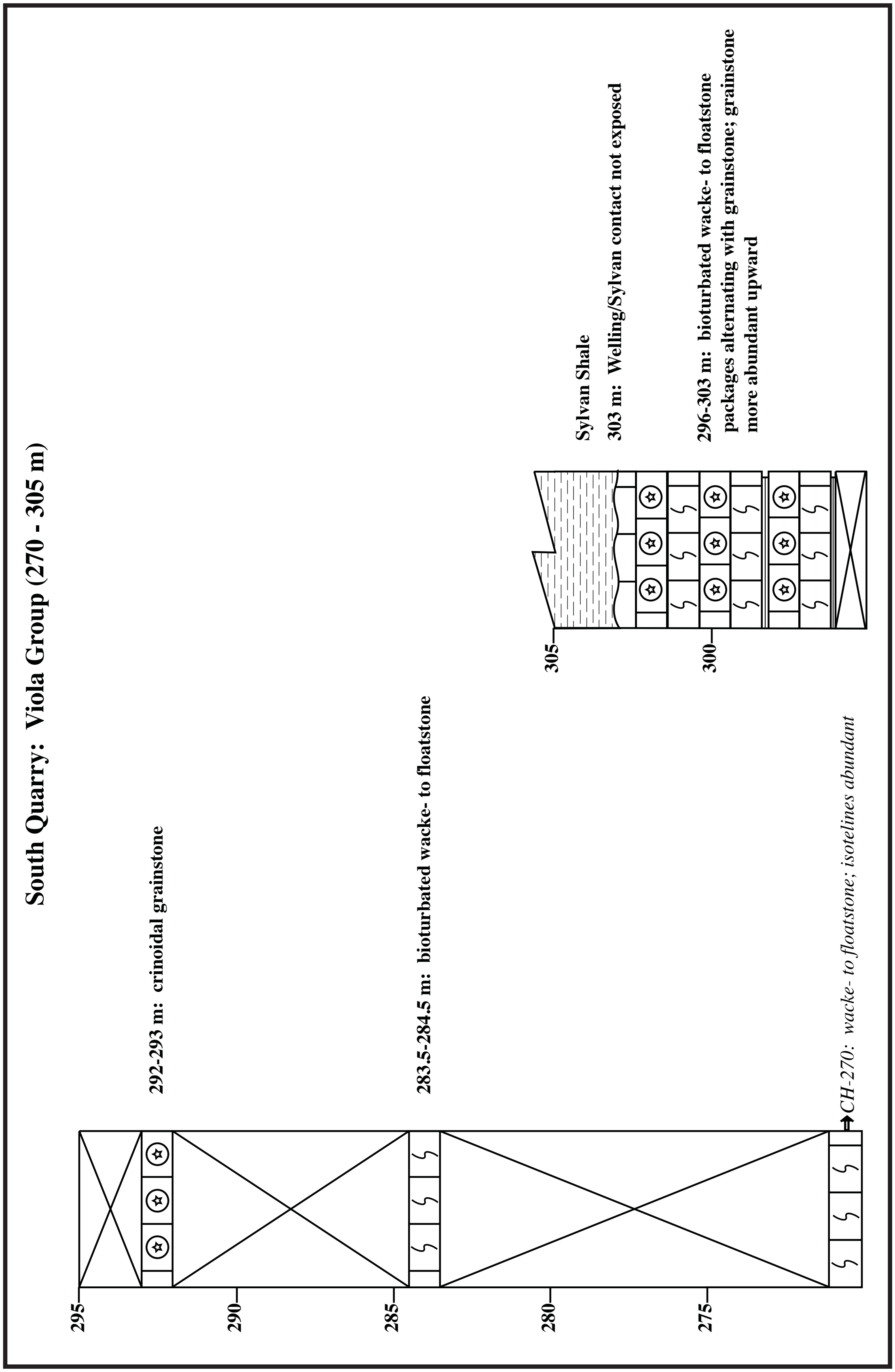
South Quarry: Viola Group (270 - 305 m)
Sylvan Shale
303 m: Welling/Sylvan contact not exposed
296-303 m: bioturbated wacke- to floatstone packages alternating with grainstone; grainstone more abundant upward
305
300
292-293 m: crinoidal grainstone
283.5-284.5 m: bioturbated wacke- to floatstone
CH-270: wacke- to floatstone; isotelines abundant
295
290
285
280
275

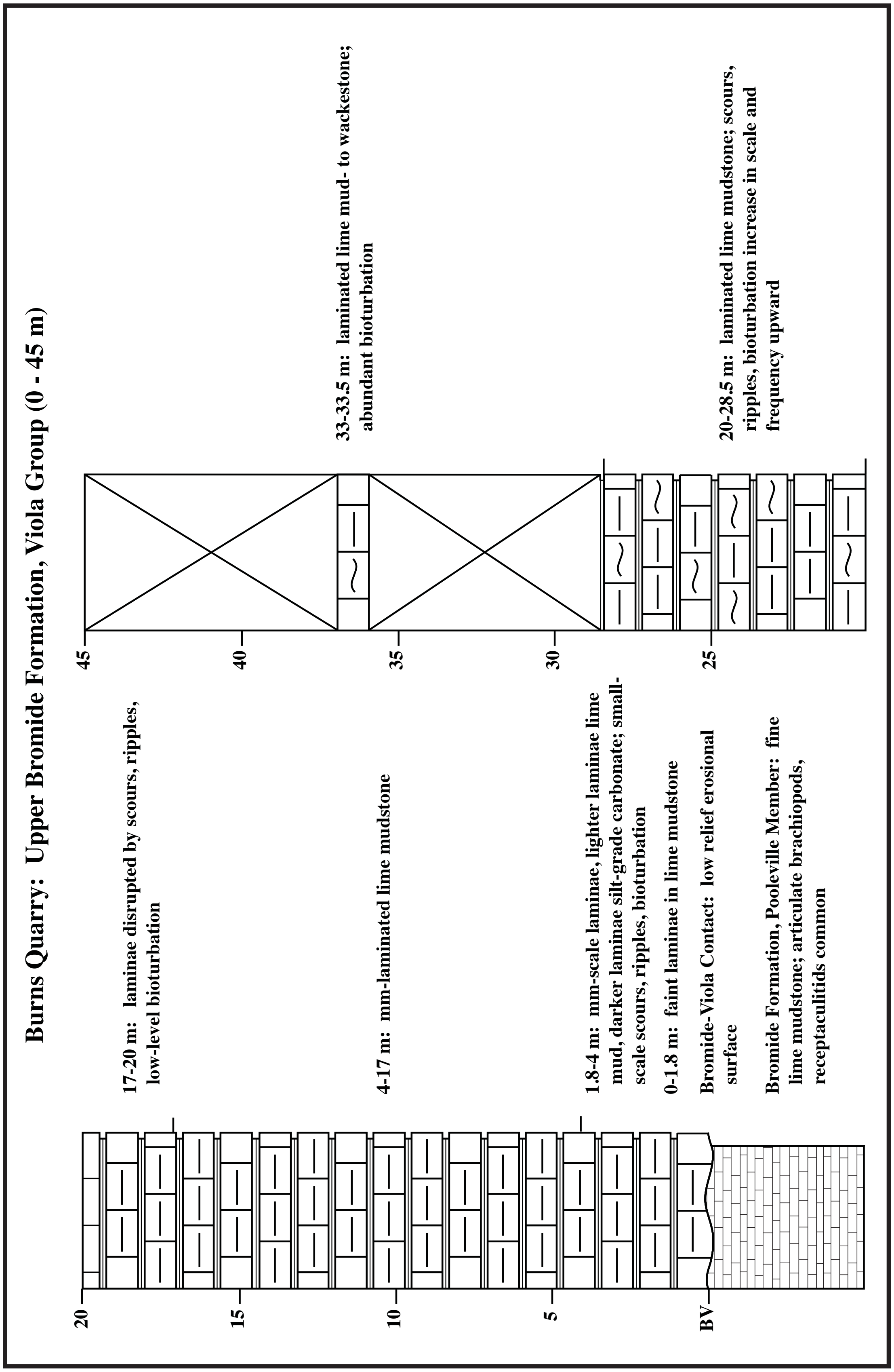
Burns Quarry: Upper Bromide Formation, Viola Group (0 - 45 m)
17-20 m: laminae disrupted by scours, ripples, low-level bioturbation
4-17 m: mm-laminated lime mudstone
1.8-4 m: mm-scale laminae, lighter laminae lime mud, darker laminae silt-grade carbonate; small-scale scours, ripples, bioturbation
0-1.8 m: faint laminae in lime mudstone
Bromide-Viola Contact: low relief erosional surface
Bromide Formation, Pooleville Member: fine lime mudstone; articulate brachiopods, receptaculitids common
33-33.5 m: laminated lime mud- to wackestone; abundant bioturbation
20-28.5 m: laminated lime mudstone; scours, ripples, bioturbation increase in scale and frequency upward
20
15
10
5
BV
45
40
35
30
25

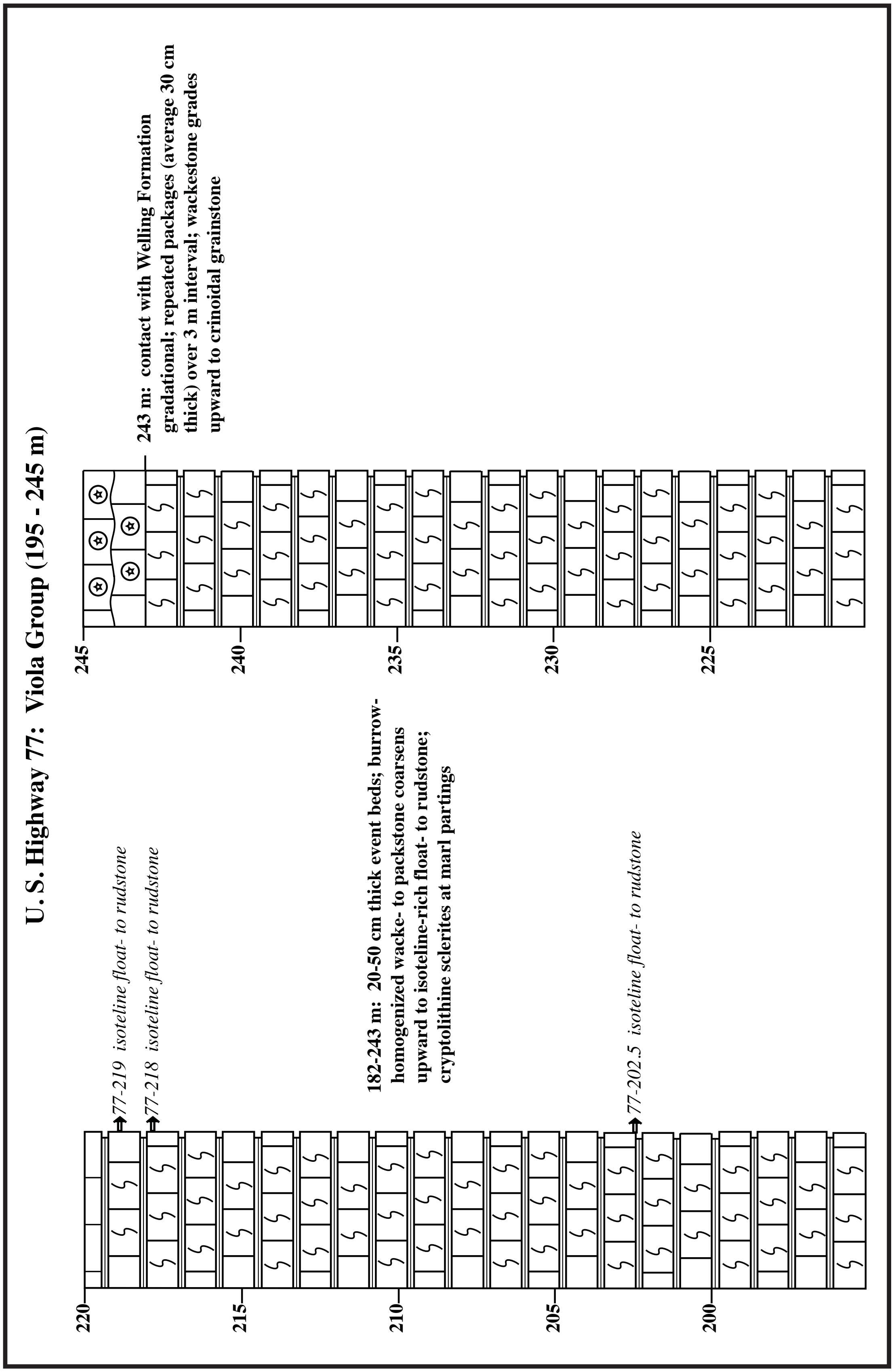
U. S. Highway 77: Viola Group (195 - 245 m)
220
215
210
205
200
77-219 isoteline float- to rudstone
77-218 isoteline float- to rudstone
77-202.5 isoteline float- to rudstone
182-243 m: 20-50 cm thick event beds; burrow-homogenized wacke- to packstone coarsens upward to isoteline-rich float- to rudstone; cryptolithine sclerites at marl partings
245
240
235
230
225
243 m: contact with Welling Formation gradational; repeated packages (average 30 cm thick) over 3 m interval; wackestone grades upward to crinoidal grainstone

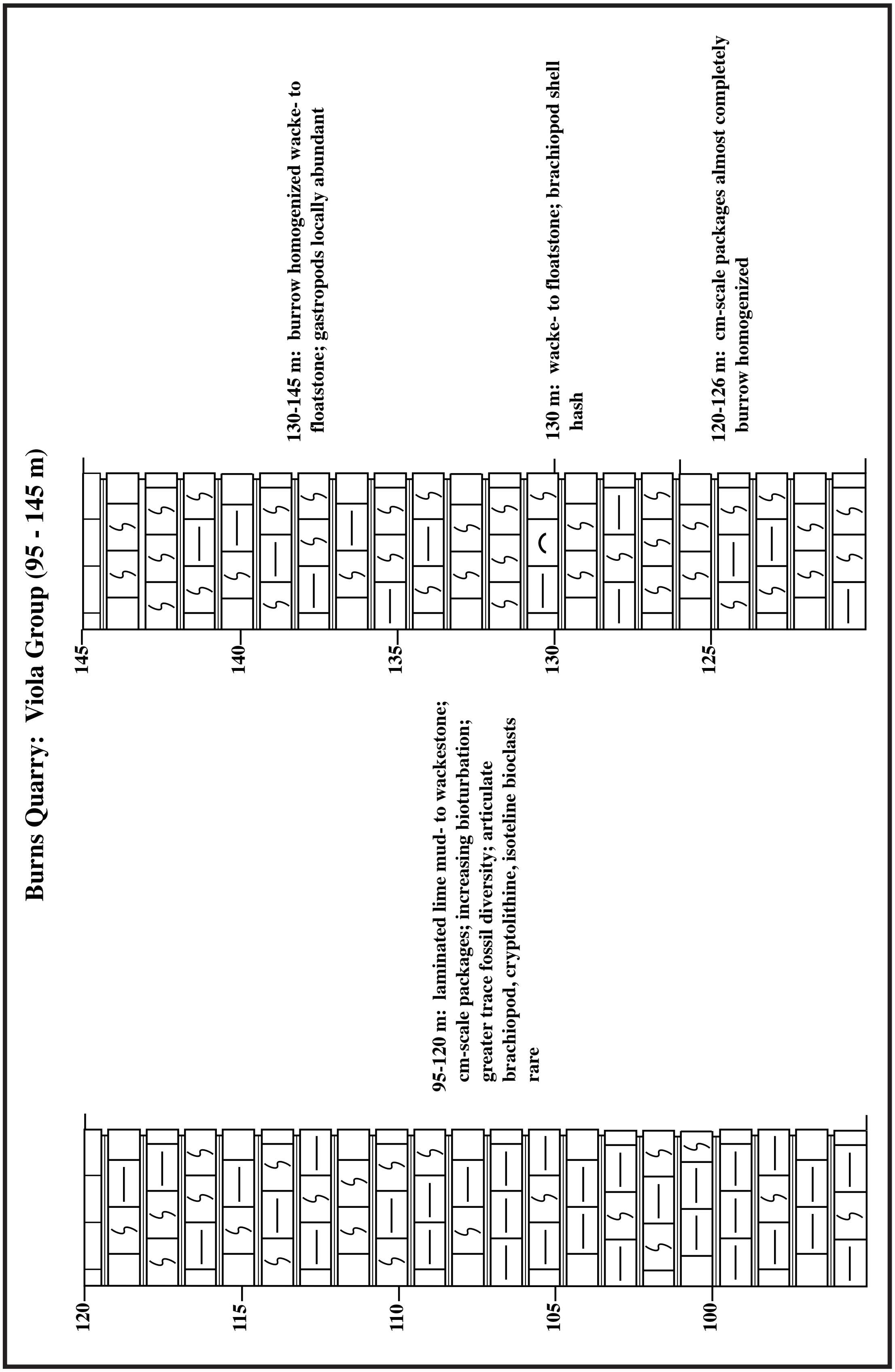
Burns Quarry: Viola Group (95 - 145 m)
130-145 m: burrow homogenized wacke- to floatstone; gastropods locally abundant
130 m: wacke- to floatstone; brachiopod shell hash
120-126 m: cm-scale packages almost completely burrow homogenized
145
140
135
130
125
95-120 m: laminated lime mud- to wackestone; cm-scale packages; increasing bioturbation; greater trace fossil diversity; articulate brachiopod, cryptolithine, isoteline bioclasts rare
120
115
110
105
100

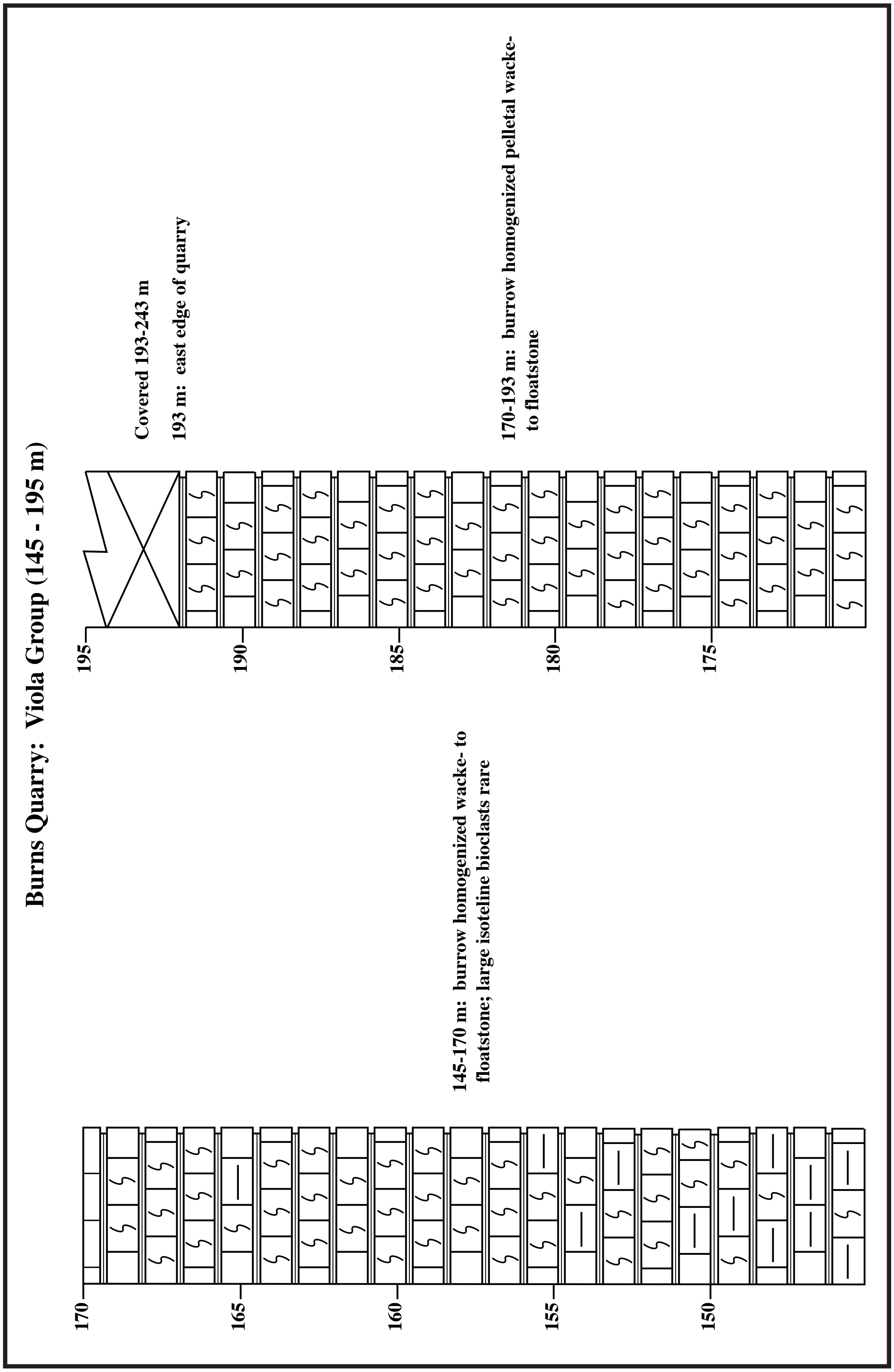
Burns Quarry: Viola Group (145 - 195 m)
Covered 193-243 m
193 m: east edge of quarry
170-193 m: burrow homogenized pelletal wacke- to floatstone
145-170 m: burrow homogenized wacke- to floatstone; large isoteline bioclasts rare
195
190
185
180
175
170
165
160
155
150

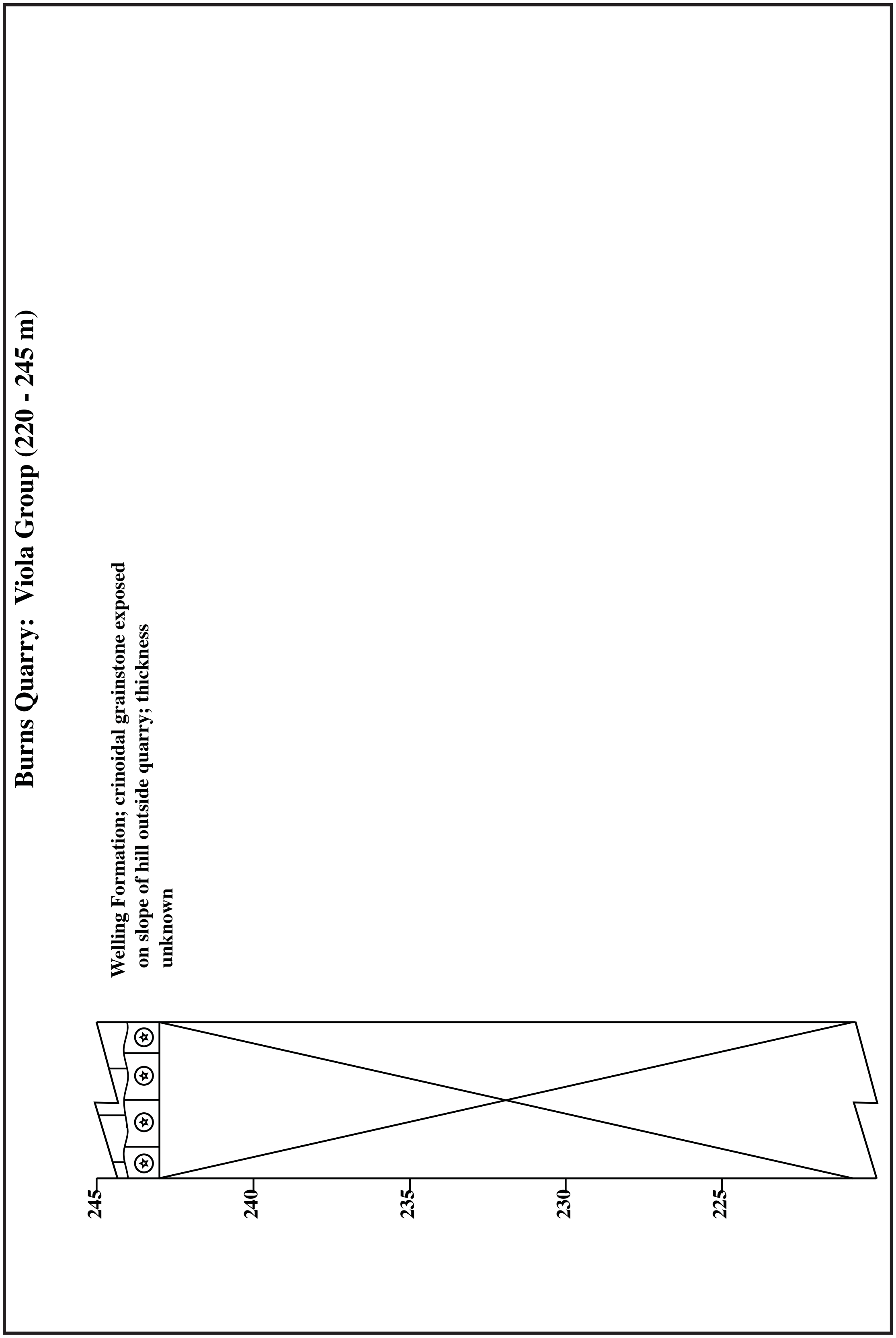
Burns Quarry: Viola Group (220 - 245 m)
Welling Formation; crinoidal grainstone exposed on slope of hill outside quarry; thickness unknown
245
240
235
230
225

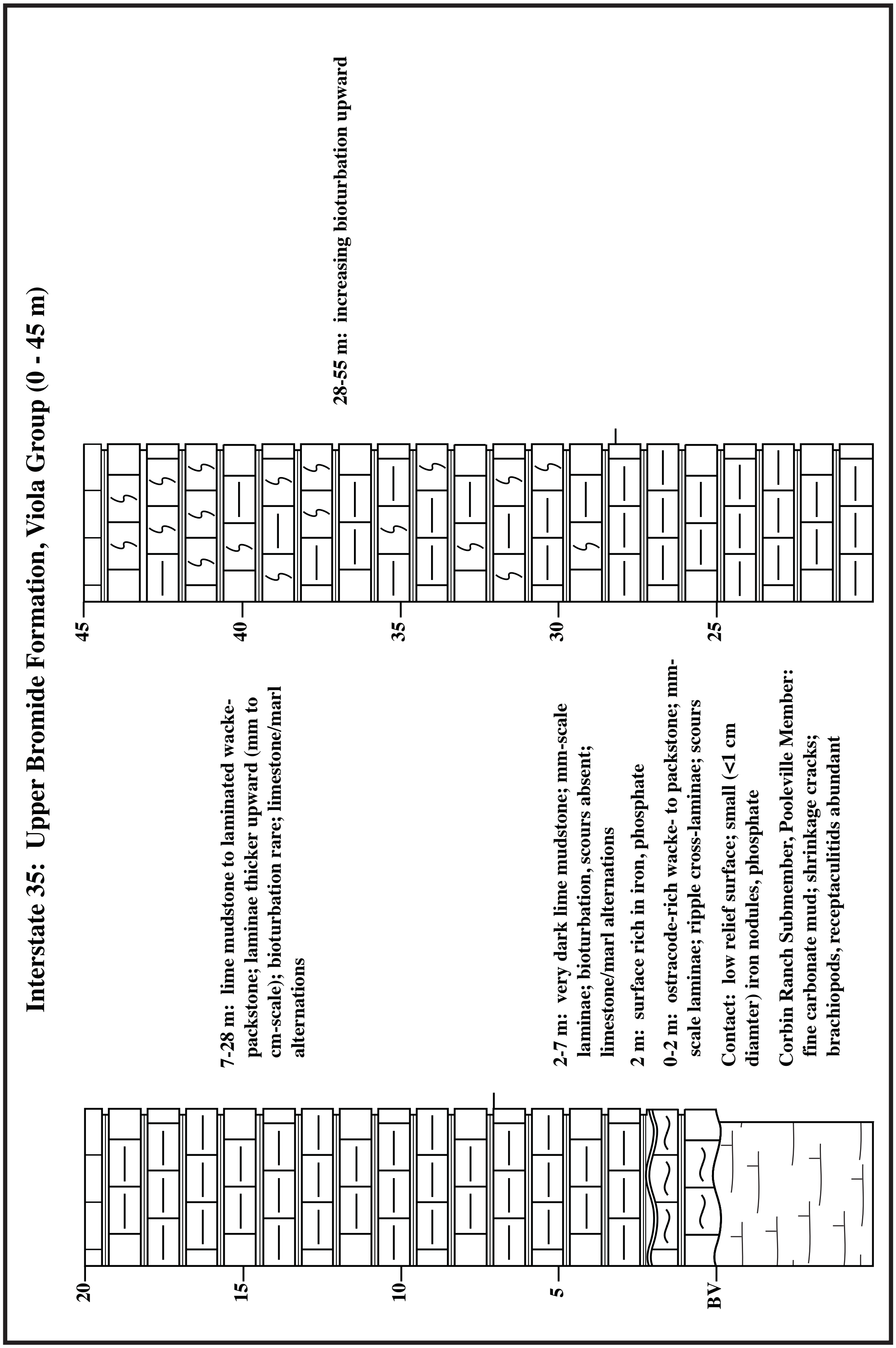
Interstate 35: Upper Bromide Formation, Viola Group (0 - 45 m)
28-55 m: increasing bioturbation upward
45
40
35
30
25
7-28 m: lime mudstone to laminated wacke-packstone; laminae thicker upward (mm to cm-scale); bioturbation rare; limestone/marl alternations
2-7 m: very dark lime mudstone; mm-scale laminae; bioturbation, scours absent; limestone/marl alternations
2 m: surface rich in iron, phosphate
0-2 m: ostracode-rich wacke- to packstone; mm-scale laminae; ripple cross-laminae; scours
Contact: low relief surface; small (<1 cm diamter) iron nodules, phosphate
Corbin Ranch Submember, Pooleville Member: fine carbonate mud; shrinkage cracks; brachiopods, receptaculitids abundant
20
15
10
5
BV

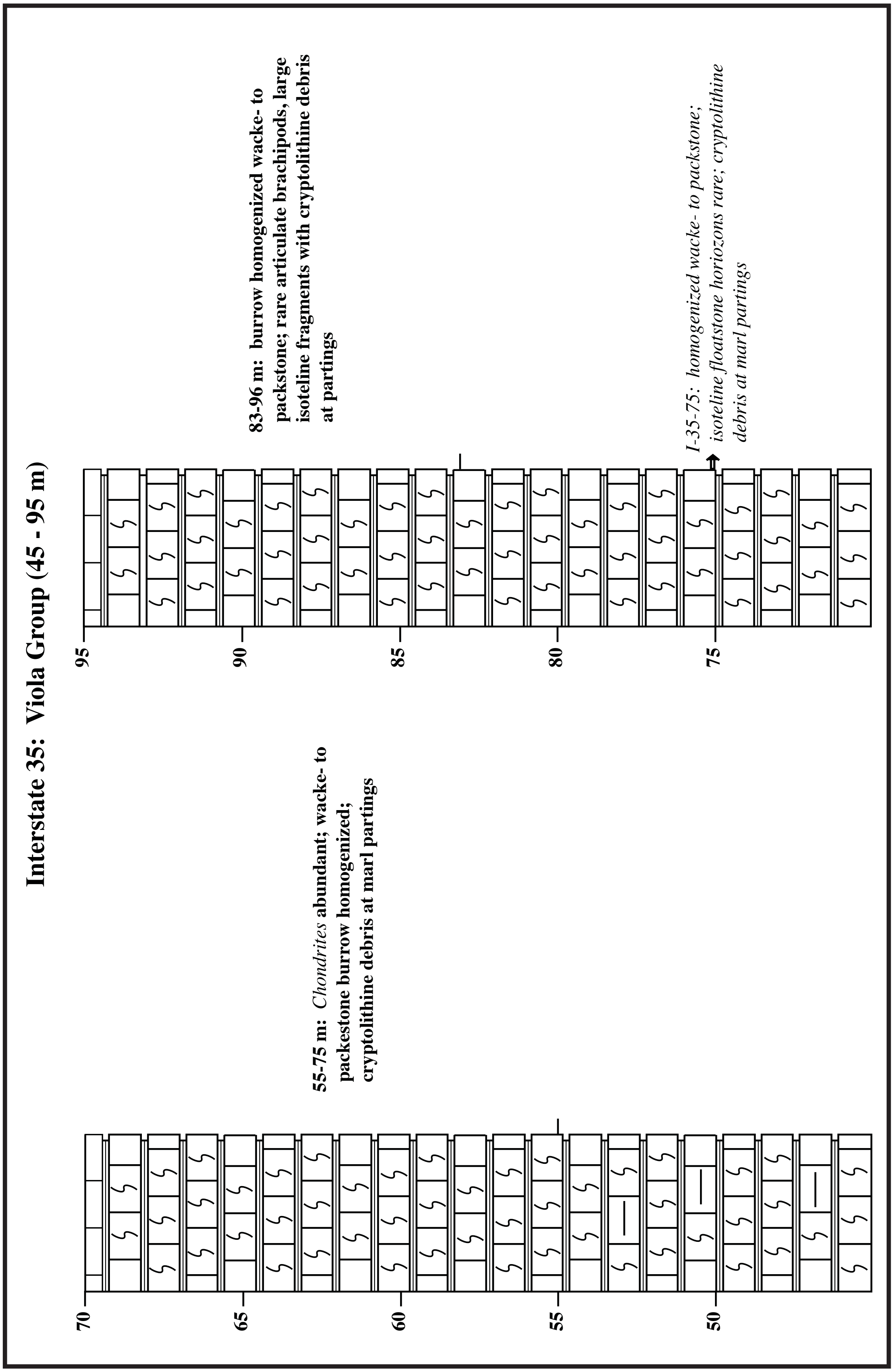
Interstate 35: Viola Group (45 - 95 m)
83-96 m: burrow homogenized wacke- to packstone; rare articulate brachipods, large isoteline fragments with cryptolithine debris at partings
I-35-75: homogenized wacke- to packstone; isoteline floatstone horiozons rare; cryptolithine debris at marl partings
95
90
85
80
75
55-75 m: *Chondrites* abundant; wacke- to packstone burrow homogenized; cryptolithine debris at marl partings
70
65
60
55
50

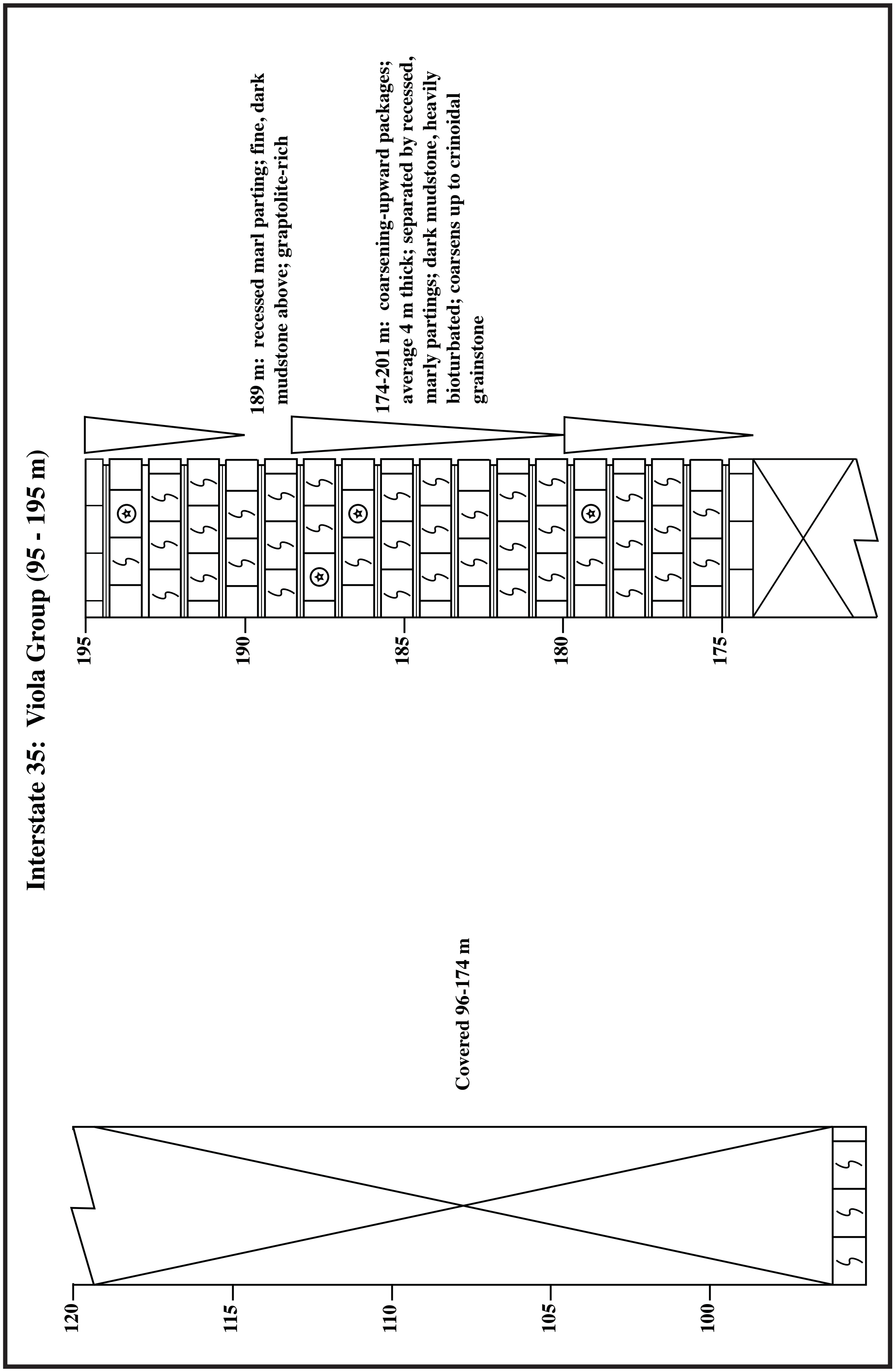
Interstate 35: Viola Group (95 - 195 m)
189 m: recessed marl parting; fine, dark mudstone above; graptolite-rich
174-201 m: coarsening-upward packages; average 4 m thick; separated by recessed, marly partings; dark mudstone, heavily bioturbated; coarsens up to crinoidal grainstone
Covered 96-174 m
195
190
185
180
175
120
115
110
105
100

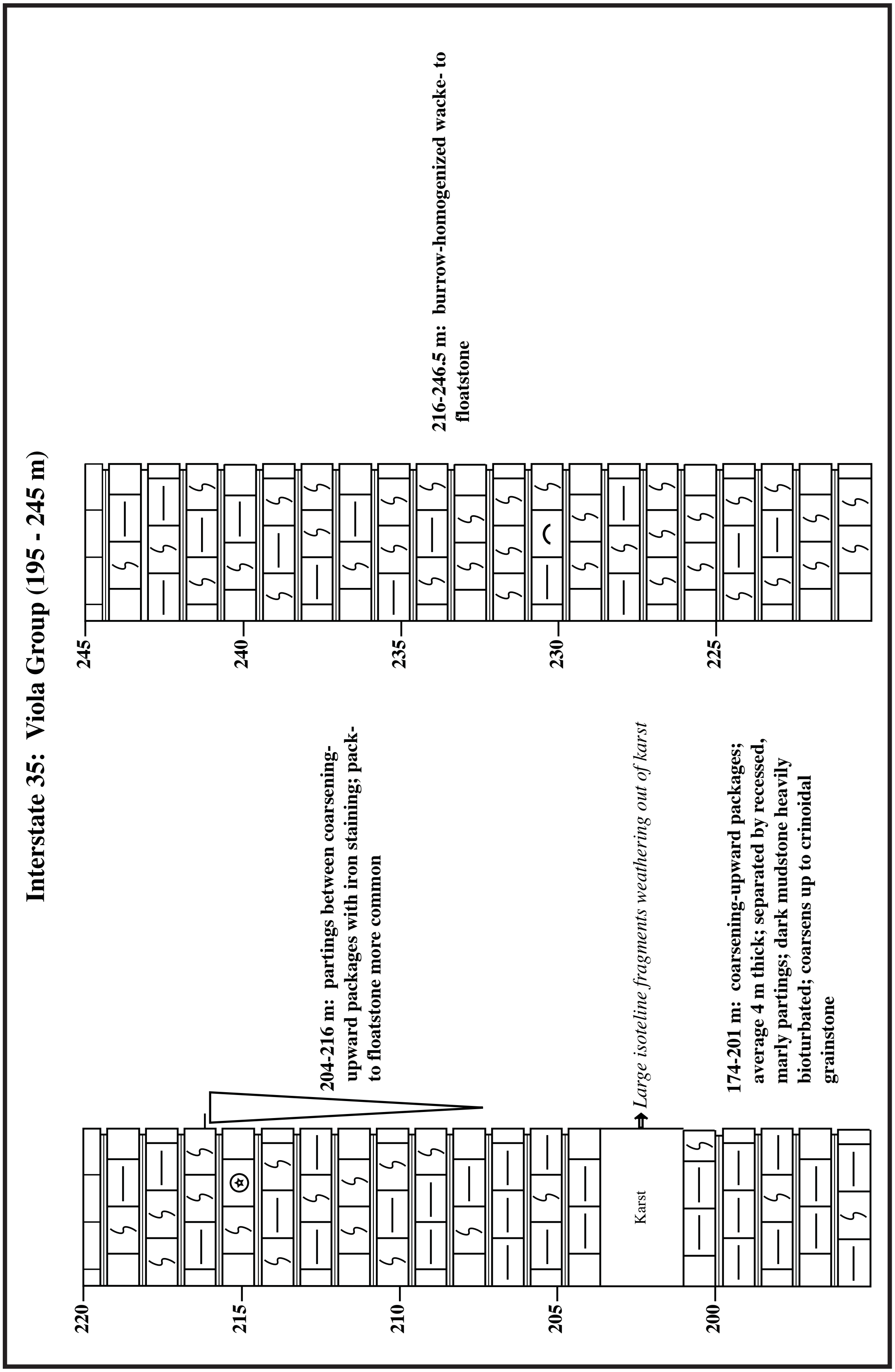
Interstate 35: Viola Group (195 - 245 m)
220
215
210
205
200
Karst
204-216 m: partings between coarsening-upward packages with iron staining; pack- to floatstone more common
Large isoteline fragments weathering out of karst
174-201 m: coarsening-upward packages; average 4 m thick; separated by recessed, marly partings; dark mudstone heavily bioturbated; coarsens up to crinoidal grainstone
245
240
235
230
225
216-246.5 m: burrow-homogenized wacke- to floatstone

Interstate 35: Viola Group (195 - 245 m)

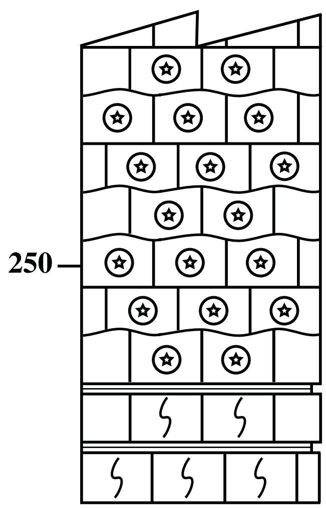

Covered to Sylvan Shale

247.5-256 m: Welling Formation; crinoidal grainstone

246-247.5 m: four packages of fine lime mudstone coarsening upward to crinoidal grainstone typical of Welling Formation

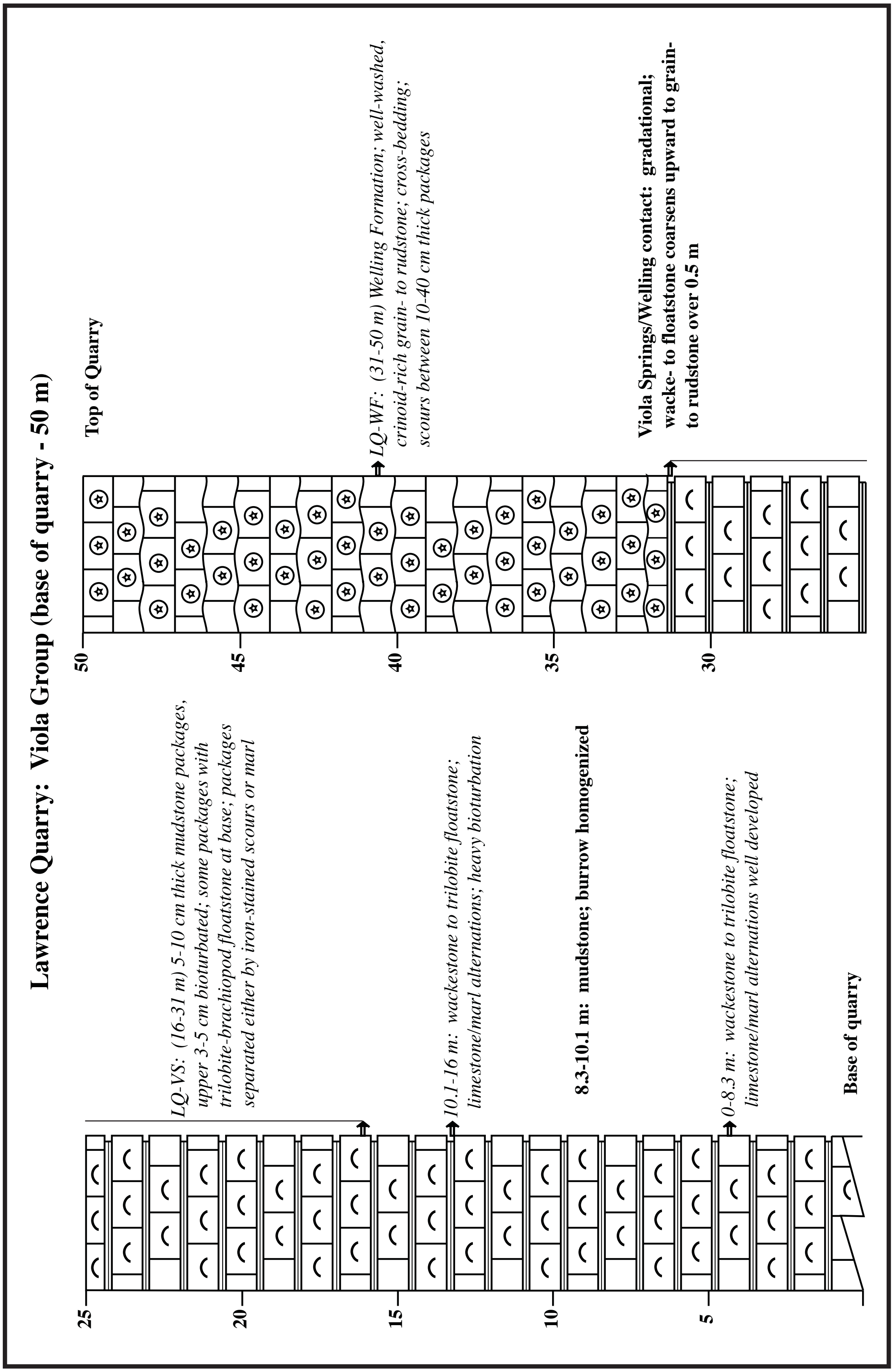
Lawrence Quarry: Viola Group (base of quarry - 50 m)
Top of Quarry
LQ-WF: (31-50 m) Welling Formation; well-washed, crinoid-rich grain- to rudstone; cross-bedding; scours between 10-40 cm thick packages
Viola Springs/Welling contact: gradational; wacke- to floatstone coarsens upward to grain- to rudstone over 0.5 m
50
45
40
35
30
LQ-VS: (16-31 m) 5-10 cm thick mudstone packages, upper 3-5 cm bioturbated; some packages with trilobite-brachiopod floatstone at base; packages separated either by iron-stained scours or marl
10.1-16 m: wackestone to trilobite floatstone; limestone/marl alternations; heavy bioturbation
8.3-10.1 m: mudstone; burrow homogenized
0-8.3 m: wackestone to trilobite floatstone; limestone/marl alternations well developed
Base of quarry
25
20
15
10
5

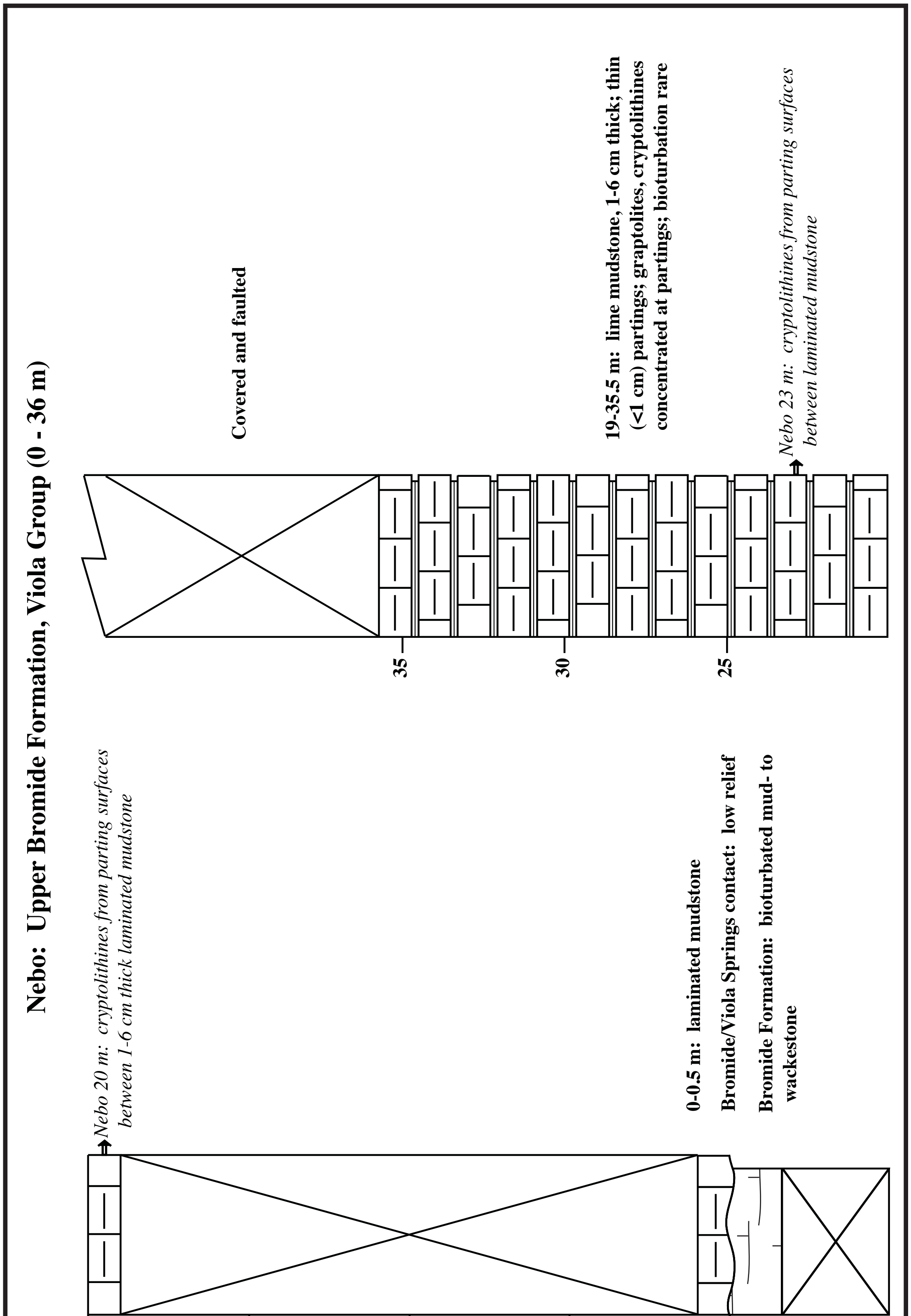
Nebo: Upper Bromide Formation, Viola Group (0 - 36 m)
Nebo 20 m: cryptolithines from parting surfaces between 1-6 cm thick laminated mudstone
0-0.5 m: laminated mudstone
Bromide/Viola Springs contact: low relief
Bromide Formation: bioturbated mud- to wackestone
Covered and faulted
19-35.5 m: lime mudstone, 1-6 cm thick; thin (<1 cm) partings; graptolites, cryptolithines concentrated at partings; bioturbation rare
Nebo 23 m: cryptolithines from parting surfaces between laminated mudstone
20
15
10
5
BV
35
30
25

Nebo: Viola Group (upper Welling Formation), base of Sylvan Shale

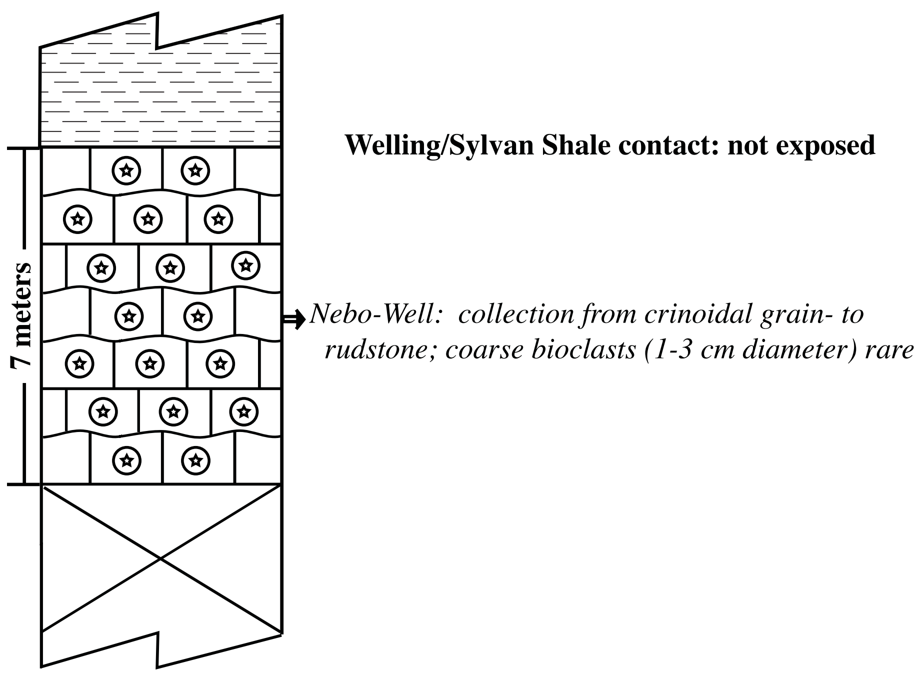

PLATES

PLATE 1

Isotelus kimmswickensis

Figures

1. UC28851A Paralectotype: broken, exfoliated cranidium x2 a) dorsal b) anterior c) lateral
2. UC28851B Paralectotype: broken, exfoliated cranidium x2 a) dorsal b) anterior c) lateral
3. OU11764 (99-30.5) mostly exfoliated transitory cranidium x8 a) anterior b) lateral c) dorsal
4. OU11765 (99-20) mostly exfoliated cranidiuim x5 a) dorsal b) lateral c) anterior
5. OU11766 (99-29) mostly exfoliated cranidium x3 in dorsal view
6. OU11767 (99-29) exfoliated cranidium x4 in dorsal view
7. OU11768 (99-08) cranidium preserving palpebral lobe and furrow x4 in dorsal view (latex cast illustrated)
8. OU11769 (99-29) cranidium x4 a) oblique b) dorsal (latex cast illustrated)
9. OU11770 (99-32) small, exfoliated pygidium x7 a) dorsal b) lateral

Plate 1

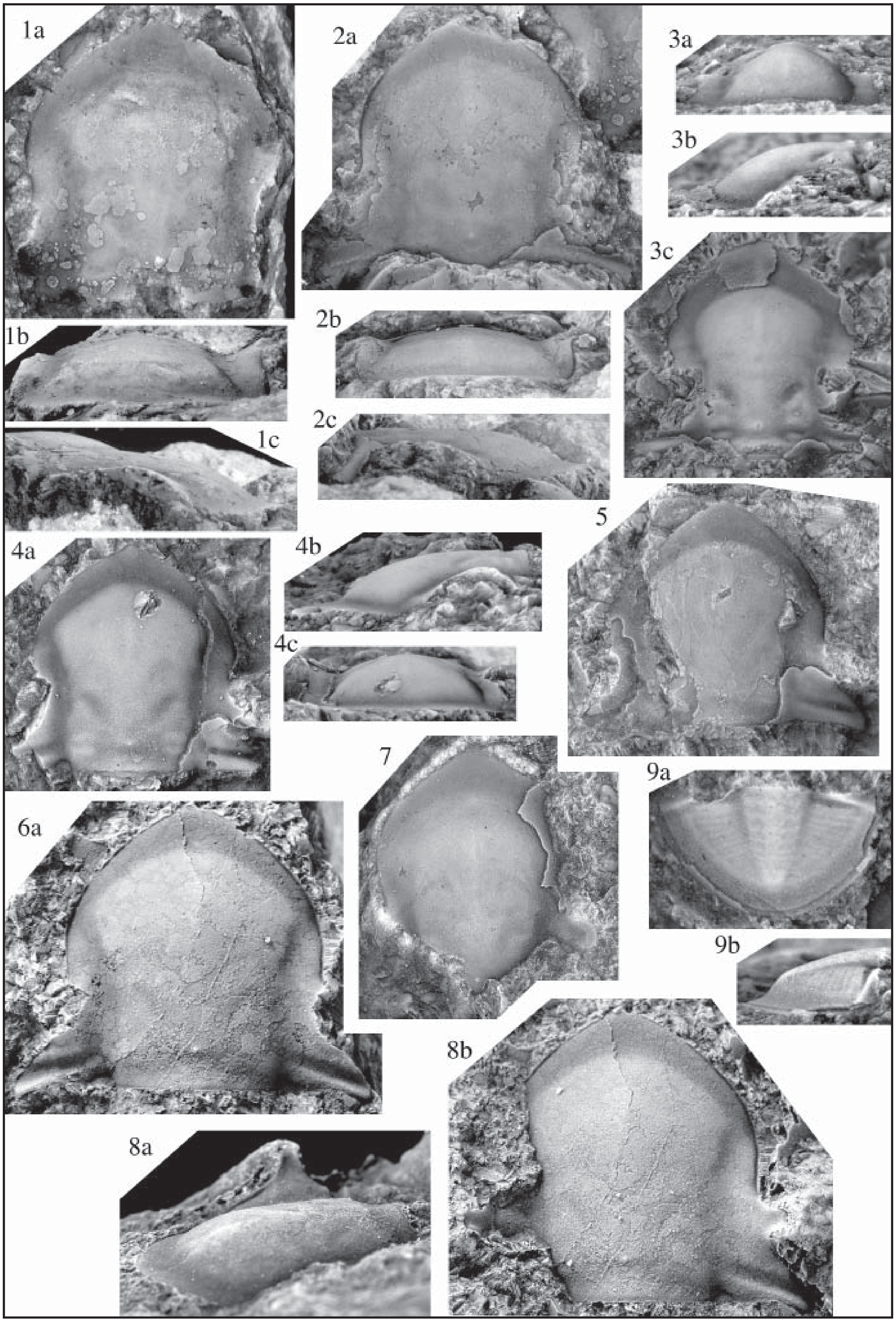

PLATE 2

Isotelus kimmswickensis, Isotelus kimmswickensis?

Figures 1-5 *Isotelus kimmswickensis*

1. UC28853 Paratype exfoliated pygidium x1.5 a) dorsal b) posterior c) lateral
2. OU11771 (99-10) small pygidium x8 a) lateral b) dorsal
3. UC28851C Paralectotype broken, exfoliated pygidium x2.5 a) dorsal b) lateral c) posterior
4. OU11772 (99-13) small exfoliated pygidium x6 a) posterior b) lateral c) dorsal
5. UC28855 Paratype broken, exfoliated pygidium x2 a) dorsal b) lateral

Figure 6 *Isotelus kimmswickensis?*

6. OU11773 (99-29) mostly exfoliated hypostome x1 a) dorsal b) lateral

Figures 7-8 *Isotelus kimmswickensis*

7. OU11774 (99-30.25) small, partly exfoliated pygidium x5 a) posterior b) lateral c) dorsal
8. OU11775 (99-32) mostly exfoliated librigena with visual surface x3 a) lateral b) dorsal

Plate 2

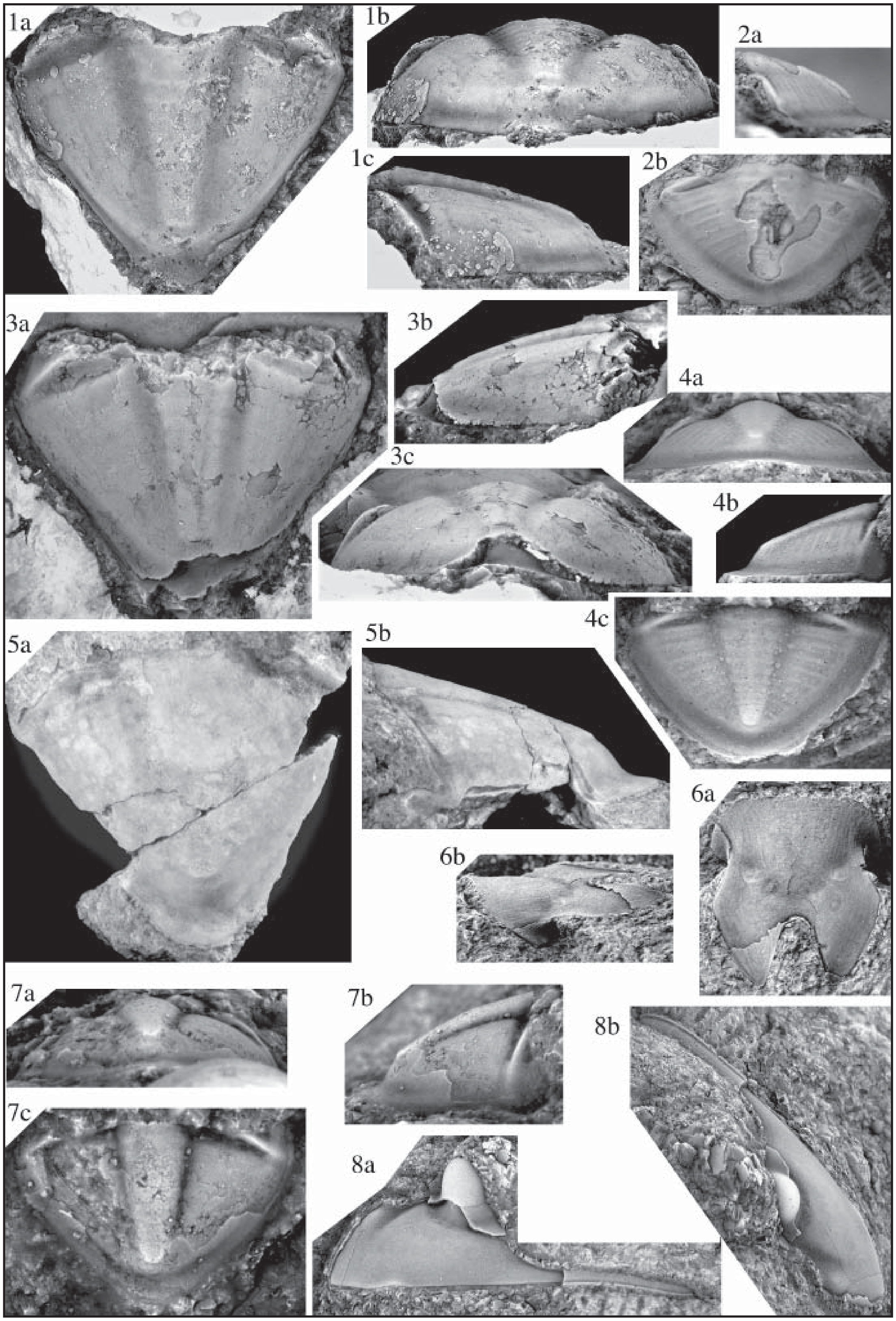

PLATE 3

Isotelus kimmswickensis, Isotelus violaensis

Figures 1-5 *Isotelus kimmswickensis*

1. OU11776 (99-20) partially exfoliated pygidium x6 a) dorsal b) posterior c) lateral
2. OU11777 (99-18) partially exfoliated pygidium x4 a) lateral b) posterior c) dorsal
3. OU11778 (99-29) broken, exfoliated pygidium x3 a) posterior b) lateral c) dorsal
4. OU11779 (99-30.25) partial, partially exfoliated pygidium a) dorsal x3 b) exoskeleton x6
5. OU11780 (99-32) broken, exfoliated pygidium in dorsal view showing relict segmentation on internal mold x2.5

Figures 6-8 *Isotelus violaensis*

6. OU11781 Paratype (99-46.5) small, partially exfoliated cranidium in dorsal view showing lateral glabellar furrows on internal mold x5
7. OU11782 Holotype: (99-48) exfoliated cranidium x2 a) dorsal b) oblique
8. OU11783 Paratype (99-40s Float) mostly exfoliated cranidium x2 a) anterior b) dorsal

Plate 3

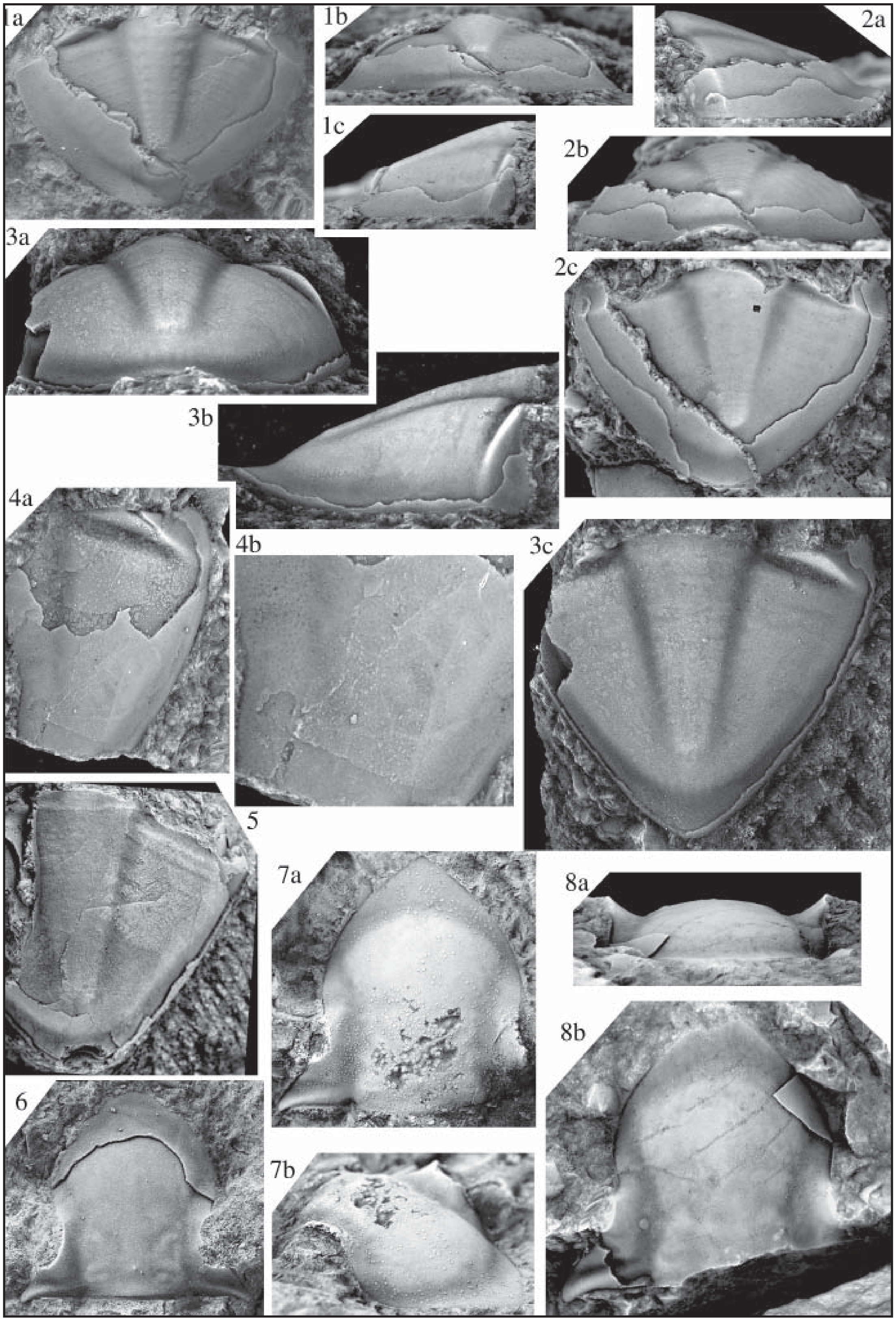

PLATE 4

Isotelus violaensis

Figures 1-5

1. OU11784 Paratype (99-39) cranidium shown x2 a) dorsal b) oblique c) anterior (latex cast illustrated)
2. OU11785 Paratype (99-48) cranidium shown x2 a) dorsal b) anterior (latex cast illustrated)
3. OU11786 Paratype (99-46) small, exfoliated pygidium x6 a) lateral b) dorsal
4. OU11787 Paratype (99-46) mostly exfoliated pygidium x5 a) posterior b) dorsal c) lateral
5. OU11788 Paratype (99-39) exfoliated cranidium x2 a) dorsal b) oblique

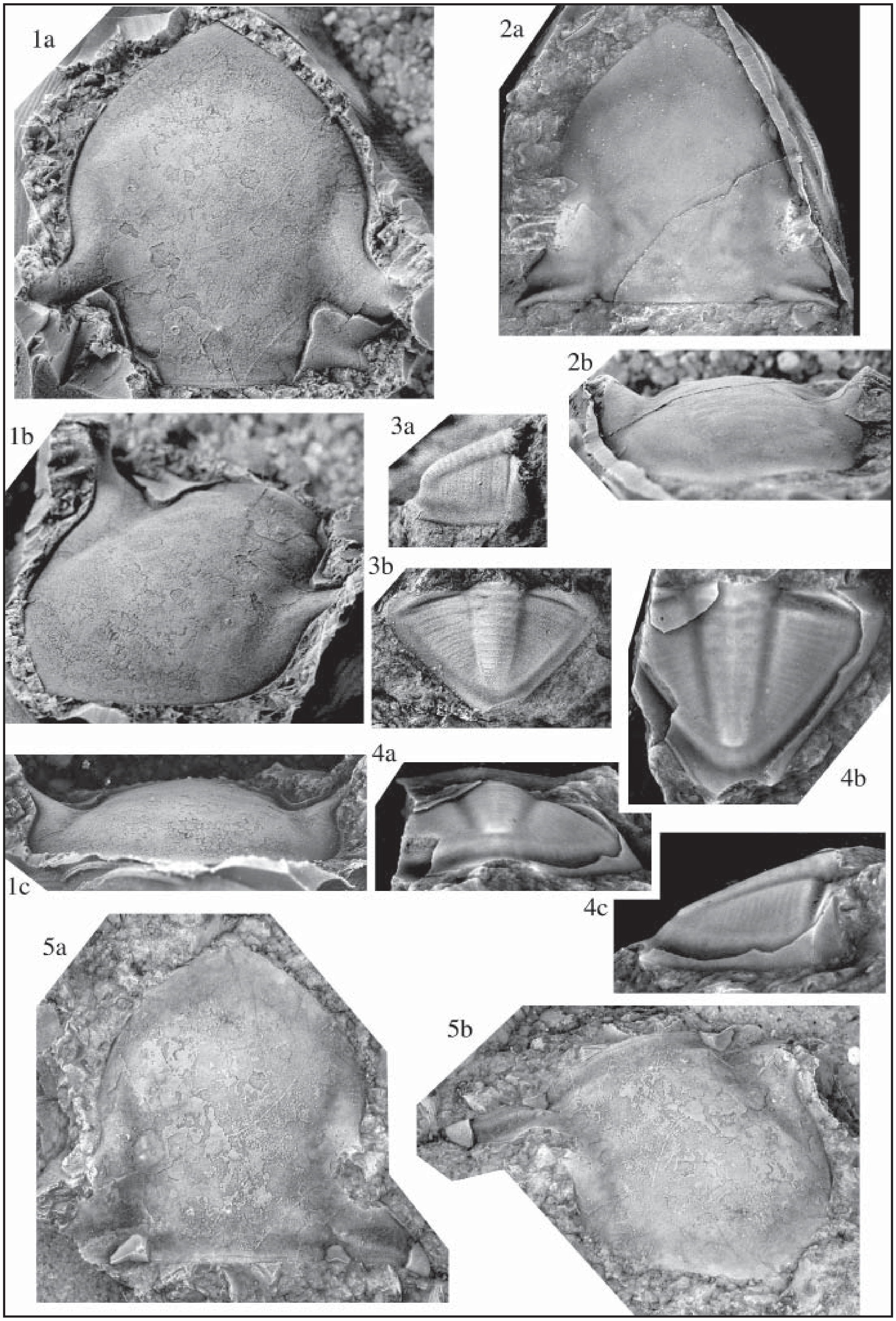
1a
2a
2b
1b
3a
3b
4b
1c
4a
4c
5a
5b

PLATE 5

Isotelus violaensis, Isotelus homalonotoides

Figures 1-4 *Isotelus violaensis*

1. OU11789 Paratype (99-40s Float) partially exfoliated pygidium x5 a) dorsal b) posterior c) lateral
2. OU11790 Paratype (99-46.5) ibrigena without visual surface shown x3 a) dorsal b) anterior c) lateral (latex cast illustrated)
3. OU11791 Paratype (99-49) partly exfoliated, broken pygidium x4 a) dorsal b) close-up of exoskeleton x8
4. OU11792 Paratype (99-40s Float) ventral view of broken hypostome x1

Figures 5-6 *Isotelus homalonotoides*

5. UC12324 Lectotype (designated herein): mostly exfoliated cranidium with missing palpebral lobes x3 a) dorsal b) lateral c) anterior
6. UC12324 Paralectotype (designated herein) complete, exfoliated pygidium x3 a) lateral b) posterior c) dorsal

Plate 5

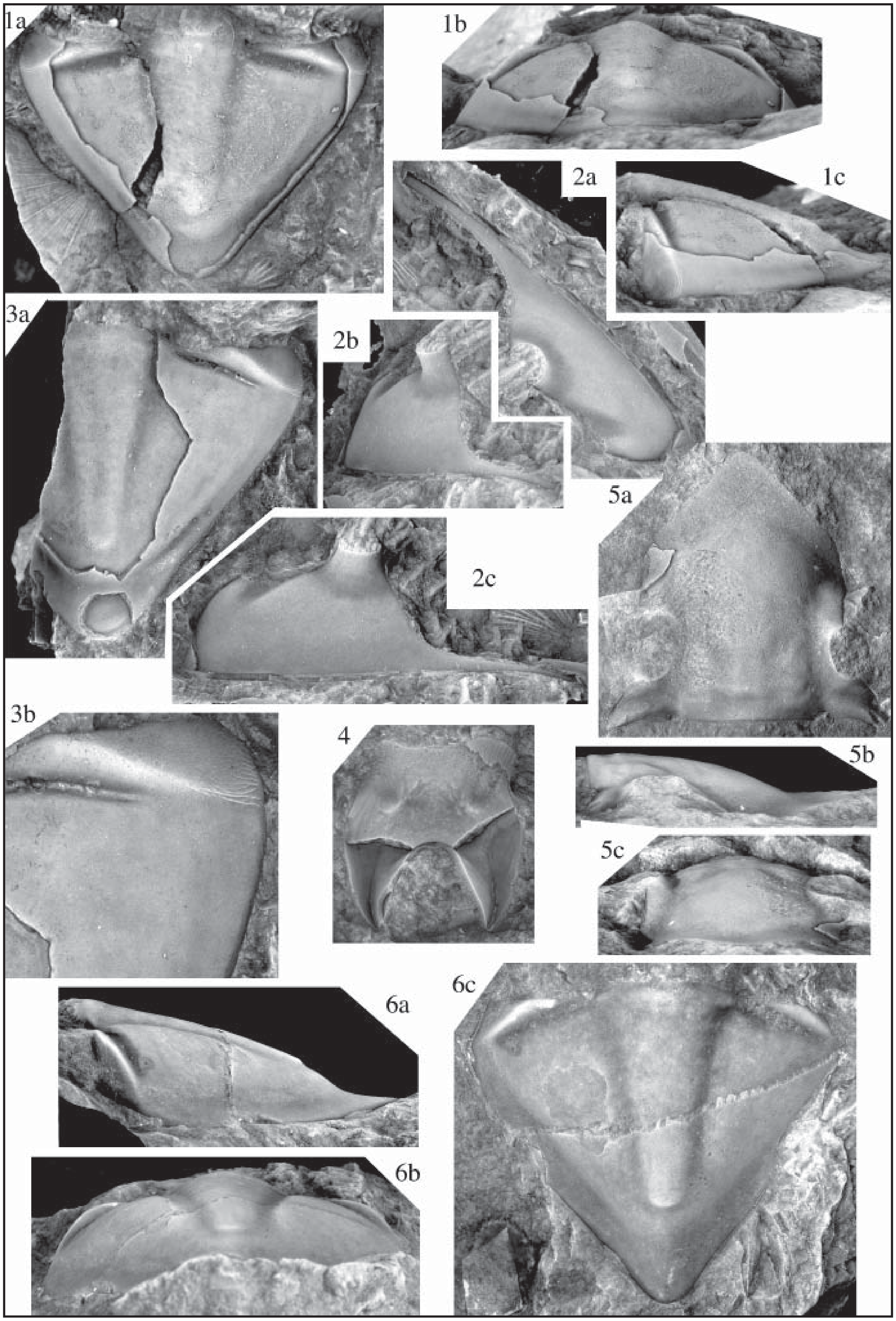

PLATE 6

Isotelus bradleyi

Figures

1. OU11793 Paratype (99-08) cranidium in dorsal view shown x8 (latex cast illustrated)
2. OU11794 Paratype (99-13) partial, testate cranidium x8 a) dorsal b) oblque c) anterior
3. OU11795 Paratype (99-33) exfoliated cranidium x5 a) anterior b) dorsal c) lateral
4. OU11796 Holotype (99-13) partly exfoliated cranidium x5 a) anterior b) dorsal c) oblique
5. OU11797 Paratype (99-33) exfoliated, broken cranidium x3 a) dorsal b) lateral
6. OU11798 Paratype (99-32) cranidium with palpebral lobes and furrows preserved, in dorsal view shown x3 (latex cast illustrated)
7. OU11799 Paratype (99-31.5) internal mold of librigena without eye stalk x4 a) dorsal b) anterior c) lateral
8. OU11800 Paratype (99-32) cranidium showing pitted exoskeleton in dorsal view shown x3 (latex cast illustrated)

Plate 6

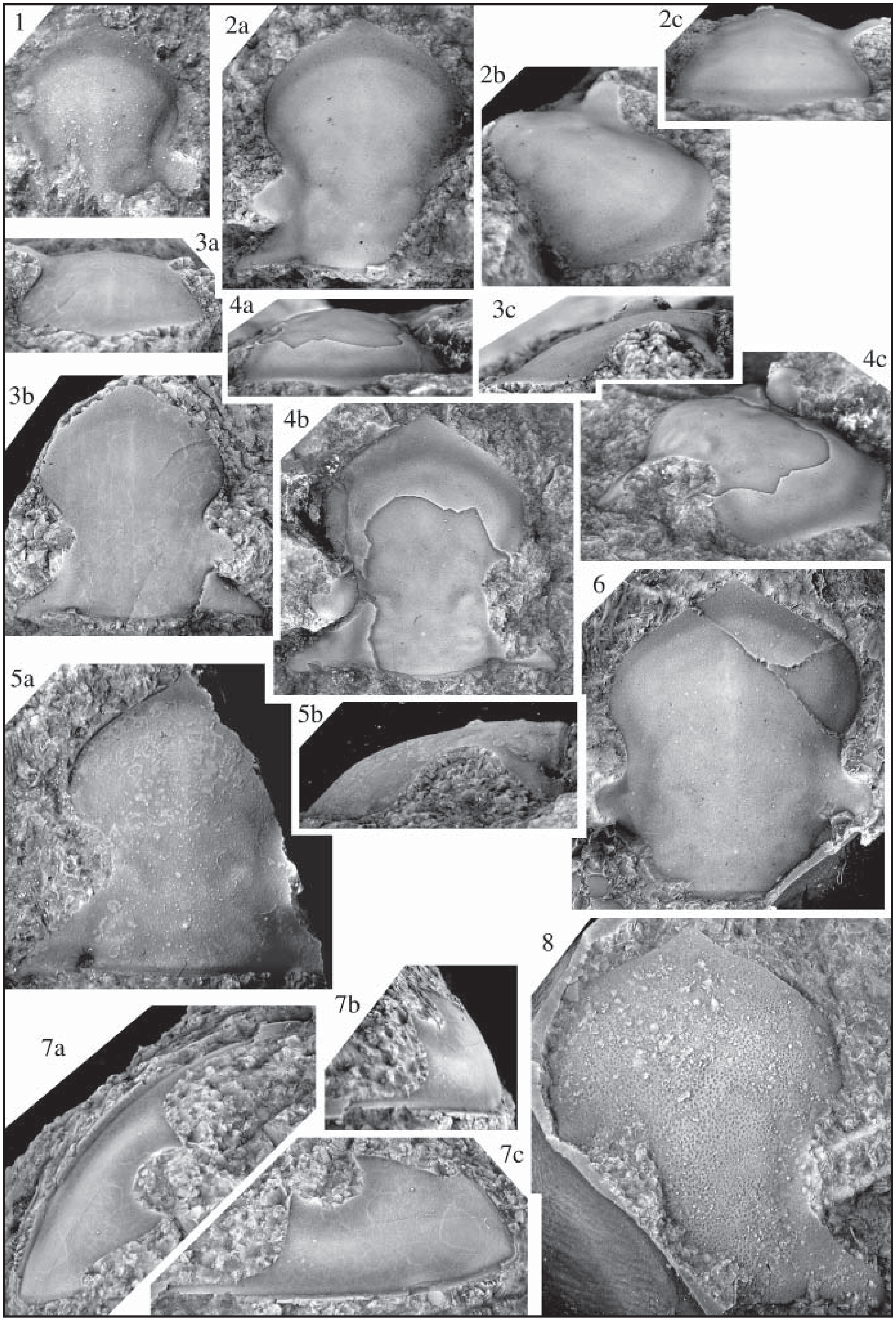

PLATE 7

Isotelus bradleyi, Isotelus cf. *I. bradleyi*

Figures 1-3 *Isotelus bradleyi*

1. OU11801 Paratype (99-32) broken, mostly exfoliated cranidium x3 a) dorsal b) anterior c) exoskeleton x8 d) lateral
2. OU11802 Paratype (LQ-VS) mostly exfoliated librigena with visual surface x2 a) lateral b) anterior c) dorsal
3. OU11803 Paratype (99-32) exfoliated cranidium with lateral glabellar furrows x3 a) lateral b) anterior c) dorsal

Figures 4-5 *Isotelus* cf. *I. bradleyi*

4. UC28871 mostly exfoliated librigenae, part of visual surface preserved; labeled I. *gigas* but facial sutures match pattern for *I.* cf. *I. bradleyi* x1.5 a) anterior b) lateral c) dorsal
5. UC28854 labeled as a paratype of I. kimmswickensis; exfoliated cranidium x2.5 a) anterior b) lateral c) dorsal

Plate 7

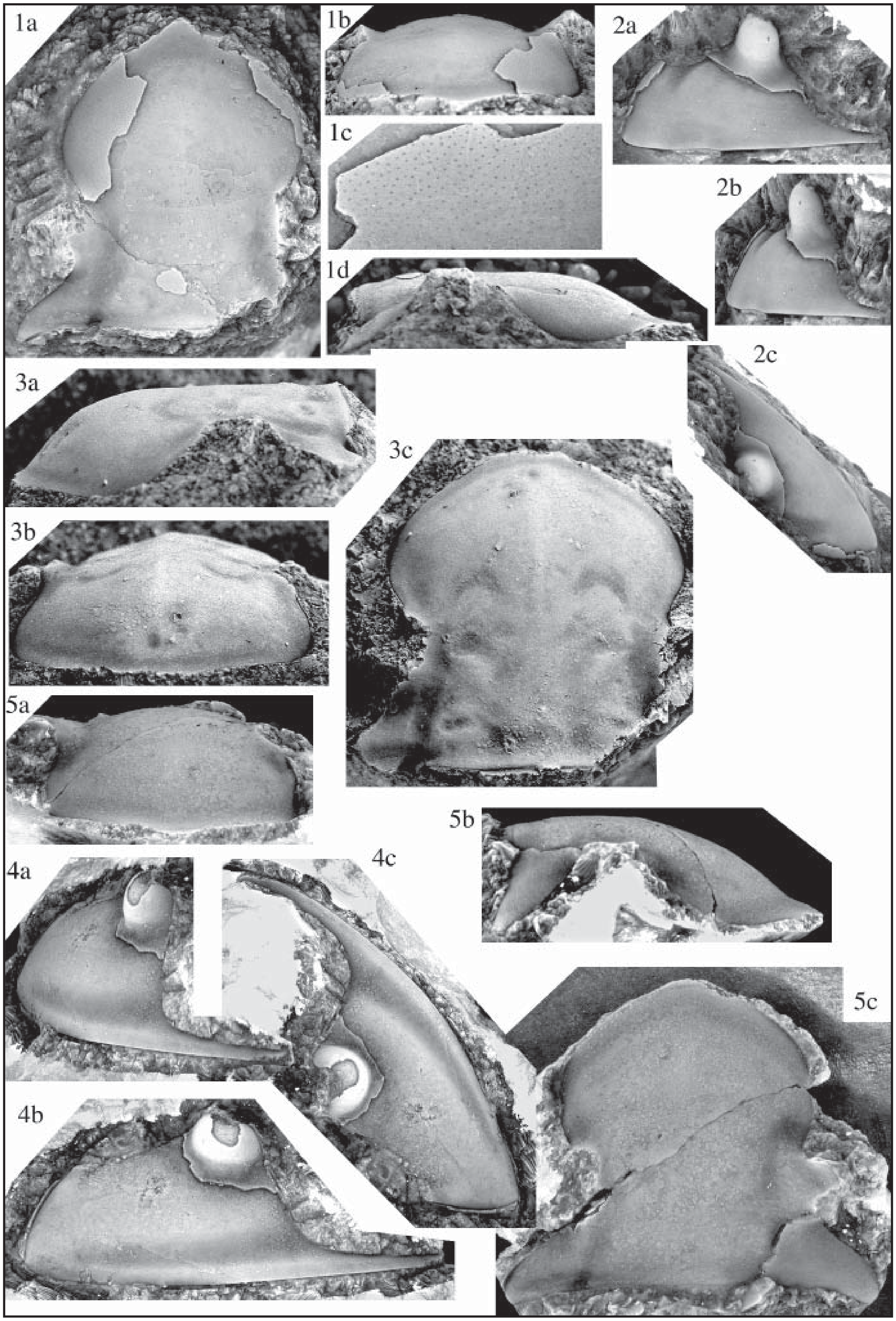

PLATE 8

Isotelus bradleyi, Isotelus skapaneidos

Figures 1-3 *Isotelus bradleyi*

1. 1. OU11804 Paratype (99-32) exfoliated broken pygidium x2 a) dorsal b) posterior c) lateral
2. OU11805 Paratype (99-32) exfoliated broken pygidium x3 a) dorsal b) posterior c) lateral
3. OU11806 Paratype (99-32) broken pygidium shown a) dorsal x2 b) close-up showing pitting on exoskeleton x6 (latex cast illustrated)

Figures 4-5 *Isotelus skapaneidos*

4. OU11807 Paratype (LQ-WF) broken pygidium x3 a) dorsal b) lateral
5. OU11808 Paratype (LQ-WF) mostly exfoliated, broken pygidium x1 a) dorsal b) lateral

Plate 8

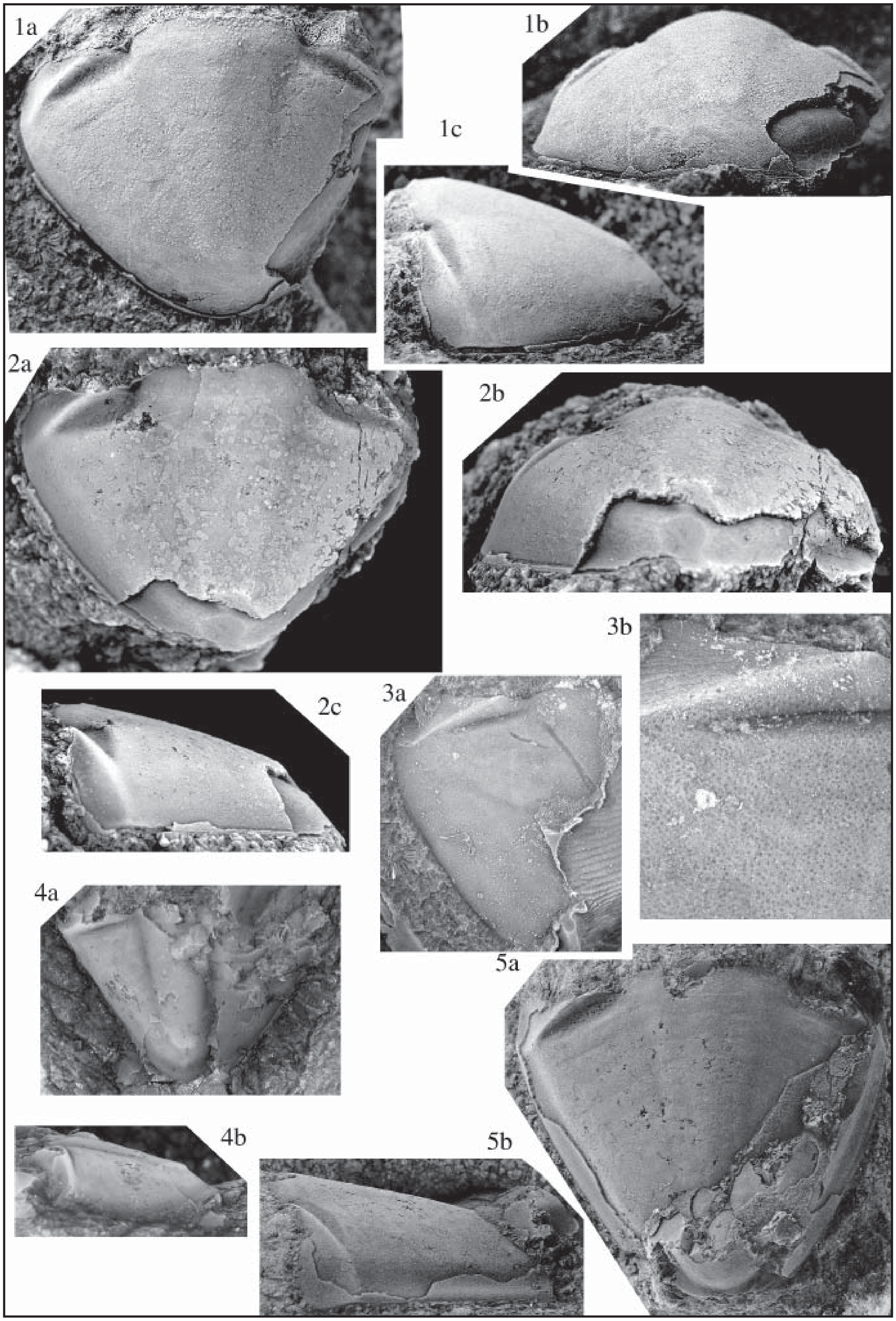

PLATE 9

Isotelus skapaneidos

Figures

1. OU11809 Holotype (LQ-WF) mostly exfoliated, nearly complete cranidium in dorsal view x1
2. OU11810 Paratype (LQ-WF) nearly complete, testate cranidium x2.5 a) lateral b) dorsal
3. OU11811 Paratype (CN-Float) testate cephalon with right side broken x1 a) dorsal b) anterior
4. OU11812 Paratype (77-216) exfoliated pygidium x1.5 a) dorsal b) lateral c) posterior

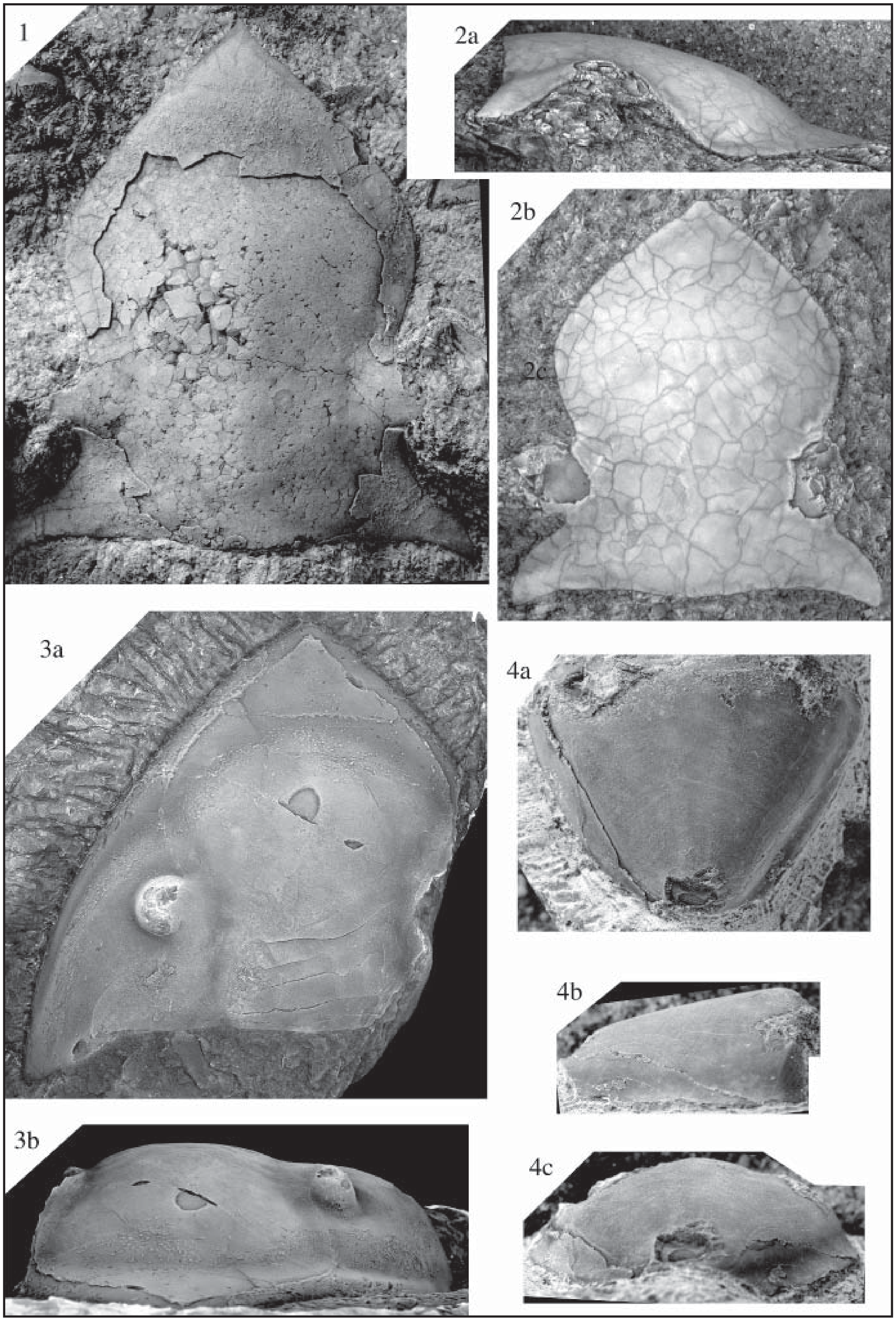
1
2a
2b
2c
3a
4a
4b
3b
4c

PLATE 10

Isotelus skapaneidos

Figures

1. OU11813 Paratype(77-Float) nearly complete individual with front of cephalon broken off, dorsal surface of pygidium weathered x1 a) lateral b) dorsal
2. OU11814 Paratype (LQ-WF) broken cranidium with exoskeleton x1.5 a) lateral b) dorsal c) anterior
3. OU11815 Paratype (LQ-WF) cephalic doublure with portions of librigenae in dorsal view x1.5

Plate 10

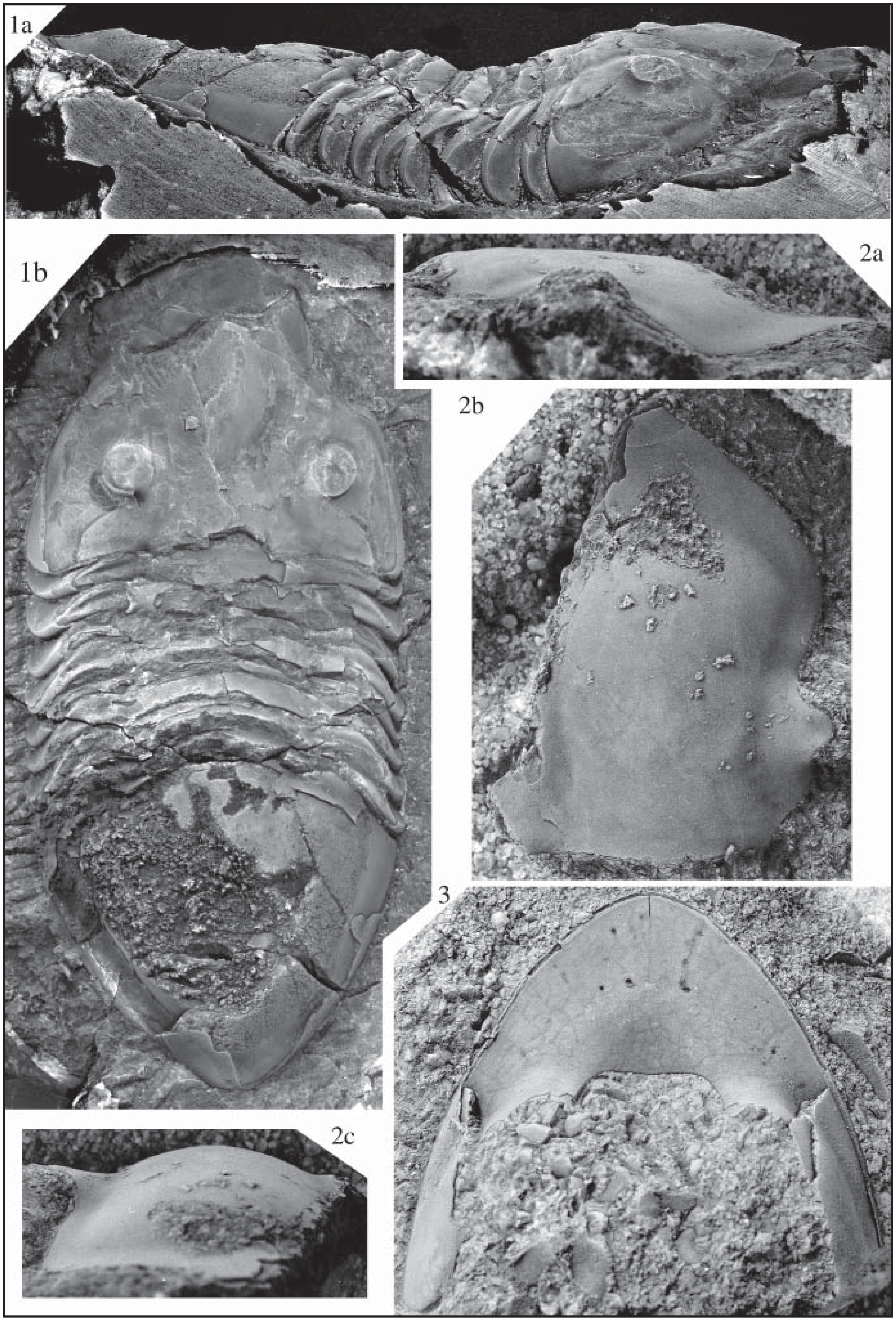

PLATE 11

Isotelus skapaneidos, Isotelus iowensis

Figures 1-2 *Isotelus skapaneidos*

1. OU11816 Paratype (77-Float) (Amoco collection) broken, testate cranidium x3 a) dorsal b) lateral
2. OU11817 Paratype (77-202.5) broken, testate cranidium in dorsal view x1.5

Figures 3-4 *Isotelus iowensis*

3. P11241 Isotelus iowensis ventral exoskeleton x1 (refigured from Slocum 1913, pl. 13, fig. 1)
4. UC6308 Holotype: Isotelus iowensis Owen 1852 x1.5

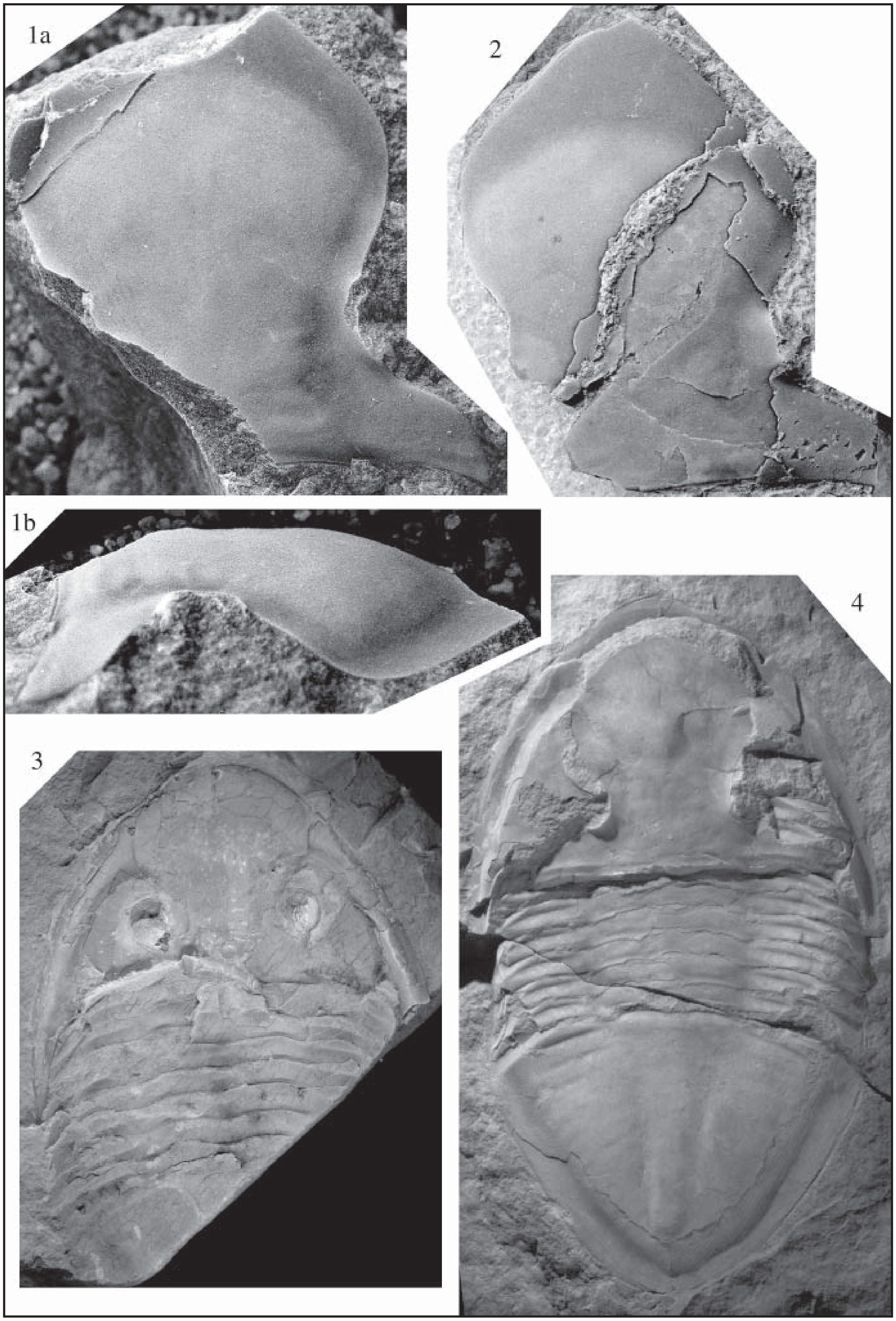
1a
2
1b
4
3

PLATE 12

Isotelus skapaneidos?, Isotelus cf. *I. iowensis*

Figure 1 *Isotelus skapaneidos?*

1. OU11818 (LQ-WF) nearly complete hypostome tentatively assigned to this species x3 a) dorsal b) lateral/oblique c) lateral

Figures 2-3 *Isotelus* cf. *I. iowensis*

2. OU3119 (BQ-Float) nearly complete individual, front of cephalon and rear of pygidium broken x0.75 in dorsal view
3. OU11819 (I-35-75) broken, testate pygidium x1 a) dorsal b) lateral

Plate 12

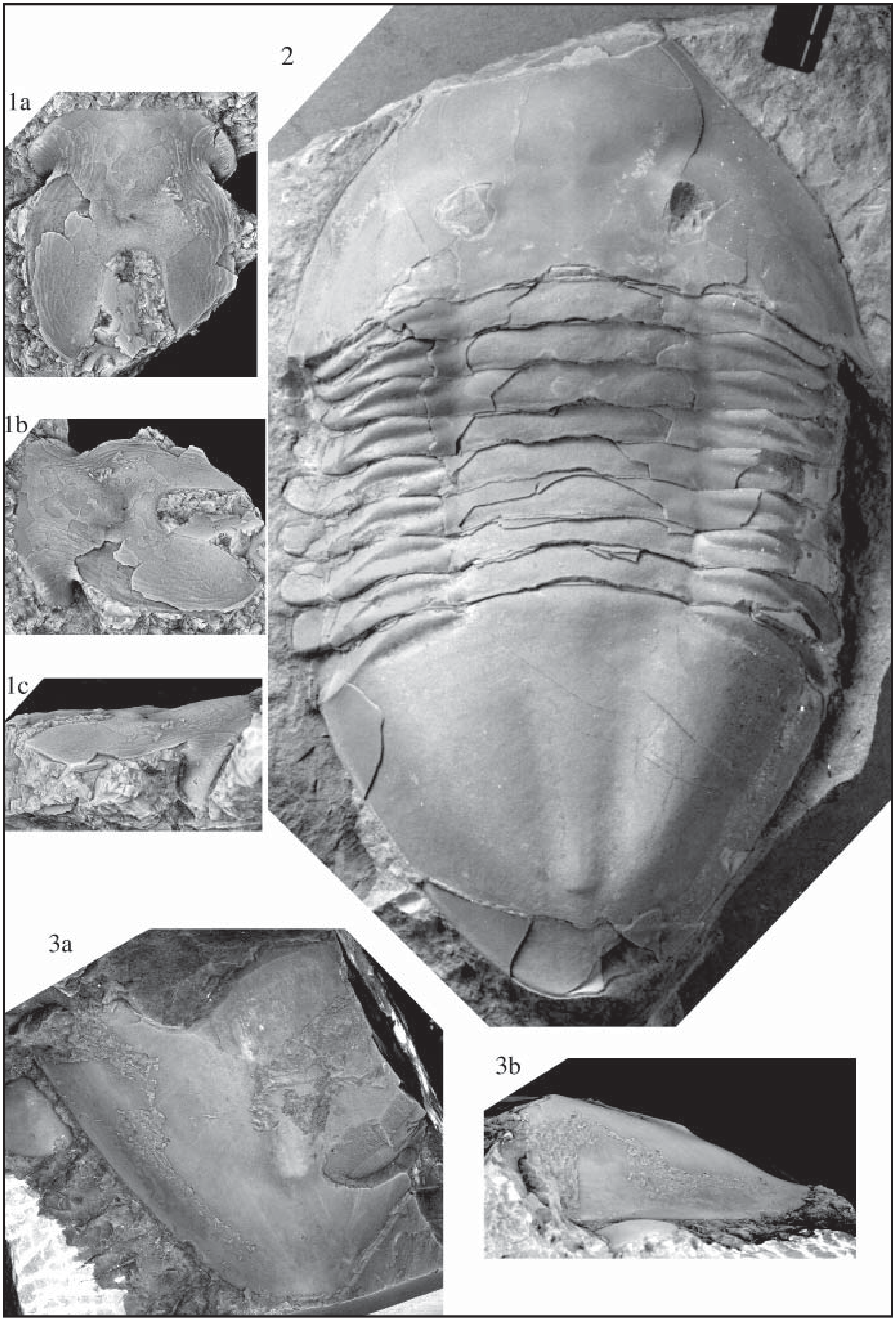

PLATE 13

Isotelus cf. *I. walcotti*

Figures

1. OU11820 (99-49.5) exfoliated anterior of cranidium in dorsal view x3
2. OU11821 (99-47) partly exfoliated librigena with visual surface x4 a) anterior b) dorsal c) lateral
3. OU11822 (99-49.5) anterior portion of cranidium x3 a) dorsal b) anterior
4. OU11823 (99-33) broken cranidium in dorsal view shown x1.5 (latex cast illustrated)
5. OU11824 (99-39) pygidium shown x1.5 a) dorsal b) posterior (latex cast illustrated)
6. OU11825 (99-49.5) exfoliated pygidium x1.5 a) dorsal b) lateral

Plate 13

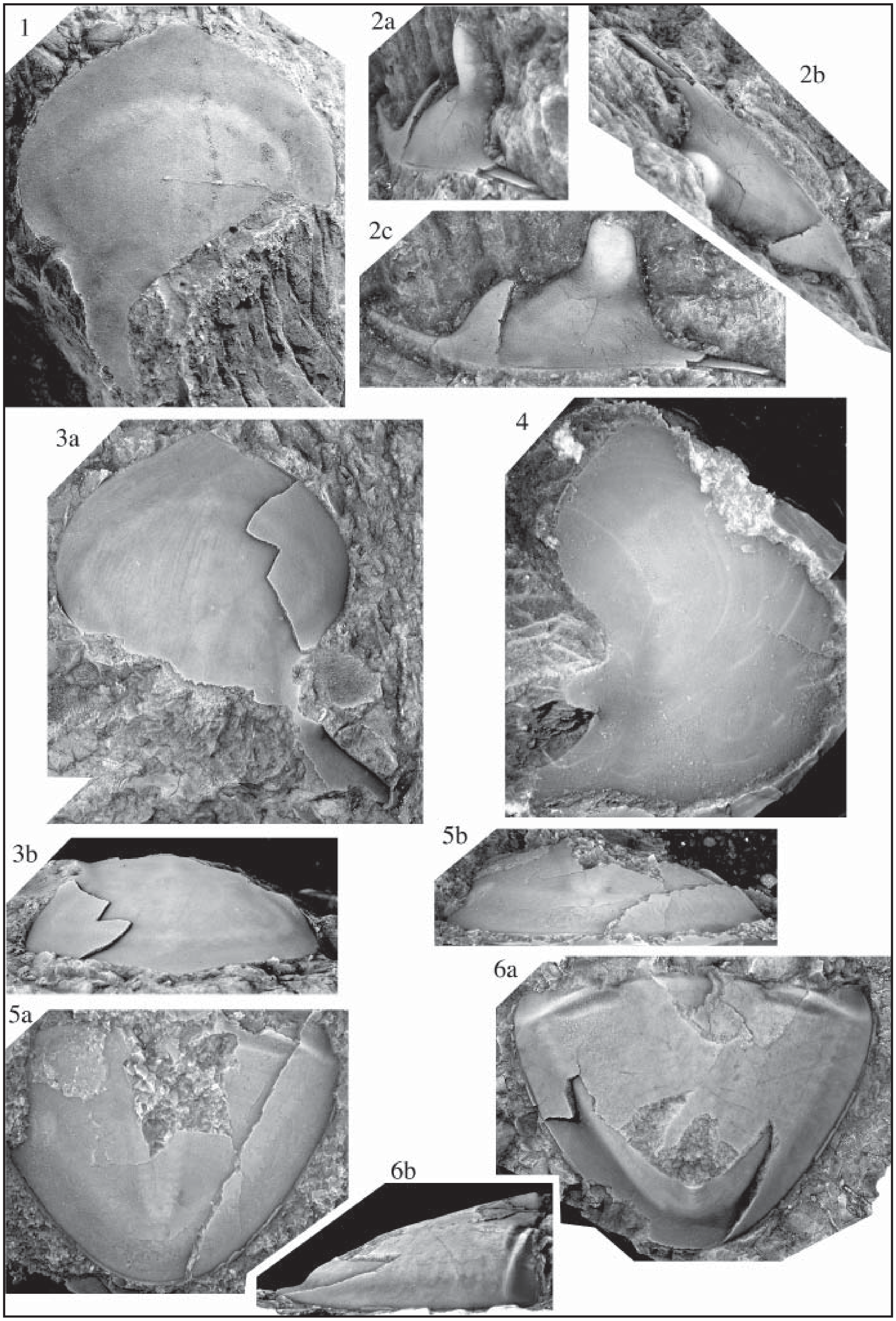

PLATE 14

Ectenaspis beckeri, Ectenaspis burkhalteri?

Figure 1 *Ectenaspis beckeri*

1. UC41151 Holotype: nearly complete, testate individual
   a) dorsal x1 b) dorsal of cephalon x2 c) lateral/oblique x1
   d) lateral x1 e) proboscis showing details of ornament x4

Figure 2 *Ectenaspis burkhalteri*

2. OU11826 (Nebo-Well) exfoliated hypostome attributed to
   E. burkhalteri in ventral view x5

Plate 14

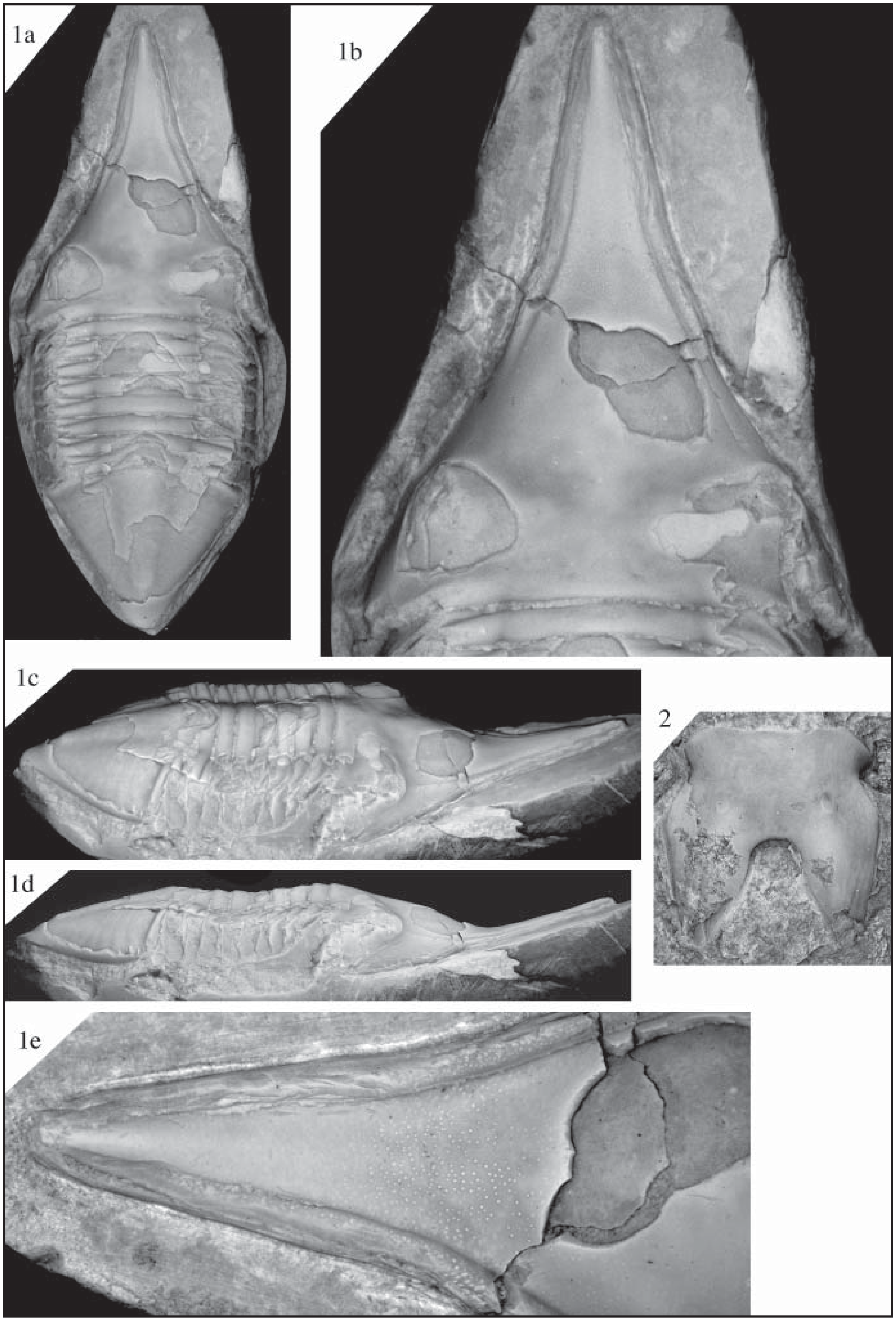

PLATE 15

Ectenaspis burkhalteri

Figures

1. OU11827 Holotype (Nebo-Well) exfoliated cranidium with anterior prolongation and right eye stalk broken a) dorsal x4 b) lateral x4 c) anterior x4 d) oblique x4 e) lateral view of palpebral lobe x8
2. OU11828 Paratype (LQ-WF) broken, crushed cranidium with one eye stalk well-preserved a) dorsal x3 b) dorsal view of palpebral lobe and eye stalk x6 c) anterior oblique x3 d) anterior of cranidium just behind where anterior prolongation is broken off showing pustules x6

Plate 15

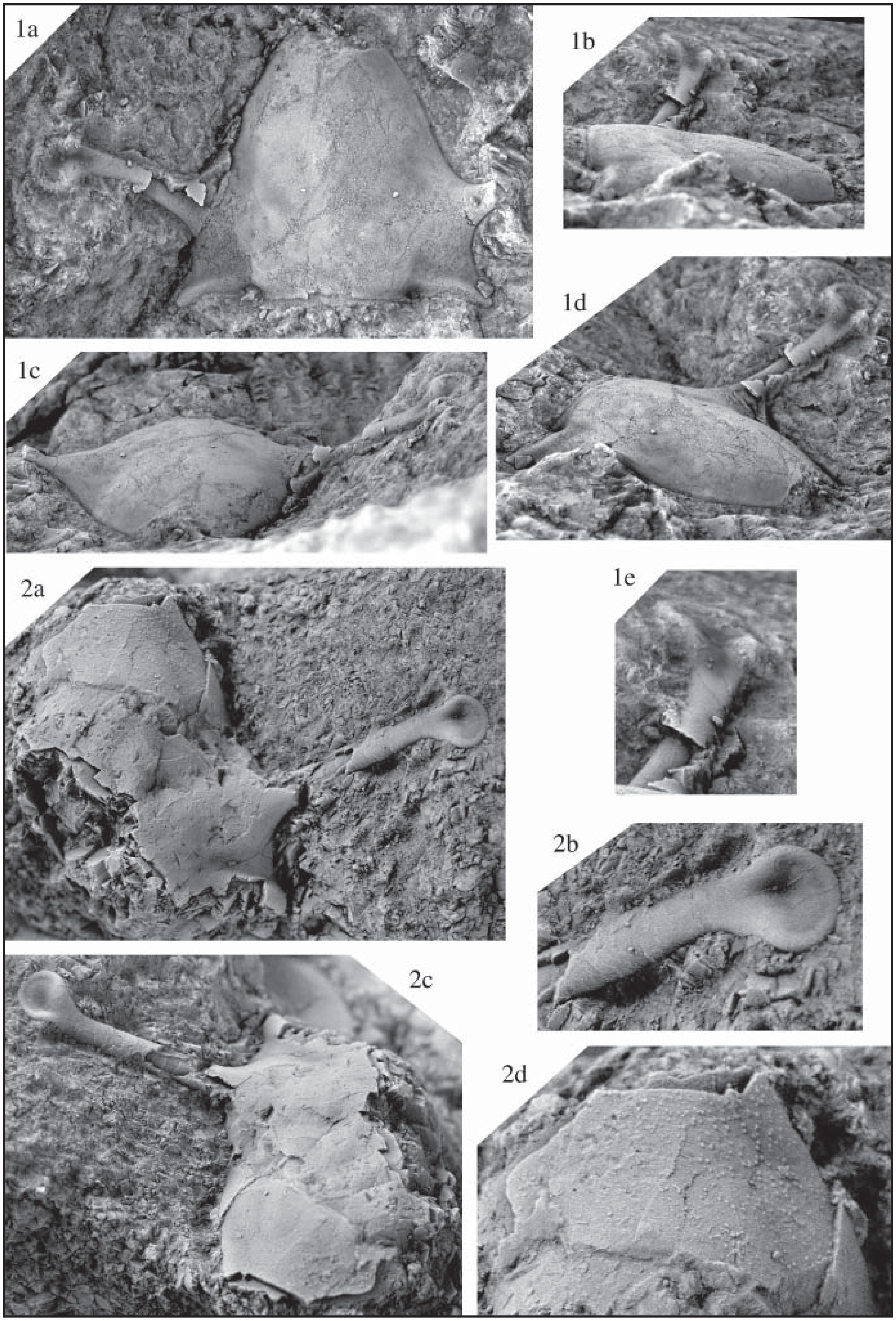

PLATE 16

Ectenaspis burkhalteri

Figures

1. OU11829 Paratype (LQ-WF) partial, testate cranidium x2 a) dorsal b) lateral
2. OU11830 Paratype (LQ-WF) partial cranidium x3 a) dorsal b) anterior oblique
3. OU11831 Paratype (LQ-WF) exfoliated anterior portion of librigena, including ventral part of eye stalk x1.5 a) posterior oblique b) lateral
4. OU11832 Paratype (LQ-WF) partly exfoliated, broken librigena missing eye stalk and most of anterior portion, with part of genal spine x1 a) lateral b) dorsal
5. OU11833 Paratype (LQ-WF) broken, testate pygidium x3 a) dorsal b) lateral

Plate 16

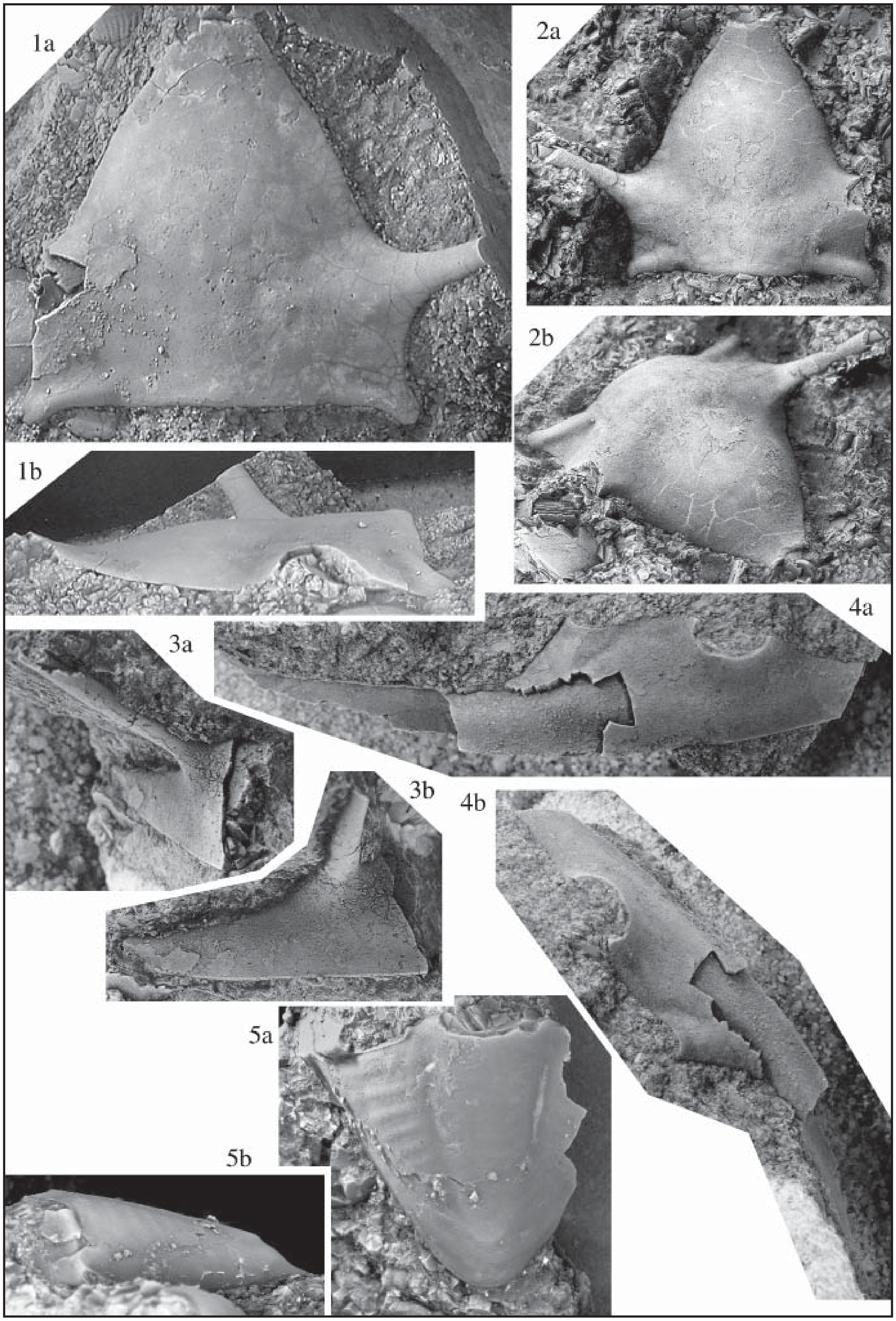

PLATE 17

Ectenaspis beckeri, Ectenaspis burkhalteri,
Stegnopsis wellingensis

Figure 1 *Ectenaspis beckeri*

1. UC41151 Holotype: pygidium x2 a) dorsal b) lateral

Figures 2-4 *Ectenaspis burkhalteri*

2. OU11834 Paratype (LQ-WF) nearly complete, testate pygidium x2 (a dorsal b) lateral
3. OU11835 Paratype (LQ-WF) testate pygidium with posterior broken x2 a) lateral b) dorsal
4. OU11836 Paratype (LQ-WF) nearly complete, testate pygidium x1.5 a) dorsal b) lateral

Figure 5 *Stegnopsis wellingensis*

5. OU11837 Holotype (LQ-WF) broken cranidium shown x1.5 a) dorsal b) anterior c) lateral (latex cast illustrated)

Plate 17

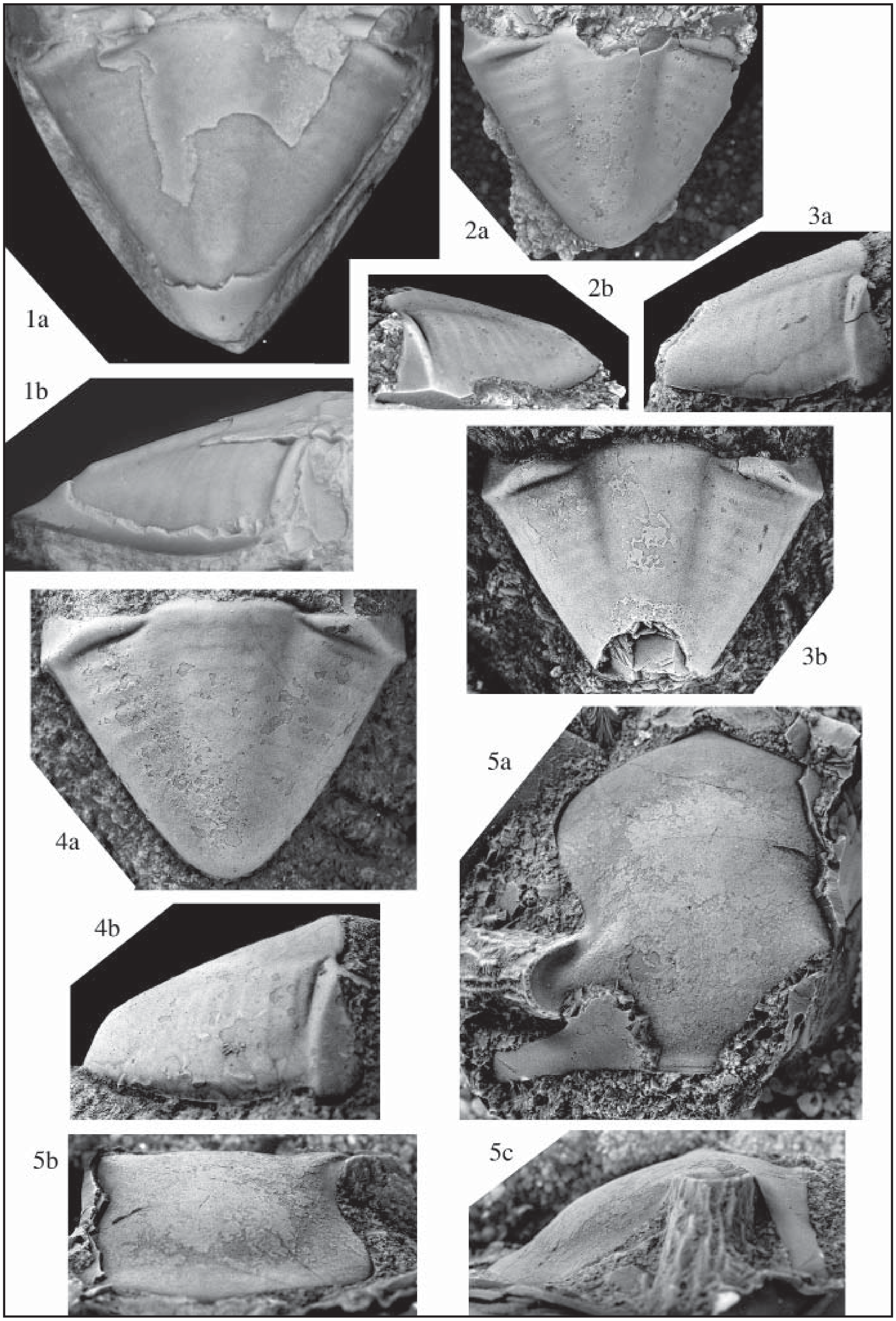

PLATE 18

Stegnopsis wellingensis, Stegnopsis erythragora

Figures 1-3 *Stegnopsis wellingensis*

1. OU11838 Paratype (LQ-WF) partial cranidium, partly testate x3 a) dorsal b) lateral c) anterior
2. OU11839 Paratype (LQ-WF) partial, exfoliated cranidium x2 a) dorsal b) anterior
3. OU11840 Paratype (LQ-WF) mostly exfoliated pygidium broken along posterior margin x1.5 a) dorsal b) posterior

Figures 4-6 *Stegnopsis erythragora*

4. OU11841 (BQ-18) meraspid cranidium tentatively assigned to this species x12 a) oblique b) lateral c) dorsal c) anterior e) details of the posterior portion of the cranidium x20
5. OU11842 (BQ-12) meraspid librigena tentatively assigned to this species x10 a) dorsal b) lateral
6. OU11843 (BQ-12) meraspid librigena tentatively assigned to this species, in dorsal view x10

Figure 7 *Stegnopsis wellingensis*

7. OU11844 Paratype (LQ-WF) mostly exfoliated pygidium, broken along posterior and left margins x1 a) dorsal b) posterior c) lateral

Plate 18

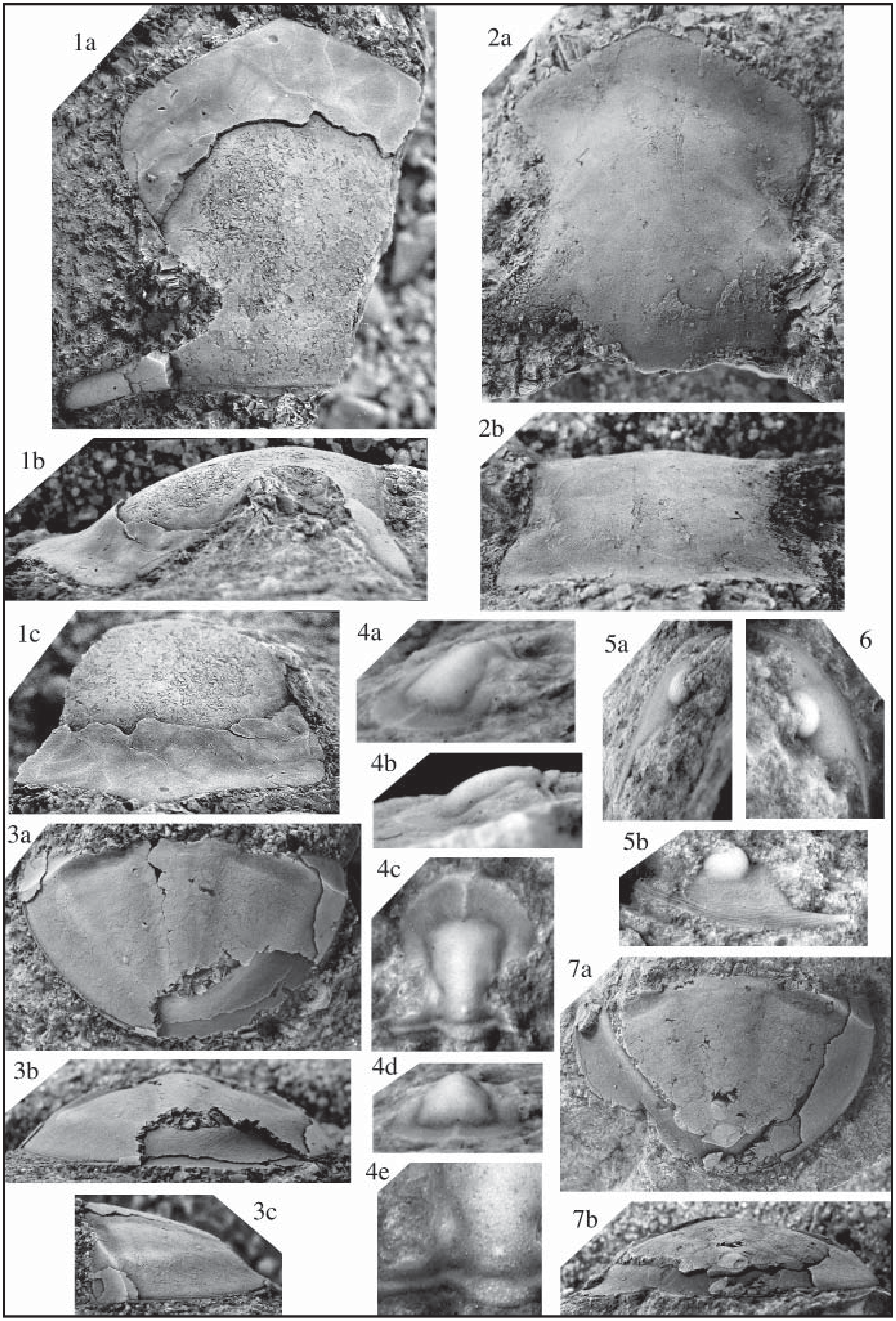

PLATE 19

Stegnopsis wellingensis, Stegnopsis erythragora

Figures 1-3 *Stegnopsis wellingensis*

1. OU11845 Paratype (LQ-WF) nearly complete pygidium shown x2 a) dorsal b) lateral c) posterior (latex cast illustrated)
2. OU11846 Paratype (LQ-WF) exfoliated pygidium in dorsal view x1.5
3. OU11847 Paratype (LQ-WF) mostly exfoliated pygidium x1.5 a) dorsal b) lateral c) posterior d) close-up of exoskeleton showing absence of ornament x6

Figures 4-5 *Stegnopsis erythragora*

4. OU11848 (BQ-24) small pygidium tentatively assigned to this species x8 a) dorsal b) posterior
5. OU11849 Paratype (77-183) nearly complete (meraspid?) cranidium x7 a) dorsal b) oblique c) lateral

Plate 19

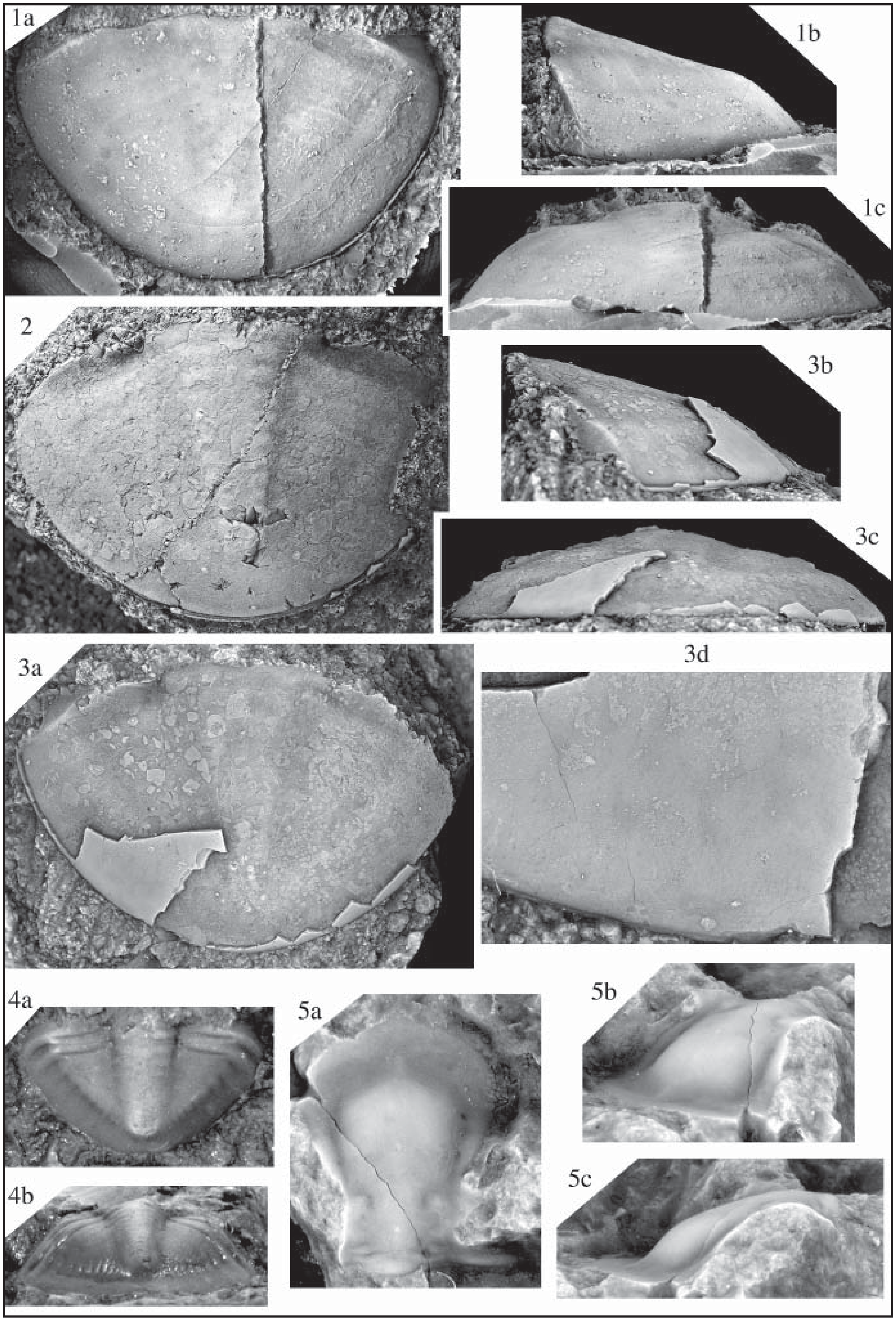

PLATE 20

Stegnopsis erythragora

Figures

1. OU11850 Paratype (Loc. G of Glaser, along Little Buckhorn Creek near the south-east margin of the Arbuckle Reservoir, Chickasaw National Recreation Area) nearly complete individual missing posterior margin of pygidium and with dorsal surface of cranidium badly weathered x1 a) dorsal b) oblique c) lateral
2. OU11851 Paratype (Nebo-Well) cranidium showing palpebral lobes shown x4 a) dorsal b) anterior c) lateral (latex cast illustrated)
3. OU11852 Paratype (Nebo-Well) cranidium in dorsal view x5
4. OU11853 Holotype (Nebo-Well) small (meraspid?) cranidium with some exoskeleton x6 a) oblique b) lateral c) dorsal

Plate 20

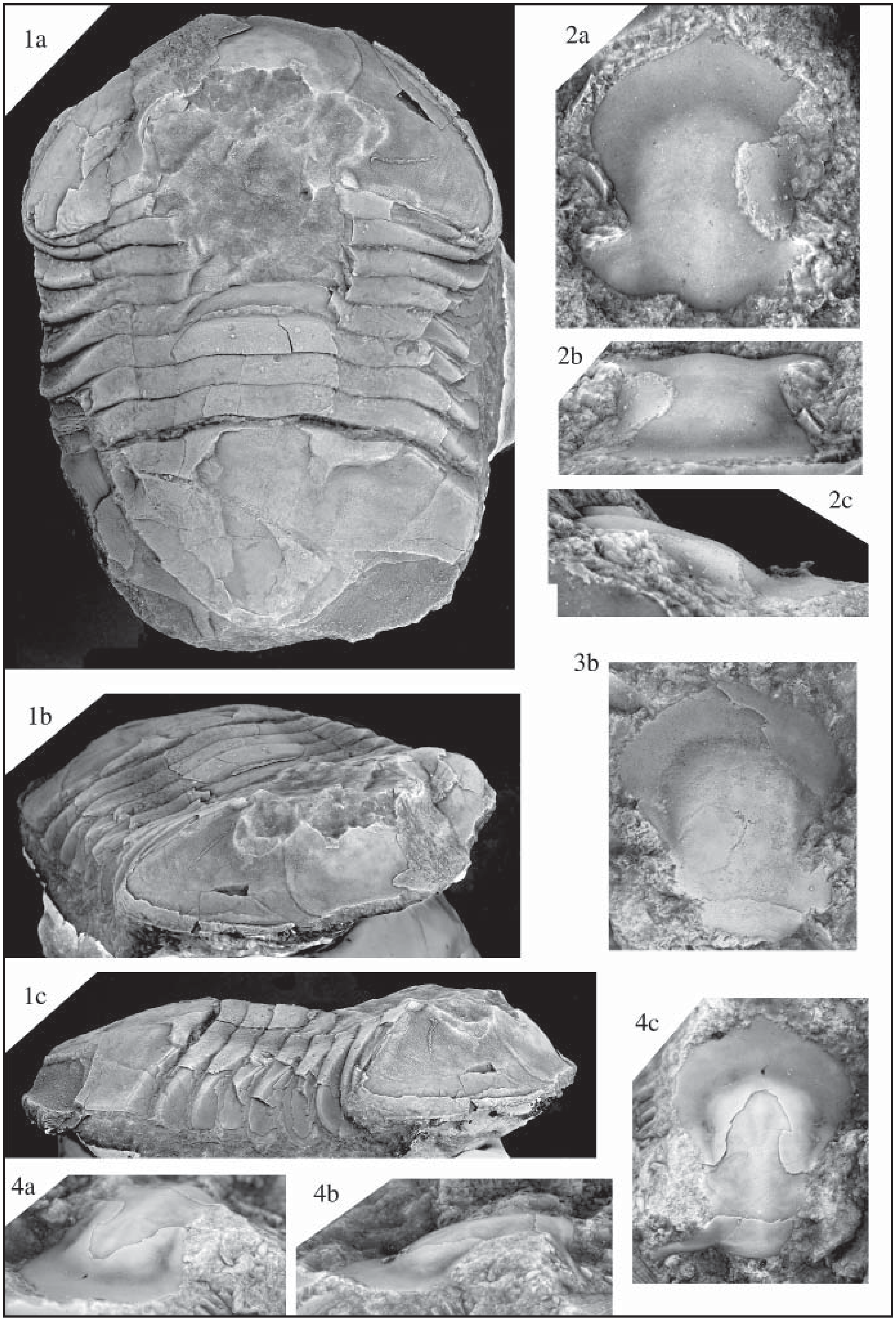

PLATE 21

Stegnopsis erythragora

Figures

1. OU11854 Paratype (Nebo-Well) testate cranidium with broken anterior margin x4 a) dorsal b) anterior c) lateral
2. OU11855 Paratype (Nebo-Well) nearly complete, exfoliated pygidium x1.5 a) posterior b) dorsal
3. OU11856 Paratype (Nebo-Well) testate pygidium x1.5 a) dorsal b) lateral c) posterior
4. OU11857 Paratype (77-183) pygidium showing sculpture shown a) dorsal x1.5 b) close-up x6 (latex cast illustrated)

Plate 21

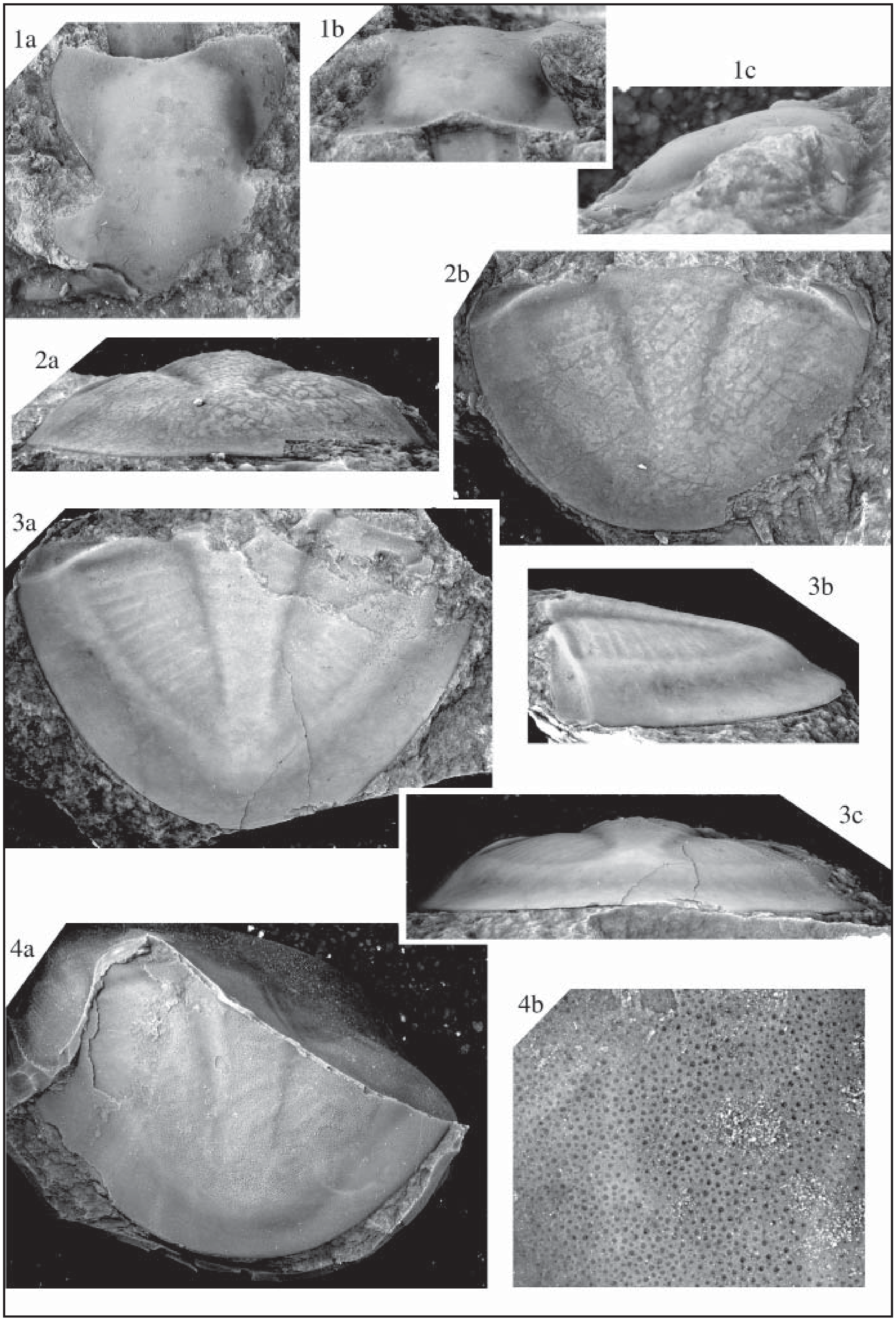

PLATE 22

Anataphrus megalophrys

Figures

1. OU11858 Paratype (LQ-VS) small (meraspid?) cranidium in dorsal view x12
2. OU11859 Paratype (LQ-VS) small (meraspid?) cranidium, testate on anterior x12 a) dorsal b) lateral c) close-up of exoskeleton x18 d) anterior
3. OU11860 Paratype (LQ-VS) small, testate cranidium x10 a) dorsal b) anterior/dorsal c) lateral
4. OU11861 Paratype (LQ-VS) small, partially testate cranidium x8 a) dorsal b) lateral c) anterior
5. OU11862 Paratype (LQ-VS) testate cranidium x7 a) dorsal b) close-up of palpebral lobe and exoskeleton x15
6. OU11863 Paratype (LQ-VS) testate cranidium x7 a) anterior b) dorsal
7. OU11864 Paratype (LQ-VS) large, testate cranidium x4 a) dorsal b) lateral c) anterior
8. OU11865 Paratype (99-49) large cranidium in dorsal view x4

Plate 22

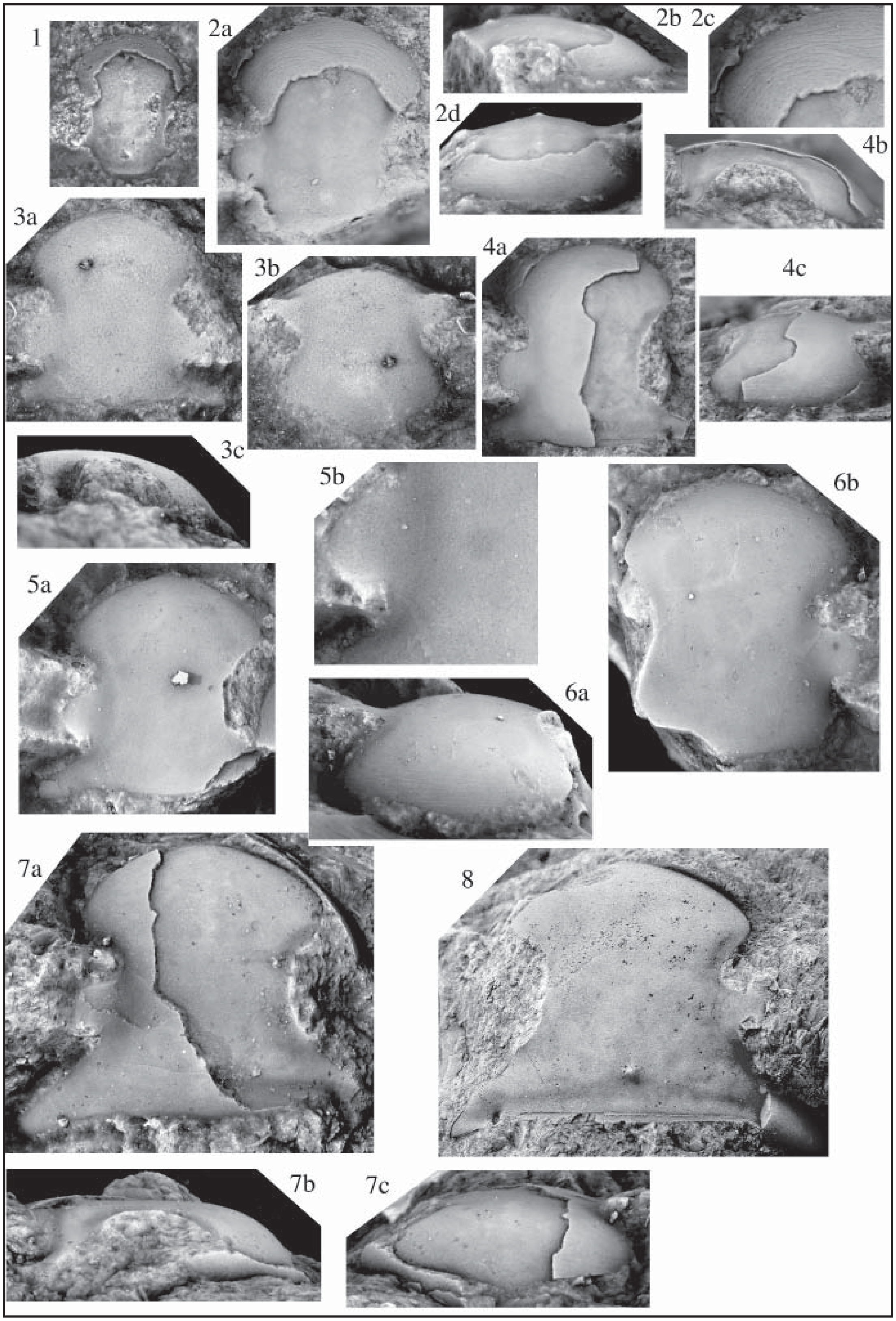

PLATE 23

Anataphrus megalophrys

Figures

1. OU11866 Holotype (LQ-VS) testate cranidium missing only right posterior fixigena a) dorsal x7 b) anterior right portion of cranidium showing lack of sculpture x12 c) anterior/dorsal
2. OU11867 Paratype (LQ-VS) nearly complete, testate hypostome x6 a) ventral b) lateral/oblique c) lateral
3. OU11868 Paratype (99-48) mostly testate librigena with visual surface x4 a) lateral b) dorsal c) anterior
4. OU11869 Paratype (99-49) mostly exfoliated librigena with visual surface x4 a) lateral b) dorsal c) anterior
5. OU11870 Paratype (LQ-VS) testate hypostome x6 a) ventral b) lateral
6. OU11871 Paratype (99-48) partly exfoliated hypostome x6 a) dorsal b) lateral
7. OU11872 Paratype (LQ-VS) partly exfoliated, transitory pygidium x10 a) lateral b) dorsal c) posterior

Plate 23

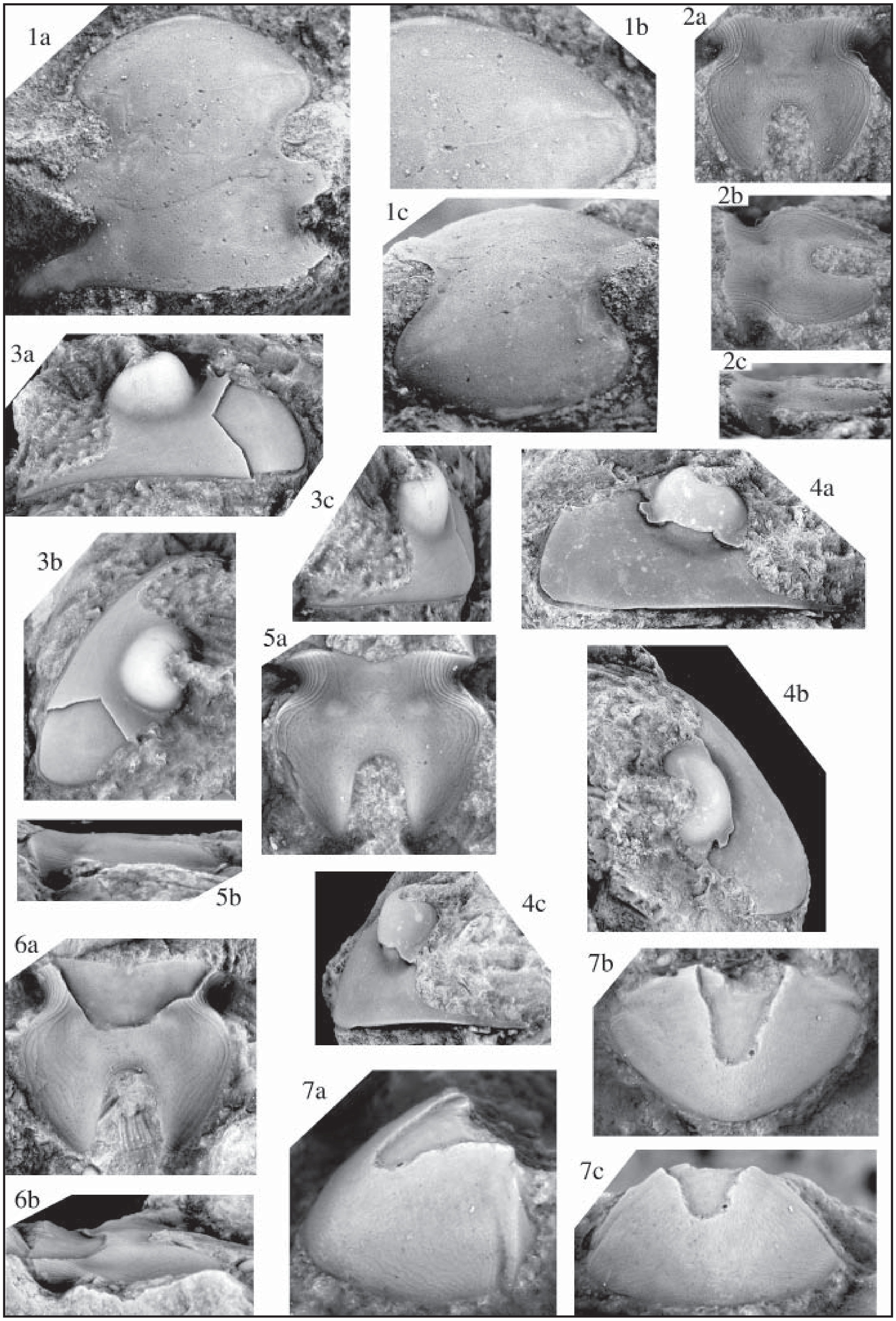

PLATE 24

Anataphrus megalophrys

Figures

1. OU11873 Paratype (LQ-VS) partly exfoliated thorax and exfoliated pygidium x4 a) dorsal b) lateral
2. OU11874 Paratype (LQ-VS) small, testate pygidium x6 a) dorsal b) posterior c) maximum view with lighting to show faint axial furrows d) lateral
3. OU11875 Paratype (99-48) partly exfoliated pygidium missing posterior margin x6 a) dorsal b) posterior c) lateral
4. OU11876 Paratype (LQ-VS) exfolilated pygidium showing relict segmentation of axis x5 a) posterior b) maximum c) lateral
5. OU11877 Paratype (LQ-VS) mostly exfoliated pygidium showing relict segmentation of axis x5 a) dorsal b) posterior c) lateral

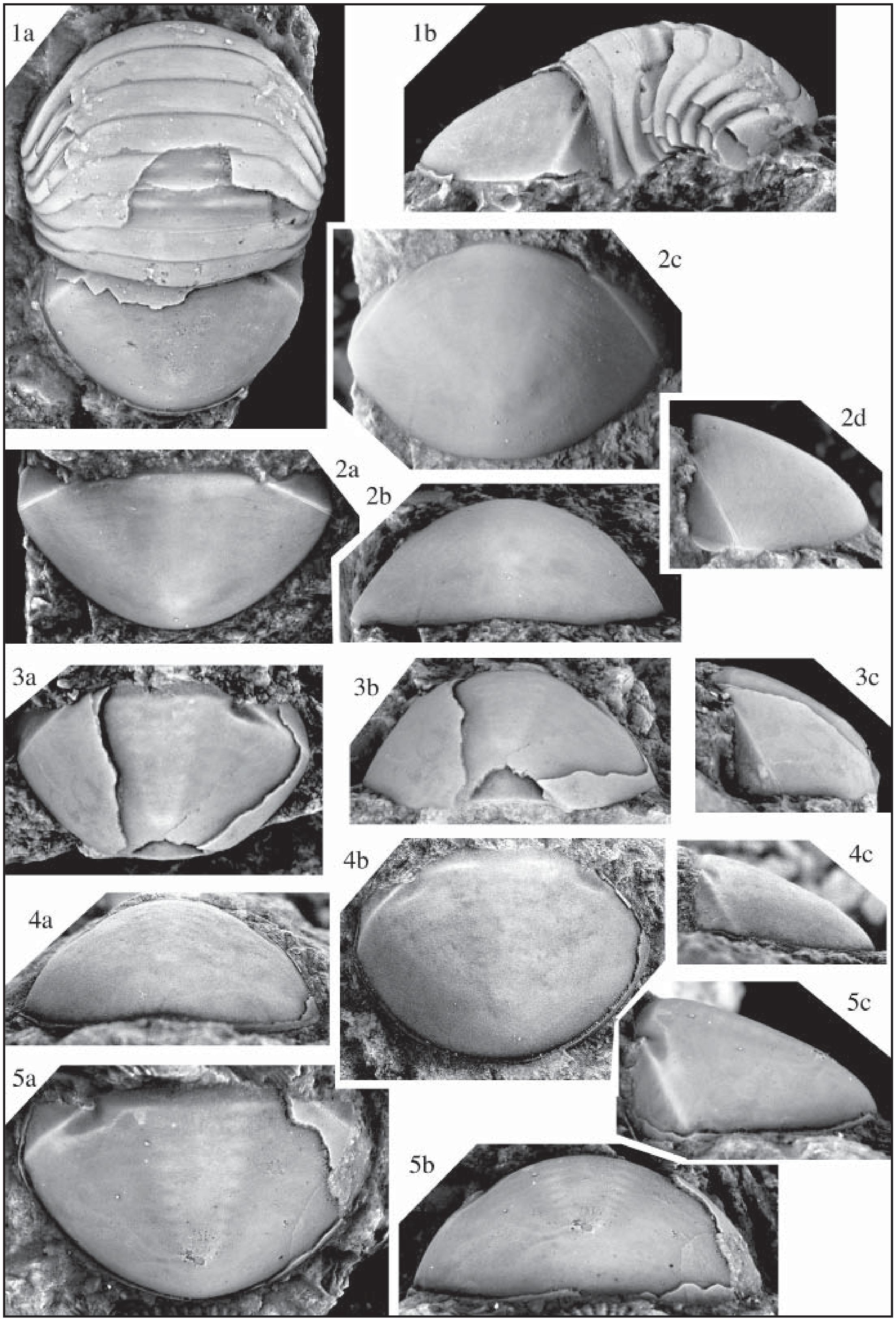
1a
1b
2a
2b
2c
2d
3a
3b
3c
4a
4b
4c
5a
5b
5c

PLATE 25

Anataphrus megalophrys, Anataphrus kermiti

Figures 1-6 *Anataphrus megalophrys*

1. OU11878 Paratype (LQ-VS) partly exfoliated, broken pygidium with right and posterior part of doublure exposed a) dorsal x4 b) close-up showing sculpture x8
2. OU11879 Paratype (LQ-VS) transitory pygidium x12 a) dorsal b) posterior c) lateral
3. OU11880 Paratype (99-48) partly exfoliated pygidium x3 a) dorsal b) posterior
4. OU11881 Paratype (99-49.5) exfoliated pygidium showing part of doublure in dorsal view x4
5. OU11882 Paratype (99-48) dorsal view of exfoliated large pygidium showing axial segmentation x4
6. OU11883 Paratype (99-48) transitory pygidium x12 a) dorsal b) posterior c) lateral

Figures 7-10 *Anataphrus kermiti*

7. OU11884 Paratype (77-218) complete, testate cranidium in dorsal view x10
8. OU11885 Paratype (77-219) cranidium x7 a) dorsal b) anterior c) lateral (latex cast illustrated)
9. OU11886 Paratype (77-219) small, testate pygidium x8 a) dorsal b) posterior c) lateral
10. OU11887 Paratype (77-219) small, nearly complete testate cranidium x4 a) anterior b) dorsal

Plate 25

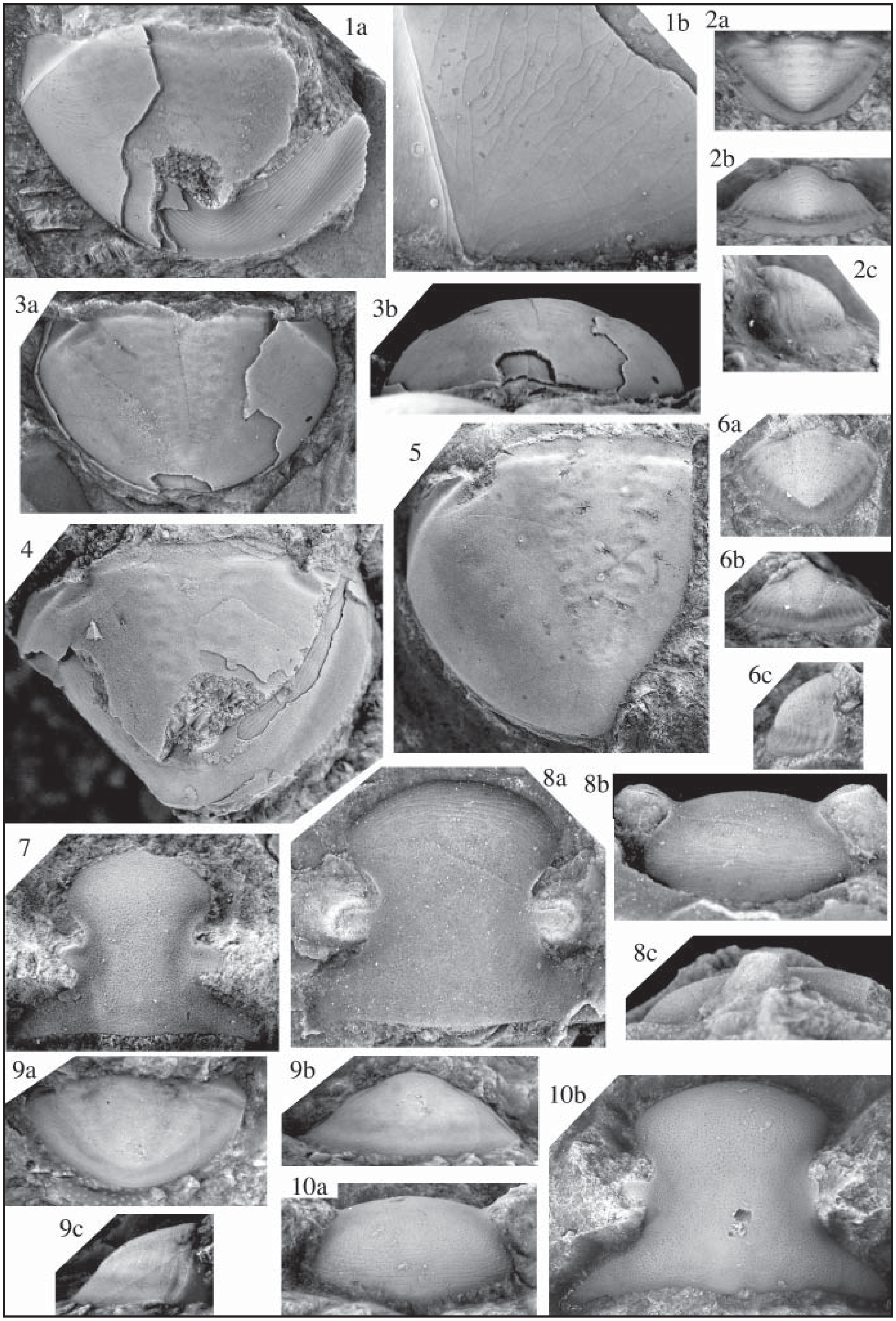

PLATE 26

Anataphrus kermiti

Figures

1. OU11888 Paratype (77-218) cranidium shoing strap-like palpebral lobes a) dorsal x4 b) lateral x4 c) palpebral lobe x8 d) anterior x4 (latex cast illustrated)
2. OU11889 Holotype (77-Float) nearly complete enrolled individual x4 a) anterior b) dorsal view of pygidium c) dorsal view of cephalon d) lateral e) dorsal view of thorax
3. OU11890 Paratype (77-219) small, exfoliated pygidium with posterior margin broken to show part of doublure x7 a) posterior b) dorsal
4. OU11891 Paratype (77-219) mostly exfoliated, transitory pygidium x10 a) dorsal b) posterior c) lateral

Plate 26

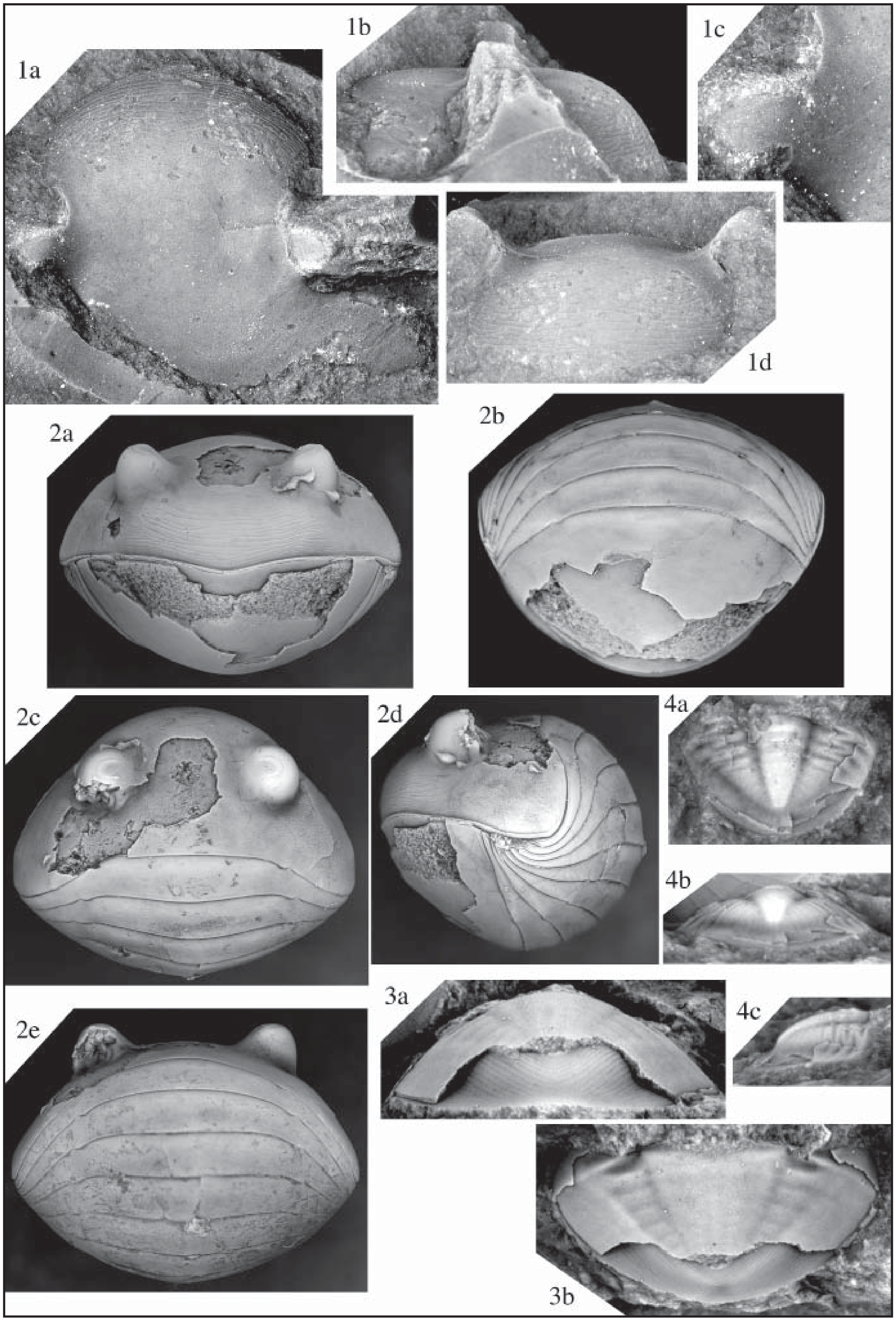

PLATE 27

Anataphrus kermiti

Figures

1. OU11892 Paratype (77-219) nearly complete cranidium a) dorsal x3 b) anterior showing terrace ridges x3 c) lateral x3 d) detail of waisted palpebral lobe, pitted exoskeleton, terrace ridges x6 (latex cast illustrated)
2. OU11893 Paratype (77-219) cranidium missing lateral posterior fixigenae and anterior of cranidium a) dorsal x3 b) dorsal view of waisted palpebral lobe x8 c) lateral view of waisted palpebral lobe x8 (latex cast illustrated)
3. OU11894 Paratype (77-219) small, testate pygidium x7 a) posterior b) maximum c) lateral
4. OU11895 Paratype (LQ-WF) testate pygidium x7 a) dorsal b) lateral c) posterior
5. OU11896 Paratype (LQ-WF) complete, testate pygidium a) maximum x2.5 b) lateral x2.5 c) detail of exoskeleton showing pitting and ridges x5

Plate 27

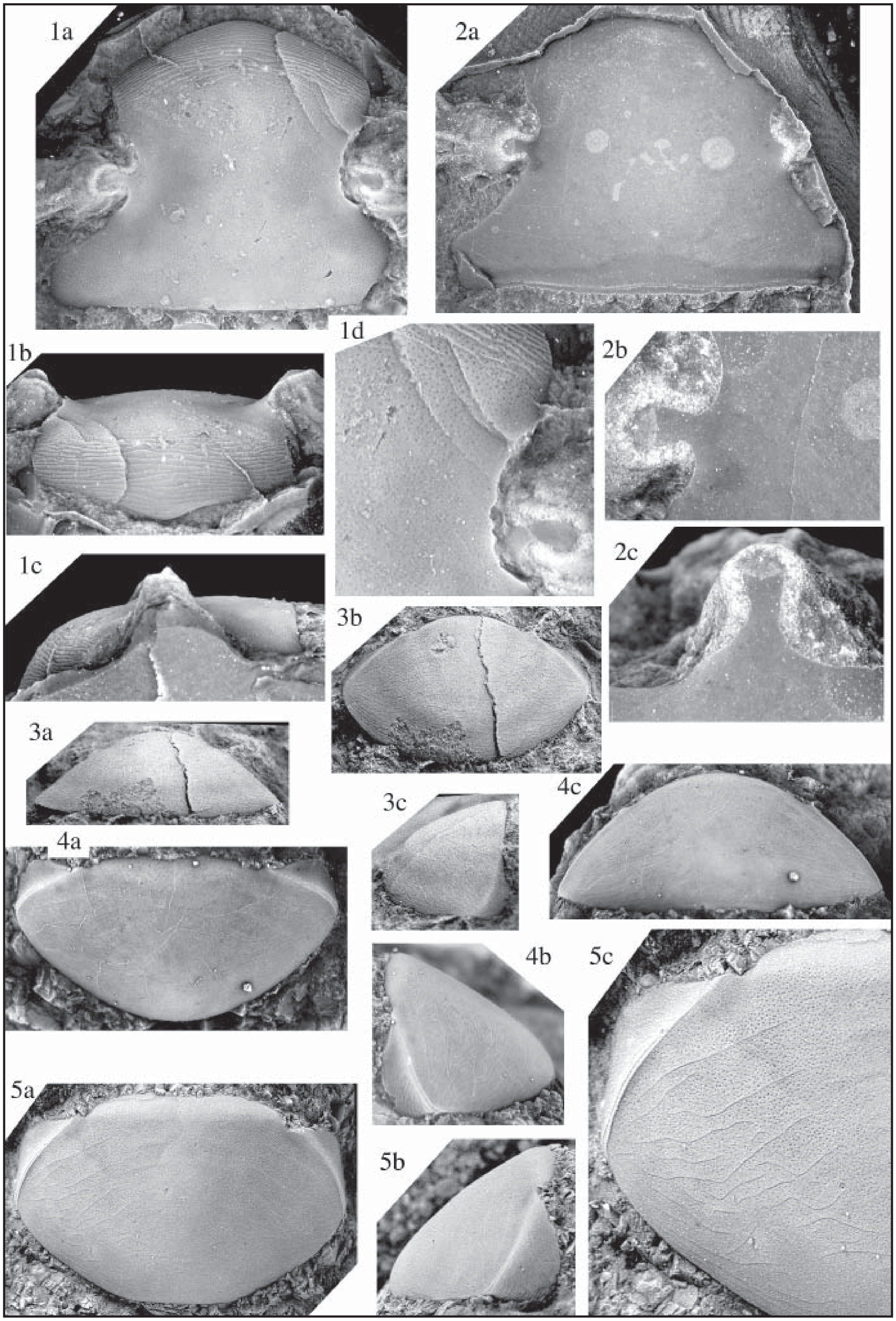

PLATE 28

Anataphrus kermiti

Figures

1. OU11897 Paratype (LQ-WF) partial cranidium a) dorsal x5 b) waisted palpebral lobe x8 (latex cast illustrated)
2. OU11898 Paratype (LQ-WF) nearly complete librigena x8 a) anterior b) dorsal c) lateral
3. OU11899 Paratype (LQ-WF) nearly complete, testate cranidium x6 a) dorsal b) anterior/oblique
4. OU11900 Paratype (Nebo-Well) testate hypostome in ventral view x4
5. OU11901 Paratype (LQ-WF) exfoliated hypostome x4 a) ventral b) lateral
6. OU11902 Paratype (LQ-WF) testate, transitory pygidium x8 a) dorsal b) posterior c) lateral
7. OU11903 Paratype (CC) testate transitory pygidium x12 a) dorsal b) lateral c) posterior
8. OU11904 Paratype (Nebo-Well) exfoliated pygidium x6 a) lateral b) posterior c) dorsal
9. OU11905 Paratype (LQ-WF) exfoliated pygidium showing axial segmentation x7 a) posterior b) lateral c) dorsal
10. OU11906 Paratype (CC) exfoliated cranidium in dorsal view x4

Plate 28

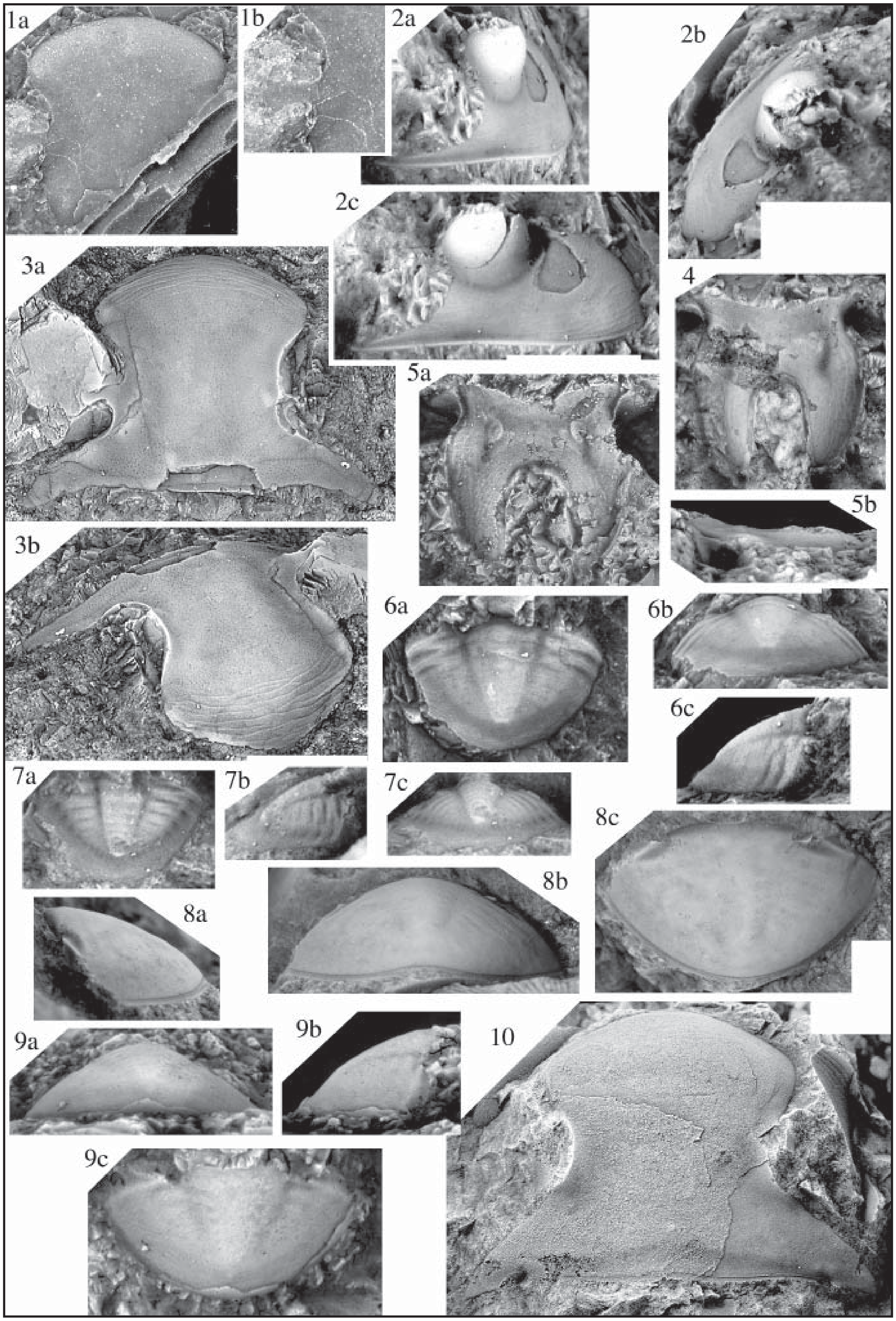

PLATE 29

Anataphrus kermiti

Figures

1. OU11907 Paratype (CC) exfoliated pygidium x6
a) maximum b) posterior c) lateral
2. OU11908 Paratype (BQ-24) small, testate cranidium x8
a) dorsal b) lateral/dorsal showing strap-like palpebral lobe
3. OU11909 Paratype (BQ-18) cranidium showing strap-like palpebral lobe x8 a) dorsal b) anterior c) lateral (latex cast illustrated)
4. OU11910 Paratype (BQ-24) cranidium showing strap-like palpebral lobe in dorsal view x8 (latex cast illustrated)
5. OU11911 Paratype (BQ-18) distorted, testate cranidium showing waisted palpebral lobe in dorsal view x5
6. OU11912 Paratype (BQ-24) testate librigena with visual surface x4 a) anterior b) dorsal c) lateral
7. OU11913 (BQ-18) exfoliated pygidium x3.5 a) dorsal
b) posterior c) lateral
8. OU11914 Paratype (77-219) small, nearly complete, partly exfoliated cranidium x10 a) dorsal b) anterior c) lateral
9. OU11915 (77-219) small, partly exfoliated cranidium x10
a) dorsal
10. OU11916 Paratype (77-219) meraspid librigena in lateral view x10
11. OU11917 Paratype (CC) transitory pygidium x10
a) posterior b) lateral c) dorsal

Plate 29

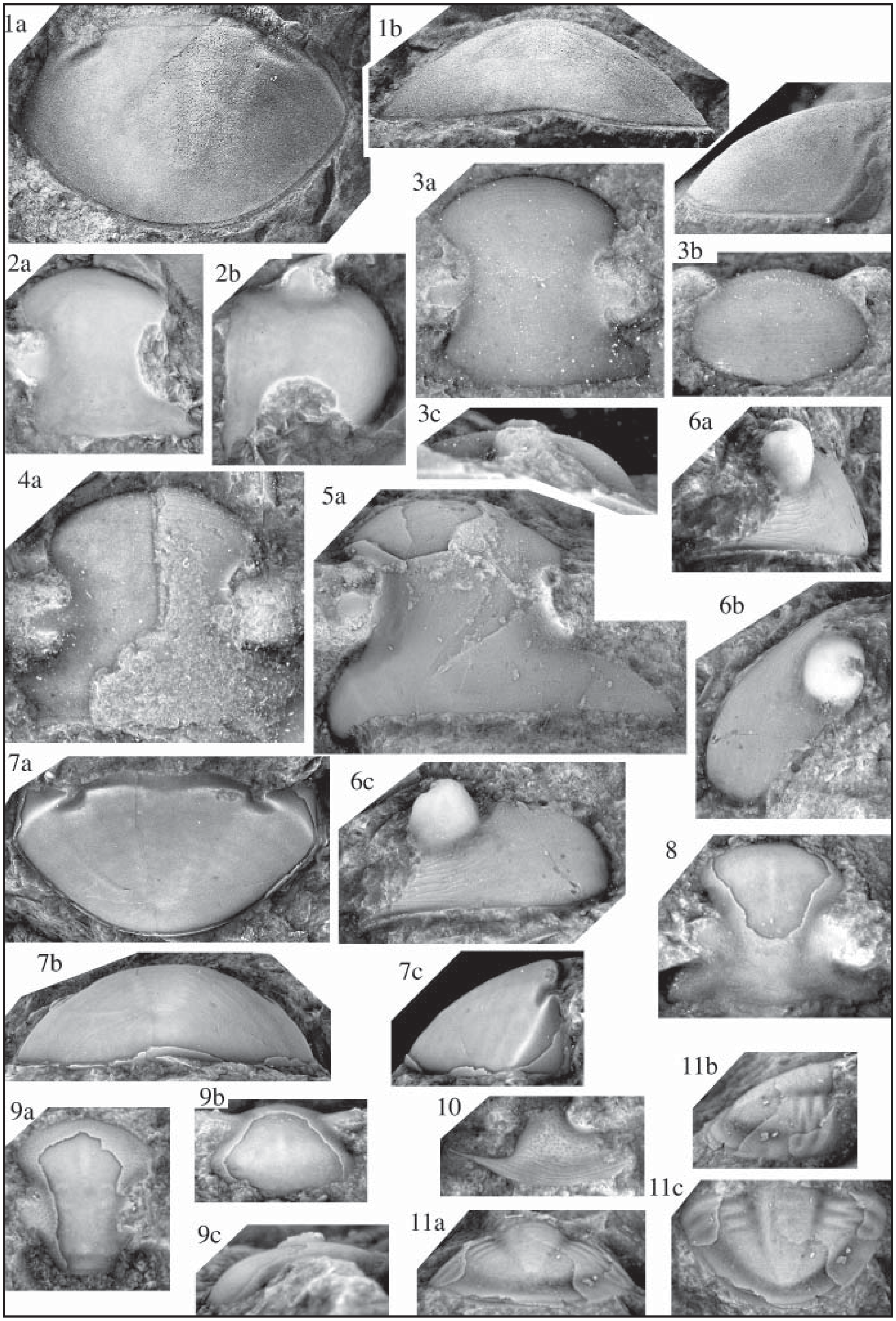

PLATE 30

Anataphrus kermiti ontogeny

Figures

1. OU11918 Paratype (BQ-12) meraspid cranidium x15
   a) dorsal b) anterior c) lateral c) oblique
2. OU11919 Paratype (BQ-18) meraspid cranidium x12
   a) dorsal b) anterior c) lateral d) oblique
3. OU11920 Paratype (BQ-12) small cranidium x10 a) dorsal
   b) oblique c) anterior d) lateral
4. OU11921 Paratype (BQ-12) meraspid librigena x10 in lateral view
5. OU11922 Paratype (BQ-24) meraspid librigena x8 in lateral view
6. OU11923 Paratype (BQ-24) meraspid librigena x8
   a) anterior b) dorsal c) lateral
7. OU11924 Paratype (BQ-12) meraspid hypostome x14 in ventral view
8. OU11925 Paratype (BQ-12) meraspid hypostome x12
   a) lateral/ventral b) ventral
9. OU11926 Paratype (BQ-24) meraspid pygidium x8 in dorsal view
10. OU11927 Paratype (BQ-24) meraspid pygidia x12
11. OU11928 Paratype (BQ-18) meraspid pygidium x15
    a) dorsal b) lateral c) posterior
12. OU11929 Paratype (BQ-12) meraspid pygidium x15
    a) dorsal b) lateral c) posterior
13. OU11930 Paratype (BQ-12) meraspid pygidium x15
    a) dorsal b) lateral c) posterior
14. OU11931 Paratype (BQ-24) meraspid pygidium x12
    a) dorsal b) posterior
15. OU11932 Paratype (BQ-24) meraspid pygidium x8
    a) dorsal b) maximum c) lateral
16. OU11933 Paratype (BQ-12) meraspid pygidium x12
    a) dorsal b) lateral c) posterior
17. OU11934 Paratype (BQ-12) meraspid pygidium x10
    a) dorsal b) lateral c) posterior
18. OU11935 Paratype (BQ-24) meraspid pygidium in dorsal view x12
19. OU11936 Paratype (LQ-WF) meraspid pygidium x8
    a) dorsal b) lateral c) posterior

Plate 30

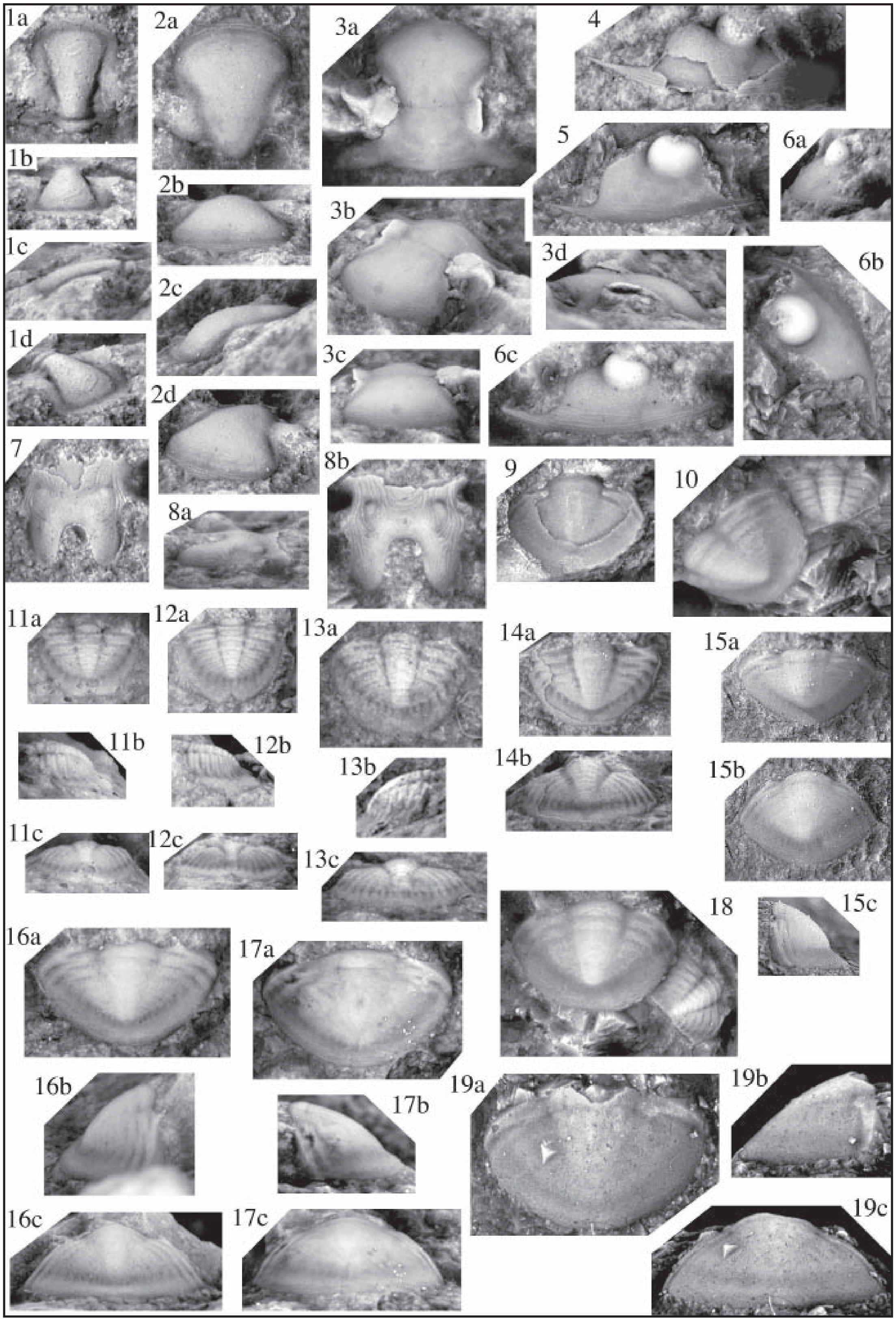
1a
2a
3a
4
1b
2b
5
6a
3b
1c
3d
6b
2c
1d
3c
6c
2d
7
8b
9
10
8a
11a
12a
13a
14a
15a
11b
12b
13b
14b
15b
11c
12c
13c
18
15c
16a
17a
16b
17b
19a
19b
16c
17c
19c

PLATE 31

Anataphrus kermiti

Figures

1. OU11937 Paratype (MC) nearly complete, partly exfoliated, enrolled individual x2.5 a) dorsal b) lateral c) anterior
2. OU11938 Paratype (BQ-Pave) complete, testate individual with slightly crushed cranidium a) lateral/dorsal x1 b) cephalon x2 c) dorsal x1
3. OU11939 Paratype (BQ-Pave) crushed, weathered complete individual x1 a) dorsal b) lateral/dorsal
4. OU11940 Paratype (LQ-WF) testate cranidium indorsal view, unblackened, dark areas indicate muscle attachment sites on ventral surface of exoskeleton x2
5. OU11941 Paratype (LQ-WF) testate pygidium, unblackened x2 a) dorsal view, dark areas along axis indicate sites of muscle attachment on ventral surface of exoskeleton b) dorsal view, lighting maximized to show faint relict segmentation on pleural regions

Plate 31